Title
A Hypothalamic Switch for REM and Non-REM Sleep

Author
Chen, Kai-Siang

Publication Date
2017

Peer reviewed|Thesis/dissertation

A Hypothalamic Switch for REM and Non-REM Sleep

By

Kai-Siang Chen

A dissertation submitted in partial satisfaction of the

requirements for the degree of

Doctor of Philosophy

in

Molecular and Cell Biology

in the

Graduate Division

of the

University of California, Berkeley

Committee in charge:

Professor Yang Dan, Chair

Professor Ehud Isacoff

Professor Lance Kriegsfeld

Professor Kristin Scott

Fall 2017

A Hypothalamic Switch for REM and Non-REM Sleep

By

Kai-Siang Chen

Abstract

A Hypothalamic Switch for REM and Non-REM Sleep

by

Kai-Siang Chen

Doctor of Philosophy in Molecular and Cell Biology

University of California, Berkeley

Professor Yang Dan, Chair

Rapid eye movement (REM) and non-REM (NREM) sleep are controlled by specific neuronal circuits. In this thesis, I show that galanin-expressing GABAergic neurons in the dorsomedial hypothalamus (DMH) comprise separate subpopulations with opposing effects on REM versus NREM sleep. Microendoscopic calcium imaging revealed diverse sleep-wake activity of DMH GABAergic neurons, but the galanin-expressing subset falls into two distinct groups, either selectively activated (REM-on) or suppressed (REM-off) during REM sleep. Retrogradely labeled, preoptic area (POA)-projecting galaninergic neurons are REM-off, whereas the raphe pallidus (RPA)-projecting neurons are primarily REM-on. Bidirectional optogenetic manipulations showed that the POA projectors promote NREM sleep and suppress REM sleep, while the RPA projectors have the opposite effects. Thus, REM/NREM switch is regulated antagonistically by galaninergic neurons with intermingled cell bodies but distinct axon projections.

Table of Contents

Chapter 1. Introduction: Neural Circuits Regulating Sleep

Chapter 2. Dorsomedial Hypothalamus in Sleep Regulation

Chapter 1. Introduction: Neural Circuits Regulating Sleep

1.0 Preface

Sleep is one of the most universal but mysterious animal behavior. In this Chapter, I review the previous research works that have helped us understand the neural circuits regulating sleep. They include the neural circuits regulating sleep-wake behaviors, and the circuits regulating rapid eye movement (REM) sleep and non-REM (NREM) sleep. At the end of this chapter, I also review some key technological innovations that are recently applied in the research of sleep circuits.

1.1 The Early History of Sleep-Wake Circuits Research

In this section, I review the scientific development of the identification and mapping of neural circuits regulating sleep and wakefulness. I especially focus on early literatures based on the studies on patients, lesions within the animal and pharmacological experiments. Novel findings by using advanced system neuroscience methods are described in Chapter 1.3.

1.1.1 Epidemics and the Patients with Sleep Disorders

Sleep is a universal biological phenomenon which can be found in most of the species in the animal kingdom. Earlier philosophers, from the period of Aristotle until the early 20 century, believed that the formation of sleep was a simple consequence of the reduction of sensory inputs and brain activities. Some leading scientists in the neuroanatomy fields, for instance, Lhermitte and Purkinje even thought that there is no specific neural pathways for sleep-wake regulation.

This concept was first challenged by a Viennese neurologist, Baron Constantin von Economo, in 1916. Dr. von Economo was investigating patients with a new type of encephalitis that swept through North America and Europe during the second decade of the 20th century. This encephalitis was later called von Economo's sleeping sickness or encephalitis lethargica and most of the patients with this disease slept excessively. Many of them slept for more than 20 hours each day, and only woke up briefly to eat and drink. Their cognitive function was intact during the waking periods, while they turned back to sleep very quickly. Patients took many weeks to recover from this syndrome (von Economo, 1930).

1.1.2 The Identification of The Ascending Arousal System

After investigations, Dr. von Economo found that these patients had lesions between the diencephalon and the midbrain. He then proposed that there is an ascending arousal system coming from the brainstem that kept the forebrain in the awake state.

Dr. von Economo's ideas didn't catch other scientists' attention much until the end of the World War II. At that period, investigators including Moruzzi and Magoun, demonstrated that this syndrome might be mediated by an ascending arousal pathway from the rostral pons to the midbrain reticular formation. Thereafter, the idea of "Ascending Arousal System" became a popular concept within the scientific field (Moruzzi, 1949; Starzl et al., 1951).

In the period between the 1970s and 1980s, scientists spent more efforts on investigating this system. One major finding within this period was that the Ascending Arousal System has two branches and each of them originates from a small group of neurons with defined neurotransmitters. The first branch of the Ascending Arousal System originates from a pair of cell groups expressing acetylcholine in the pedunculopontine (PPT) and laterodorsal tegmental nuclei (LDT). These neurons' activities are the highest during wakefulness and REM sleep but are silent during NREM sleep. These cholinergic neurons project to the thalamus and activate the thalamic relay neurons involving in the thalamus-cortex transmission, which may ultimately lead to cortical activations (Hallanger et al., 1987; Krout et al., 2002; McCormick, 1989; Saper et al., 2001; Strecker et al., 2000).

1.1.3 Monoaminergic Neurons in Wakefulness Regulation

The second branch of this system is independent of the thalamus. The origin of this branch comes from different nuclei expressing monoamines, including the noradrenergic neurons in the locus coeruleus (LC), the serotoninergic neurons in the dorsal and median raphe nuclei, the dopaminergic neurons in the ventral periaqueductal gray matter, and the histaminergic neurons in the tuberomammillary nucleus (TMN). These monoaminergic neurons have the highest activities during wakefulness, lower activities during NREM sleep, and the lowest activities during REM sleep. These neurons activate the neurons in the basal forebrain, the lateral hypothalamus and finally cause the cortical activation (Aston-Jones and Bloom, 1981; Estabrooke et al., 2001; Gerashchenko et al., 2003; Jones, 2003; Lee et al., 2005; Mileykovskiy et al., 2005; Ranson, 1939; Rasmussen et al., 1984; Saper, 1985; Saper et al., 2001; Steininger et al., 1999; Verret et al., 2003).

1.1.4 Identification of Sleep-Promoting Regions

The other major finding contributed by Dr. von Economo was the first identification of a brain region that may induce sleep. Opposite to the major population of the encephalitis lethargica patients, a subset of them have the opposite symptom – they became insomniac and only slept a few hours per day. Dr. von Economo found these patients' basal ganglia and adjacent anterior hypothalamus were lesioned. Follow up animal experiments demonstrated and confirmed that the damage of the lateral preoptic (LPO) area would cause a similar phenomenon.

In the period of the 1980s to 1990s, investigators were interested in identifying the synaptic inputs to the wake-active monoaminergic neurons which might be involved in the regulation of sleep. Within the ventrolateral preoptic area (VLPO), a dense cluster of sleep-active GABAergic neurons expressing a neuropeptide galanin were found projecting to all major arousal cell groups in the hypothalamus and the brainstem. These results suggested that the VLPO lesion could be a potential reason that caused the insomnia in the patients that Dr. von Economo studied. Indeed, in the animal research, the lesions within the VLPO dramatically decreased the NREM sleep (Chamberlin et al., 2003; Chou et al., 2002; Gallopin et al., 2000; Gaus et al., 2002; John et al., 2004; Ko et al., 2003; Köhler et al., 1986; Lu et al., 2002; Lu et al., 2000; McGinty and Sterman, 1968; Nauta, 1946; Sherin et al., 1998; Sherin et al., 1996; Suntsova et al., 2002; Vincent et al., 1982; von Economo, 1930).

Are there other major sleep promoting regions in the brain that can promote sleep in addition to the VLPO area? How could these sleep and wake neurons interact to change the brain states? Future research applying novel system neuroscience methods may help us have deeper understanding of the working principle of sleep-wake regulations.

1.2 REM Sleep Circuits

In this section, I review the scientific development on the discovery of REM sleep and the mapping of the neural circuits regulating REM and NREM sleep. I especially focus on early literature based on human studies, brain waves recording, lesions within the animal, and pharmacological experiments. I also discuss the formation of the working model for REM-NREM sleep control. Novel findings by using advanced system neuroscience methods would be described in the later section.

1.2.1 The Discovery of REM Sleep

Earlier literatures written in Rome and India suggest that different types of sleep exist. Besides, the studies on dogs show that the dogs were moving and twitching only during a certain period of sleep (Morrison, 2011).

In 1937, Richard Klaue, a German scientist, first identified a period of fast electrical brain activities in cats that were sleeping. Seven years later, in 1944, Ohlmeyer found a 90 minutes ultradian cycle of sleep which is involved in the regulation of male erections during sleep. Thereafter, in 1952, Eugene Aserinsky, Nathaniel Kleitman, and William C. Dement identified the phases of REM during sleep, and built up their connection with dreaming by measuring the eye movement event and the accompanying electrical activity in the children of Aserinsky and Kleitman. Dement designed experiments to deprive REM sleep which helped to understand the physiological function of REM sleep (Aserinsky, 1996; Aserinsky and Kleitman, 1953; Dement, 1960).

1.2.2 Cholinergic and Monoaminergic Regulatory of REM Sleep

After the discovery of REM sleep, the regulatory mechanism of REM sleep became a major topic in sleep research. In the following two decades after REM sleep was identified, Michel Jouvet and others performed a series of lesion studies to identify the brain region responsible for generating REM sleep. Their work demonstrated that neurons in the pontine tegmentum (dorsolateral pons) enable and regulate REM sleep by large excitotoxic lesions or transections of pons. Jouvet found that the lesion of the reticular formation within the brainstem inhibited REM sleep and later publications indicated that REM sleep can happen in a cat even without its forebrain (Jouvet, 1962; Webster and Jones, 1988).

In addition to the lesions studies, EEG recording data in the cats suggested that prior to and during REM sleep, there are high-voltage EEG waves coming from the pons, lateral geniculate and occipital cortex (called PGO waves). These PGO waves are generated by a group of burst cholinergic neurons in the pedunculopontine (PPT) and laterodorsal tegmental (LDT) nuclei and time locked to the burst of firing from these neurons (Sakai and Jouvet, 1980).

On the contrary, the activities of noradrenergic neurons in the locus coeruleus (LC), the serotoninergic neurons in the dorsal and median raphe nuclei, the dopaminergic neurons in the ventral periaqueductal gray matter and the histaminergic neurons in the tuberomammillary nucleus (TMN) are completely silent during REM sleep (Aston-Jones and Bloom, 1981; Hobson et al., 1975; Steininger et al., 1999; Takahashi et al., 2010; Trulson et al., 1981).

1.2.3 Examination of The Importance of Cholinergic and Monoaminergic Systems in REM Sleep Regulation

The reciprocal relationship between the activities of these monoaminergic neurons and the pedunculopontine and laterodorsal tegmental nuclei suggested that their interaction may regulate the alternation of REM and NREM sleep.

By using Lottka-Volterra equations, McCarley and Hobson came up with a differential equation model (a predator-prey model) of REM/NREM sleep regulatory mechanism. In their model, the cholinergic neurons act like prey. The increase of their activities during REM sleep excites monoamine neurons. Nonetheless, the monoaminergic neurons are like predators – the increase of their activities decreases the activities of cholinergic neurons and causes the termination of REM sleep. This model however, still has its weakness, since the substantial time delay required in a predator-prey model is difficult to be explained in neural circuits in which the neural transmission time is at the scale of milliseconds (Hobson et al., 1975; McCarley and Hobson, 1975; Pace-Schott and Hobson, 2002).

Even with this weakness, this model of the interaction between the cholinergic and monoaminergic neurons regulating sleep has its own experimental support. Luppi performed pharmacological experiments in which he applied cholinergic drugs to the mesopontine tegmentum and found the increase of REM sleep. However, when he applied drugs that activated the monoaminergic neurons, REM sleep was suppressed (Luppi et al., 2006).

On the other hand, other lesion studies challenged the importance of these cholinergic and monoaminergic neurons in REM sleep regulation – the lesions of these nuclei have limited effect on REM sleep. Lesions with electrolytes within the pedunculopontine tegmental nucleus (PPT) of cats had mild effects on the reduction of the number of transitions into REM sleep, while lesions within the laterodorsal tegmental nucleus (LDT) or locus coeruleus (LC) had no effects on REM sleep. Follow up experiments with more precise lesions within the pedunculopontine tegmental nucleus (PPT) or the laterodorsal tegmental nucleus (LDT) in rats showed little effects on REM sleep regulation. Complete removal of locus coeruleus (LC) with specific toxins also showed no clear effects on REM sleep regulation. These evidences collectively challenged the significance of these cholinergic-monoaminergic models as crucial regulators of REM sleep and their role in switching on and off REM sleep (Blanco-Centurion et al., 2007; Lu et al., 2006; Shouse and Siegel, 1992; Webster and Jones, 1988).

1.2.4 Identification of REM Sleep Promoting Neurons in the Brainstem

Given the weakness of the cholinergic-monoaminergic models, scientists were searching for other possible regulators that might be the key control of REM sleep. Investigators were looking at the expression pattern of immediately early genes (e.g. *c-fos*) during augmented REM sleep. In these studies, the *c-fos* expression level within the pedunculopontine tegmental nucleus (PPT) or the laterodorsal tegmental nucleus (LDT) is very low. However, three other brain regions were found with much higher expression level of *c-fos* - the sublaterodorsal nucleus (SLD), the precoeruleus region (PC), and the medial parabrachial nucleus (MPB) (Boissard et al., 2002; Lu et al., 2006).

To examine the role of sublaterodorsal nucleus (SLD) in REM sleep regulation, a GABA antagonist, bicuculline, was injected within the sublaterodorsal nucleus to inhibit these neurons. These injections activated the sublaterodorsal nucleus and elicits REM sleep-like behavior. Lesions within the sublaterodorsal nucleus in cats and rats both affected the REM sleep, while the effects were more profound in the rats (Boissard et al., 2002; Hendricks et al., 1982; Lu et al., 2006; Sastre et al., 1996; Shouse and Siegel, 1992).

To identify inputs that may modulate the sublaterodorsal nucleus activities and that may be involved in REM sleep regulation, retrograde tracers were injected into the sublaterodorsal nucleus. GABAergic inputs were mostly identified within the ventrolateral periaqueductal gray matter (vLPAG) and lateral pontine tegmentum (LPT).

These two regions both receive synaptic inputs from the extended VLPO (eVLPO) and the orexin-expressing neurons within the lateral hypothalamus. The eVLPO neurons are GABAergic and are activated during REM sleep and the orexin-expressing neurons are silent during REM sleep and excitatory. Also, these GABAergic neurons within the ventrolateral periaqueductal gray matter and lateral pontine tegmentum projecting to the REM sleep-activate sublaterodorsal nucleus. Taken together, the ventrolateral periaqueductal gray matter and the lateral pontine tegmentum were proposed to be silent during REM sleep and can suppress REM sleep. This idea was tested by the injections of GABA agonist into the ventrolateral periaqueductal gray matter and lesion studies. In both cases, the increase of REM sleep was observed (Lu et al., 2006).

To further examine the relationship between the ventrolateral periaqueductal gray matter, lateral pontine tegmentum, and the sublaterodorsal nucleus, retrograde tracers were injected into the ventrolateral periaqueductal gray matter and the lateral pontine tegmentum. These tracers which labeled sublaterodorsal nucleus GABAergic neurons and other experiments showed that the sublaterodorsal nucleus may innervate GABAergic neurons within the ventrolateral periaqueductal gray matter and lateral pontine tegmentum. These anatomical results raise possibilities that the sublaterodorsal nucleus may for an inhibitory loop with the ventrolateral periaqueductal gray matter and lateral pontine tegmentum which may control the switch of REM sleep (Crochet et al., 2006; Lu et al., 2006; Sapin et al., 2009; Sastre et al., 1996).

1.2.5 Glutamatergic Systems in REM Sleep Regulation

In addition to the GABAergic neurons, the glutamatergic neurons are intermingled with the REM-active, GABAergic neurons within the REM sleep promoting regions. These neurons have long-range projections to other REM-active region and may activate these neurons and promote REM sleep. For instance, glutamatergic neurons within the sublaterodorsal nucleus express *c-fos* during REM sleep. These neurons project to brainstem and spinal inhibitory systems which could hyperpolarize motor neurons and lead to muscle atonia (Lu et al., 2006; Luppi et al., 2013; Luppi et al., 2006; Shouse and Siegel, 1992; Webster and Jones, 1988).

Besides, there are other glutamatergic neurons which are intermingled with REM-inactive GABAergic neurons. These neurons project to the spinal cord and may support motor tone when the animals are in NREM sleep. The inhibitory inputs to these neurons may contribute the muscle atonia during REM sleep. Other glutamatergic neurons in the precoeruleus region and the parabrachial nucleus may contribute to the activation of cortical EEG by activating the forebrain (Burgess et al., 2008; Lu et al., 2006; Vetrivelan et al., 2009).

In the lateral and posterior hypothalamus, in addition to the orexin-expressing neurons that might be involved in the regulation of wakefulness, there is a large number of neurons that may regulate REM sleep. Neurons expressing the neuropeptide melanin-concentrating hormone (MCH) are intermingled with orexin-expressing neurons and share similar projection targets. However, these neurons expressing neuropeptide melanin-concentrating hormone have the highest activities during REM sleep. These neurons also express neurotransmitter GABA and both the melanin-concentrating hormone and GABA are inhibitory. Injection of melanin-concentrating hormone into the ventricle promoted REM sleep while MCH antagonists inhibited REM sleep. Nevertheless, the knockout mice of melanin-concentrating hormone or the melanin-concentrating hormone receptor 1 have no clear effect changing the total amount of REM sleep, which raises the question as to whether this peptide is really involved in the REM sleep regulation and more follow up experiments are needed (Adamantidis et al., 2008; Elias et al., 2001; Hassani et al., 2009; Verret et al., 2003; Willie et al., 2008).

1.2.6 The Flip-Flop Model for the REM/NREM Sleep Circuits

It was later proposed by Saper and other investigators from Harvard that a flip-flop switch could be used to describe the circuit mechanism regulating REM sleep through the mutually inhibitory interaction between REM-active and REM-inactive neurons, especially in the pons. Based on this model, each side of this model inhibit the other side. If one side's activities is slightly higher than the other side, it will become a forward feedback loop and quickly turn the activities of the other side off. Even though the classical electronic flip-flop switch is composed of a single electronic component at each side, which allows the circuit to switch immediately, the brain circuits are composed of a large number of neurons within different nuclei, making it difficult to use this model to simply explain the switching mechanism (Saper et al., 2001; Takahashi et al., 2010; Wright et al., 1995).

1.2.7 Searching for the REM/NREM Switch

The weakness of the REM sleep flip-flop model mentioned earlier mainly comes from the large cell numbers of each group (NREM and REM-active). Also, the long-range projection of each group of neurons may decrease the efficiency of this switching mechanism. Third, the discrete distribution of each type of neurons makes this mechanism difficult to work.

The ideal REM/NREM switch, if it exists, should overcome the three major weakness above. Theoretically, if we can identify a brain region with a small number of GABAergic neurons that are composed of both REM-active and REM-inactive neurons with distinct projection targets (projecting to REM-active and REM-inactive regions individually) and mutually inhibiting one another, this region would possibly function as the center for switching on and off REM sleep.

The traditional system neuroscience methods were not able to dissect circuits like this due to lack of tools to specifically manipulate and record neurons based on cell types and projection targets. In the later section, I will discuss how the breakthrough of system neuroscience methods make it possible to dissect such circuits, and how we use novel tools to identify and build up the neural circuits switching on and off REM sleep.

1.3 Novel Circuit Methods in Sleep Circuits Studies

In the last section of this chapter, I review the novel system neuroscience methods in combination with molecular, cellular genetics and imaging techniques which have advanced in the last decade. These have made huge breakthroughs within this field. Also, I will review some key articles on techniques that have addressed questions in the sleep field that were not possible to be answered with traditional methods.

1.3.1 Challenges

As I addressed in the earlier sections, the major research methods that were applied within the research of sleep circuits were lesion studies, electrical stimulation and pharmacology experiments (Weber and Dan, 2016).

The major problem of applying lesion studies and electrical stimulation in sleep studies is that there are sleep/wake and NREM/REM sleep –active neurons located within the same nucleus. When investigators applied these techniques in the study, it was not possible to selectively activate or inhibit the function of a subset of neurons, which make the results hard to interpret.

The pharmacological experiments, on the country, have better cell-type resolution, since the combinations of different agonist and antagonist may help us dissect the function of different neurotransmitters in the regulation of sleep. The limitation of these methods is the kinetics. The time for the drugs to start to function and dysfunction is hard to predict. Also, the long lasting periods of these drugs make the effective time difficult to interpret. This is also true for the lesions studies, which cause the effect to vary from time to time.

Lastly, the recording techniques lacked the cell type with traditional *in vivo* extracellular recordings, which make the recording data hard to be combined with the manipulation experiments. The *in vivo* calcium imaging with 2-photon microscope and specific mouse Cre-lines may help solve these problems. However, the 2-photon imaging is limited to the superficial regions of the brain, while most of the sleep regulatory nuclei are located in the deep brain which makes this idea not possible.

1.3.2 Novel System Neuroscience Methods and Their Application in Sleep Circuit Research

These challenges strongly limited the research progress of sleep circuits in the past decades. In the past few years, there were many new tools that were developed which may help solve these problems. Here, I am reviewing some of these key tools that significantly contribute to the research of sleep circuits.

1.3.2.1 Deep Brain *in vivo* Calcium Imaging in Free Moving Animals

The major challenge for applying the imaging methods in sleep research was due to the limitation of the working distance of 2-photon microscopy and the animals having difficulty to sleep with the head-fix setting which is required for most of the traditional microscopy.

In 2011, Mark J Schnitzer's group at Stanford University published a paper describing the new method for building up a miniaturized fluorescence microscopy and combined it with a gradient refractive index (GRIN) objective lens which allows scientists to observe the activities of neurons within the deep brain regions. In combination of this technology with new versions of GCaMP, a genetic-encoded calcium indictor, and specific mouse Cre-lines, imaging specific cell types within the deep brain regions and understanding their activities became possible (Chen et al., 2013; Ghosh et al., 2011).

The first application of using this tool in sleep research was published in 2015, where the author used this technique to image the neurons within the dorsal pons. There are multiple types of neurons within this region which is important for sleep regulations, but their activities are still unclear. Using this technique, the author demonstrated that the glutamatergic neurons are mostly activated during REM sleep while the GABAergic neurons are mostly activated during the wakefulness periods. These results indicated the potential function of these two types of neurons in sleep regulation (Cox et al., 2016).

1.3.2.2 Optogenetic Manipulations

Another challenge for the sleep circuit research is the lack of good tools to manipulate the activities of neurons in the cell-type specific manners. The traditional electrical stimulation always activate a large volume of neurons without any cell type specificity. Pharmacological experiments, on the other hand, can manipulate the activities in a more specific ways, while the slow kinetics limit the temporal precision of the data interpretation (Weber and Dan, 2016).

In 2005, Deisseroth's group at Stanford University first published the paper "Millisecond-timescale, genetically targeted optical control of neural activity", which opened the era for optogenetics. In combination of specific mouse Cre-lines with light-sensitive ion channels, Deisseroth's group demonstrated the methods for manipulating the activities of neurons in cell type-specific manners (Boyden et al., 2005).

The first application of using optogenetics for *in vivo* experiments was done by a collaboration between Deisseroth's and de Lecea's group. In their paper, "Neural substrates of awakening probed with optogenetic control of hypocretin neurons", they used a specific Cre line to label orexin neurons in the lateral hypothalamus and performed optogentic manipulations. Their results supported the role of orexin neurons in promoting wakefulness. Thereafter, many groups have been applying this technique to dissect sleep circuits and other fields (Adamantidis et al., 2007; Chung et al., 2017; Jego et al., 2013; Xu et al., 2015).

1.3.2.3 Optrode Recording

The major advantage of *in vivo* calcium imaging is being able to record a large number of neurons simultaneously. However, the temporal resolution of *vivo* calcium imaging is not as good as traditional *in vivo* electrical recording methods, due to the limitation of the slow kinetics of the calcium indicators.

In 2011, Deisseroth's group published "Optetrode: a multichannel readout for optogenetic control in freely moving mice", which describe a method for recording the neuron activities in a cell type specific manner. They designed a tetrode with an optical fiber in the center, and expressed light-sensitive cation channel, channelrhodopsin, into specific neurons. Then from their electrode recording, they were able to tell which neurons are responsive to the laser stimulation that activates neurons expressing channelrhodopsin. With this method, they were able to record the activities of specific type of neurons and to know their correlation with specific animal behaviors.

In 2015, the optrode recording was first applied in sleep research. Investigators were using optrodes to record the neurons within the basal forebrain, and tried to record the activities of different types of neurons across the brain. They found most of the neurons within the basal forebrain are most active during wakefulness, while a subset of GABAergic neurons expressing somatostatin are most activated during NREM sleep. These recording data revealed a novel sleep-activated population that was not possible to tell by traditional recording methods (Xu et al., 2015).

1.3.2.4 Novel Viral Tools for Circuit Mapping

The research breakthrough of the viral development also helped the progress of system neuroscience. Here, I want to especially mention the invention of two new viral tools which are especially useful for circuit mapping.

The first one is applying rabies virus for monosynaptic retrograde tracing. Callaway's group at Salk Institute first used genetic methods to modify rabies virus and its receptor which made the rabies virus carry fluoresce reporters and only travel to one synapse at one time. This tool has been widely used within the field of system neuroscience and made the monosynaptic retrograde tracing possible, which is an essential step for mapping out a specific circuit (Callaway and Luo, 2015; Wickersham et al., 2007).

The first application of this tool in the sleep field was for validating the monosynaptic connection between ventral medulla and its downstream ventral periaqueductal region (vlPAG). Investigators found the ventral medulla GABAergic neurons can promote REM sleep and vlPAG can inhibit REM sleep. By injecting rabies into vlPAG and in situ hybridization, they were able to identify the presynaptic GABAergic neurons at ventral medulla and to confirm the connection between these two regions (Weber et al., 2015).

The other one is a new tool generated by Schaffer's and Karpova's group, called rAAV2-retro virus. Though the rabies virus is a good tool for synaptic tracing, the rabies virus strongly affects the infected neurons' health and makes it not possible for manipulation and recording experiments. This new tool, rAAV2-retro, however, can label the neuron based on their projection and still keep the neurons healthy. Schaffer's and Karpova's group have demonstrated this virus can be used for *in vivo* calcium imaging and gene-editing. Future development of this tool with optogenetics, mice genetics and deep brain imaging can help us understand the neural circuits regulating sleep more profoundly (Tervo et al., 2016).

Chapter 2. Dorsomedial Hypothalamus in Sleep Regulation

2.0 Preface

A prominent feature of sleep in mammals, birds, and reptiles is the repeated alternation between REM and non-REM sleep, but the underlying circuit mechanism remains unclear. Here I report a novel mechanism regulating the REM-NREM switch. Using cell-type-specific microendoscopic calcium imaging, I found that GABAergic neurons in the dorsomedial hypothalamus that also express the sleep-related neuropeptide galanin consist of two functionally antagonistic populations: they are either selectively active during REM sleep (REM-on) or selectively suppressed during REM sleep (REM-off). Using a novel viral tool for retrograde labelling combined with imaging and optogenetic manipulations, I showed that the two types of GABAergic/galaninergic neurons project to distinct targets and exert opposing effects on REM vs. non-REM sleep without affecting wakefulness. These findings demonstrate a striking circuit motif, in which two groups of neurons, residing in the same nucleus and using the same neurotransmitters (both GABA and galanin), promote two mutually exclusive brain states by projecting to distinct downstream targets.

2.1 Introduction

REM and NREM sleep are distinct brain states associated with different mental experience and functional roles (Brown et al., 2012). During NREM sleep the electroencephalogram (EEG) is dominated by large-amplitude slow-wave activity, but during REM sleep the EEG is desynchronized (Aserinsky and Kleitman, 1953; Dement, 1958; Jouvet, 1962). The switch between REM and NREM sleep occurs multiple times each day, but the neural circuit controlling the switch remains poorly understood.

REM and NREM sleep are regulated by multiple groups of neurons in the brainstem and hypothalamus (Brown et al., 2012; Jouvet, 1962; Saper et al., 2010; Scammell et al., 2017; Weber and Dan, 2016). In the brainstem, some neurons powerfully promote NREM to REM transitions, while others sustain NREM sleep and suppress REM sleep (Anaclet et al., 2014; Boissard et al., 2003; Clement et al., 2011; Hayashi et al., 2015; Hobson et al., 1975; Lu et al., 2006; Sapin et al., 2009; Sastre et al., 1996; Van Dort et al., 2015; Weber et al., 2015). In the lateral hypothalamus, melanin-concentrating hormone (MCH)-expressing neurons are most active during REM sleep (Hassani et al., 2009). Their brief optogenetic activation strongly promotes REM sleep, while their chronic activity is found to be important for NREM sleep (Blanco-Centurion et al., 2016; Ferreira et al., 2017; Jego et al., 2013; Konadhode et al., 2013; Tsunematsu et al., 2014). The dorsomedial hypothalamus (DMH) also plays a key role in sleep regulation, as its lesion increased both NREM and REM sleep and decreased wakefulness during the subjective day (Aston-Jones et al., 2001; Chou et al., 2003). However, the underlying circuit mechanism is not well understood. Neurons in the DMH exhibit diverse brain-state-dependent firing patterns (Findlay and Hayward, 1969), which is partly due to the existence of multiple cell types. A recent study using single-cell RNA sequencing showed that, as a molecular marker, galanin labels a subtype of GABAergic neurons in the hypothalamus (Romanov et al., 2017). This neuropeptide is strongly implicated in sleep regulation (Sherin et al., 1998; Steiger and Holsboer, 1997), and it is densely expressed in the DMH.

In my doctoral research, I examined the role of galanin-expressing DMH neurons in sleep regulation using microendoscopic calcium imaging, virus-assisted circuit tracing, and bidirectional optogenetic manipulations. I found that while DMH GABAergic neurons exhibit diverse brain state-dependent activity, the galanin-expressing subpopulation consists of two distinct groups with opposing effects on REM versus NREM sleep. These two neuronal groups can be separated on the basis of their axonal projections, but their cell bodies are intermingled in the DMH. The physical proximity between these functionally antagonistic populations could facilitate their reciprocal inhibitory interactions to induce the rapid switch between REM and NREM sleep.

2.2 Methods

2.2.1 Animals

All experimental procedures were approved by the Animal Care and Use Committee at the University of California, Berkeley. Optogenetic manipulation and viral tracing experiments were performed in male or female GAL-Cre mice (GENSAT, stock number KI87). Calcium imaging experiments were performed in male or female GAL-Cre mice and GAD2-Cre mice (Jackson Laboratory, stock numbers 010802). Animals were housed on a 12-h dark/12-h light cycle (light on between 7:00 and 19:00). Animals with implants for EEG/EMG recordings, optogenetic stimulation or calcium imaging were housed individually.

2.2.2 Surgical Procedures

Adult (6- to 12-week old) mice were anaesthetized with isoflurane (5% induction, 1.5% maintenance) and placed on a stereotaxic frame. Body temperature was kept stable throughout the procedure with a heating pad. After asepsis, the skin was incised to expose the skull, and the overlying connective tissue was removed. A craniotomy (0.5-1 mm diameter) was made for virus injection, optical fiber implantation, or GRIN lens implantation. The stereotaxic coordinates were as follows. DMH: anteroposterior (AP) -1.5 mm, mediolateral (ML) 0.3 mm, dorsoventral (DV) 4.8-5.0 mm; POA: AP 0 mm, ML 0.3 mm, DV 5.0-5.2 mm; RPA: AP -6 mm, ML 0 mm, DV 5.6-5.8 mm.

The following viral vectors were used in this study. AAV2-EF1α-DIO-ChR2–eYFP, AAV2-EF1α-DIO–eYFP (produced by University of North Carolina Vector Core), AAV1-Syn-DIO-GCaMP6f (University of Pennsylvania Vector Core, ~10^{12} vector genomes per milliliter; injection after 10× dilution), rAAV2-retro-EF1α-DIO-ChR2-eYFP, rAAV2-retro-EF1α-DIO-iC++-eYFP, rAAV2-retro-EF1α-DIO-GCaMP6s, rAAV2-retro-EF1α-mCherry, rAAV2-retro-EF1α-eYFP, AAV2-CAG-DIO-TVA-mCherry (10^{12} to 10^{13} vector genomes per milliliter; AAV preparation followed previously reported protocol (Maheshri et al., 2006; Zhang et al., 2016)) and RV-ΔG-eGFP+EnvA (10^{8} to 10^{9} vector genomes per milliliter; preparation followed previously reported protocol (Osakada and Callaway, 2013; Zhang et al., 2016)). For injection, virus was loaded into a sharp micropipette mounted on a Nanoject II attached to a micromanipulator and slowly injected into the target area (for imaging, 500 nL unilateral, into DMH, POA or RPA; for optogenetic activation of DMH galaninergic neurons or their axons, 500 nL/hemisphere, bilateral, into the DMH; for optogenetic manipulation of POA-projecting neurons, 500 nL/hemisphere, bilateral, into the POA; for optogenetic manipulations of RPA-projecting neurons, 600 nL into the RPA). To trace the axon collaterals of subgroups of DMH galaninergic neurons projecting to either the POA or the RPA, AAV2-CAG-DIO-TVA-mCherry was first injected into the DMH (500 nL, unilateral) of GAL-Cre mice. Three weeks later, RV-ΔG-eGFP+EnvA (500 nL) was injected into the POA or RPA of these mice.

For EEG and EMG recordings, a reference screw was inserted into the skull on top of the cerebellum. Two stainless steel screws were inserted into the skull 1.5 mm from midline and 1.5 mm anterior to the bregma, and two others were inserted 3 mm from the midline and 3.5 mm

posterior to the bregma. One EMG electrode was inserted into the neck musculature. Insulated leads from the EEG and EMG electrodes were soldered to a pin header, which was secured to the skull using dental cement.

For calcium imaging, mice were implanted with a GRIN lens (600 μm diameter, 7.3 mm long, Inscopix). A 600 μm diameter optical fiber (Thorlabs) with sharpened tip was inserted into a polyimide tube (625 μm diameter, cut to 7.3 mm, Vention) and implanted to 200 μm above the target brain area. The polyimide tube was then secured to the skull using dental cement, and the optical fiber was retracted. The GRIN lens was then inserted through the polyimide tube into the target area. A heat-shrinkable tube with paper tape above was used as protective cap to cover the GRIN lens. After > 3 weeks, the tape was removed to expose the GRIN lens and a miniaturized, single-photon, fluorescence microscope (Inscopix) was lowered over the implanted GRIN lens until the GCaMP6 fluorescence was visible under illumination with the microscope's LED. The microscope's baseplate was then secured to the skull with dental cement darkened with carbon powder for subsequent attachment of the microscope to the head. After recovery from surgery, I did not observe any gross behavioral abnormality, and these mice exhibited normal sleep–wake cycles. After surgery, mice were allowed to recover for at least 2 weeks before experiments.

For optogenetic manipulations, mice were implanted bilaterally with optical fibers. After surgery, mice were allowed to recover for at least 2 weeks before experiments.

2.2.3 Polysomnographic Recordings

EEG and EMG electrodes were connected to flexible recording cables via a mini-connector, and recordings were made in the animal's home cage placed in a sound-attenuated box. Recordings started after at least 1 h of habituation. All signals were acquired using TDT RZ5 amplifier (bandpass filter, 1–750 Hz; sampling rate, 1,500 Hz). I used the difference between the voltage potentials recorded from the EEG electrode and the reference electrode as EEG signal and the difference between the potentials from the EMG electrode and reference electrode as EMG signal.

Spectral analysis was carried out using fast Fourier transform, and NREM, REM and wake states were semi-automatically classified using a custom-written sleep analysis software (MATLAB, Mathworks) for each 5 s epoch (wake: desynchronized EEG and high EMG activity; NREM sleep: synchronized EEG with high power at 0.5–4 Hz and low EMG activity; REM sleep: desynchronized EEG with high power at theta frequencies (6–9 Hz) and low EMG activity).

2.2.4 Optogenetic Manipulations

I performed optogenetic manipulation experiments 4 to 6 weeks after injection of AAV expressing ChR2. Recordings took place during the light cycle (10:00 to 19:00) in the mouse's home cage placed within a sound-attenuating chamber. For optogenetic manipulations of DMH neurons, each trial consists of a 20 Hz pulse train lasting for 120 s (for optogenetic activation) or constant light lasting for 60 s (for optogenetic inhibition) using a blue 473-nm laser (6 mW at fiber tip, Shanghai Laser). The inter-trial interval was randomly distributed, from 5 to 30 minutes, controlled by the TDT system.

2.2.5 Transition Analysis

To quantify transition probabilities between brain states, I discretized time into 20 s bins and aligned all laser stimulation trials from all *N* mice by the onset of laser stimulation at time 0. To determine the transition probability from state *X* to *Y* for time bin *i*, $P_i(X, Y)$, I first determined the number of trials (*n*) in which the animal was in brain state *X* during the preceding time bin *i-1*. Next, I identified the subset of these trials (*m*) in which the animal transitioned into state *Y* in the current time bin *i*. The transition probability $P_i(Y|X)$ was computed as *m/n*. In Fig. 1d, each bar represents the transition probability averaged across three consecutive bins. To compute the baseline transition probabilities, I averaged across all time bins excluding the laser stimulation period and the 2 min period following laser stimulation.

2.2.6 Calcium Imaging

Imaging sessions took place during the light cycle in the home cage placed within a sound-attenuated chamber. The animal was briefly anesthetized with isoflurane to secure the microscope to the baseplate and to focus it to a given field of view. The animal was then allowed to recover from anesthesia and habituate in their home cage for at least 30 minutes prior to imaging. Calcium activity was acquired using the nVista hardware and nVista HD software (Inscopix), with a 5 Hz image acquisition rate using 0.2-0.7 mW illumination. EEG and EMG were acquired using TDT system-3 controlled by OpenEx software (TDT) (see above). An output signal (5 Hz) delivered from the Inscopix system to the TDT system throughout the recording session was used to synchronize the timing between the imaging and EEG/EMG recordings. Each recording session lasted 30-120 min, and for each mouse the data from a single recording session was included.

2.2.7 Calcium Imaging Analysis

Imaging data were processed in Mosaic (Inscopix) and MATLAB (Mathworks). First, the acquired images were spatially downsampled by a factor of 4. To correct for lateral motion of the brain relative to the GRIN lens, I used the motion correction function in Mosaic, as in previous studies (Mukamel et al., 2009; Resendez et al., 2016). Regions of interest (ROIs) were then identified using an established algorithm based on principal and independent component analyses (PCA-ICA) followed by visual inspection (Mukamel et al., 2009; Resendez et al., 2016). The pixel intensities within each ROI were averaged to create a fluorescence time-series. For individual neurons, the Z-score was calculated as the difference between the calcium activity at each bin and the averaged calcium activity of the whole recording time, divided by the standard deviation of the whole recording time.

Activity map was computed as follows:

$$m_{x,y} = \langle \langle (f_{x,y}(t) - f_{x,y}) / (f_{x,y} + f) \rangle_w^3 \rangle_t$$

Where $m_{x,y}$ is the activity at pixel (*x*,*y*), brackets indicate averaging, $f_{x,y}(t)$ is the fluorescence value at frame *t*, $f_{x,y}$ is the average of $f_{x,y}(t)$ over time, *f* is the average of $f_{x,y}$ over *w*, and *w* is a sliding window of 2 x 2 pixels (~ 5 x 5 μm)(Pinto and Dan, 2015).

2.2.8 Histology and Immunohistochemistry

Mice were deeply anesthetized and transcardially perfused with 0.1M PBS followed by 4% paraformaldehyde in PBS. After removal, brains stayed overnight in 4% paraformaldehyde. For cryoprotection, brains were stored in 30% sucrose (w/v) in PBS solution for at least one night. Brains were sliced in 50 μm coronal sections using a cryostat (Thermo Scientific). For immunohistochemistry, non-specific binding sites were blocked by incubating the brain sections in 10% goat serum (Millipore) in PBST (0.3% Triton X-100 in PBS). To amplify the fluorescence of axon fibers expressing eYFP or eGFP I applied antibodies for GFP (GFP-1020, Aves Labs, 1:1000). Brain sections were incubated with the primary antibody diluted in blocking solution for two nights. A species-specific secondary antibody conjugated with green Alexa fluorophore (1:1000; goat anti chicken) was diluted in PBS and applied for 2 hrs at room temperature. Fluorescence images were taken using 20×, 0.75 NA objective in a high-throughput slide scanner Nanozoomer 2.0 RS (Hamamatsu), a fluorescence microscope (Olympus BX53) or a confocal microscope (LSM 710, Zeiss).

2.2.9 Axon arborization analysis

Consecutive 50 μm coronal sections were collected and stained using Hoechst. Slides were scanned using a Nanozoomer (Hamamatsu). All images were acquired using identical settings and were analyzed using ImageJ and MATLAB as previously described (Chung et al., 2017). Images were background subtracted, thresholded, and pixels above this threshold were interpreted as positive signals. Pixels at the tissue borders with fluorescence artifact were excluded from the analysis. Each brain sample was aligned to the Allen Mouse Brain Atlas (Oh et al., 2014). The eGFP-labelled axon signal was quantified for each region and averaged across samples (Do et al., 2016; Zhang et al., 2016).

2.2.10 Statistics

For optogenetic experiments, GAL-Cre mice were randomly assigned to control (injected with AAV expressing eYFP) and experimental groups (injected with AAV expressing ChR2-eYFP or iC++-eYFP). For optogenetic, imaging, and rabies-mediated tracing experiments, GAL-Cre mice were randomly assigned to POA- or RPA- retrograde experiments. No randomization was used for calcium imaging (for both GAL-Cre and GAD2-Cre mice) and AAV anterograde tracing (GAL-Cre mice). Investigators were not blinded to animal identity and outcome assessment.

Statistical analysis was performed using MATLAB, R or Python. The selection of statistical tests was based on reported previous studies. All statistical tests were two-sided. The 95% confidence intervals for brain state probabilities were calculated using a bootstrap procedure: for an experimental group of n mice, with mouse i comprising mi trials, I repeatedly resampled the data by randomly drawing for each mouse mi trials (random sampling with replacement). For each of the 10,000 iterations, I recalculated the mean probabilities for each brain state across the n mice. The lower and upper confidence intervals were then extracted from the distribution of the resampled mean values. To test whether a given brain state was significantly modulated by laser stimulation, I calculated for each bootstrap iteration the difference between the mean probabilities

during laser stimulation and the baseline values without laser stimulation (identical duration to laser stimulation). From the resulting distribution of difference values, I then calculated a P value to assess whether laser stimulation significantly modulated brain states or transitions between brain states. The investigators were not blinded to allocation during experiments and outcome assessment.

2.3 Microendoscopic Calcium Imaging of DMH Neurons

To measure the activity of DMH galaninergic neurons across brain states, I used a galanin (GAL)-Cre mouse line (Gerfen et al., 2013), in which the specificity of GAL-Cre expression in the DMH has been validated previously by *in situ* hybridization (2011 Allen Institute for Cell Science. Allen Mouse Brain Connectivity Atlas. Available from http://connectivity.brain-map.org/transgenic/experiment/100138525). A Cre-inducible adeno-associated virus (AAV) expressing the calcium indicator GCaMP6f (Chen et al., 2013) was injected into the DMH, and imaging was performed through a gradient refractive index (GRIN) lens coupled to a miniaturized integrated fluorescence microscope in freely moving mice (Cox et al., 2016; Ghosh et al., 2011). During each imaging session, brain states were classified based on EEG and electromyogram (EMG) recordings (Figures 1A and 1B). Calcium activity of the galaninergic neurons varied strongly across brain states (Figure 1C). In particular, for each of the 36 imaged neurons the activity was significantly different between REM and NREM sleep ($p < 0.05$, Wilcoxon rank sum test). Some neurons were selectively activated during REM sleep ("REM-on" neurons), while others were selectively suppressed ("REM-off" neurons). These neurons were often observed in the same field of view (Figures 1B and 1C), and they appeared to be spatially intermingled (Figure 1E).

To quantify the relative activity of each neuron in different brain states, I plotted its REM-NREM modulation index ($Z_{REM} - Z_{NREM}$, where Z is Z-scored calcium activity averaged within each brain state) versus the wake-NREM modulation index ($Z_{wake} - Z_{NREM}$). The galaninergic neurons fell into two distinct clusters (Figure 1D, black dots). The REM-NREM modulation index exhibited a clear bimodal distribution ($P = 0.003$, Hartigan's dip test), with the two peaks corresponding to the REM-on and REM-off neurons. However, the wake-NREM modulation index showed a unimodal distribution centered around 0 ($P = 0.98$, Hartigan's dip test), indicating that the overall activity was similar during wakefulness and NREM sleep.

Interestingly, when I imaged the sleep-wake activity of DMH GABAergic neurons in GAD2-Cre mice, I found a much higher degree of functional heterogeneity, with different neurons preferentially active during wake, REM, or NREM states (Figure 1F and 1G). Both the REM-NREM and wake-NREM modulation indices showed unimodal distributions ($P = 0.60$ and 0.94, respectively, Hartigan's dip test), and the GABAergic neurons were scattered in all quadrants with no apparent clustering (Figure 1D, gray dots). This suggests that, as a subpopulation of DMH GABAergic neurons, the galaninergic neurons are especially involved in regulating REM and NREM sleep.

2.4 Axon Projections of DMH Galaninergic Neurons

Given the similar transmitter phenotypes of REM-on and REM-off DMH neurons (both are GABAergic and galaninergic), I wondered whether they can be distinguished based on their projection targets. Anterograde tracing of DMH galaninergic axons using Cre-inducible AAV expressing enhanced yellow fluorescent protein (eYFP) revealed projections to multiple brain regions, including the preoptic area (POA), lateral hypothalamus (LHA), dorsomedial region of the thalamus, periaqueductal gray (PAG), dorsolateral pons, and raphe pallidus (RPA) (Figures 2A and 2B). Such broad projections are consistent with previous findings in the rat (Aston-Jones et al., 2001; Chou et al., 2003).

To determine whether these divergent projections originate from different subsets of DMH neurons or reflect collateral projections from the same population, I selectively labeled the neurons projecting to each area. To target the POA-projecting population, which contains the largest number of DMH-galaninergic axons and was proposed to be important for sleep regulation (Chou et al., 2003), I injected AAV expressing avian-specific retroviral receptor (TVA) fused with mCherry (AAV2-CAG-DIO-TVA-mCherry) into the DMH of GAL-Cre mice. A glycoprotein (G)-deleted, EnvA-pseudotyped rabies virus (RV) expressing enhanced green fluorescent protein (RV-ΔG-eGFP+EnvA) was then injected into the POA to infect the TVA-expressing galaninergic neurons that project to the POA (Miyamichi et al., 2011; Zhang et al., 2016) (Figure 2C). Analysis of eGFP-labeled axons showed that, in addition to the POA, these DMH neurons also project to the LHA and thalamus (Figures 2D and 2G). However, in the RPA region I found no labeled axon. Conversely, when I performed the complementary experiments to label the RPA-projecting DMH neurons by injecting RV-ΔG-eGFP+EnvA into the RPA (Figure 2E), I found few eGFP-labeled axons in the POA (Figures 2F and 2H), suggesting that the POA and RPA projections originate from different neurons.

To test directly the relationship between the DMH neurons projecting to the POA and RPA, I performed simultaneous retrograde tracing from the two target areas. After injecting Cre-inducible rAAV2-retro (a designer AAV variant with high retrograde efficiency) (Tervo et al., 2016) expressing eGFP and mCherry into the POA and RPA, respectively (Figure 2I), I found strong expression of both eGFP and mCherry in the DMH but very little overlap between them (Figures 2J and 2K). This indicates that the POA- and RPA-projecting DMH galaninergic neurons form largely distinct subpopulations.

2.5 Activity of POA- and RPA-Projecting Neurons

I next measured the sleep-wake activity of the POA- or RPA-projecting subpopulation using calcium imaging. Cre-inducible rAAV2-retro expressing GCaMP6s was injected into the POA or RPA of GAL-Cre mice, and a GRIN lens was implanted into the DMH (Figures 3A and 3B, 3E and 3F). Both subpopulations of DMH galaninergic neurons showed brain-state-dependent calcium activity. The POA-projecting neurons were selectively suppressed during REM sleep (Figures 3C and 3D), with all 28 cells showing lower activity during REM than NREM sleep ($P < 0.001$; Wilcoxon rank sum test), and 26/28 cells showing lower activity during REM sleep than wakefulness ($P < 0.05$). In contrast, most of the RPA-projecting neurons were selectively activated during REM sleep (Figures 3G and 3H; 52/55 showed higher activity during REM sleep than both NREM sleep and wakefulness, $P < 0.05$, Wilcoxon rank sum test). For both the POA- and RPA-projecting subpopulations, the wake-NREM modulation index showed unimodal distributions around 0. Thus, the two galaninergic subpopulations defined by their projection targets largely segregate into the REM-on and REM-off functional categories.

2.6 POA-Projecting Neurons Suppress REM and Promote NREM Sleep

To test whether each subpopulation of DMH neurons play any causal role in sleep regulation, I manipulated their activity optogenetically. To express channelrhodopsin 2 (ChR2) in the POA-projecting neurons, I injected Cre-inducible rAAV2-retro-ChR2-eYFP into the POA of GAL-Cre mice and implanted an optic fiber into the DMH (Figure 4A). Laser stimulation (20 Hz, 2 min/trial, randomly applied every 5–30 min) caused a significant decrease in REM sleep ($P < 0.001$, bootstrap) and a complementary increase in NREM sleep ($P < 0.001$), with no significant change in wakefulness ($P = 0.18$; Figures 4B and 4C). To distinguish whether the laser-induced suppression of REM sleep was due to a decrease in its initiation or maintenance, I analyzed the transition probability between each pair of brain states (Figure 4I). Laser activation of the POA-projecting neurons caused marked decreases in NREM→REM and REM→REM transitions ($P < 0.05$, bootstrap), indicating a suppression of both the initiation and maintenance of REM sleep (Figure 4D).

Since the rAAV2-retro-DIO-ChR2-eYFP injected into the POA can also infect POA-projecting neurons outside of the DMH, in principle the effect of laser stimulation in the DMH could be mediated by the axons of these non-DMH neurons that pass through the DMH. I thus tested the effect of activating DMH neuron axons in the POA. Following the injection of AAV2-EF1α-DIO-ChR2-eYFP into the DMH of GAL-Cre mice, which labels only the DMH neurons, laser stimulation of their axons in the POA also suppressed REM sleep ($P < 0.001$) and promoted NREM sleep ($P = 0.013$; Figures 5A-5C). This further indicates that the POA projection of DMH galaninergic neurons is REM suppressing.

I next tested the effect of inactivating the POA-projecting DMH galaninergic neurons. To express the inhibitory opsin iC++ in these neurons (Berndt et al., 2016), I injected Cre-inducible rAAV2-retro-EF1α-DIO-iC++-eYFP into the POA of GAL-Cre mice. Laser stimulation (constant light, 1 min/trial, randomly applied every 5–30 min) significantly increased REM sleep ($P < 0.001$) and decreased NREM sleep ($P < 0.05$; Figures 6A-6C). In control mice expressing eGFP without ChR2 or iC++, laser stimulation had no effect ($P > 0.7$; Figures 7A-7C), and the effects of laser stimulation were significantly different between ChR2 and eGFP mice ($P < 0.001$, bootstrap) and between iC++ and eGFP mice ($P < 0.001$).

2.7 RPA-Projecting Neurons Promote REM and Suppress NREM Sleep

Finally, I tested the effects of activating and inactivating the RPA-projecting DMH galaninergic neurons. After injecting Cre-inducible rAAV2-retro-ChR2-eYFP into the RPA of GAL-Cre mice, laser stimulation in the DMH strongly increased REM sleep ($P < 0.001$, bootstrap) and decreased NREM sleep ($P < 0.001$; Figures 4E-4G). These effects were caused by increases in both NREM→REM and REM→REM transitions (Figure 4H), indicating enhancement of both the initiation and maintenance of REM sleep. In contrast, iC++-mediated inactivation of these neurons caused decreased REM sleep ($P = 0.014$) and increased NREM sleep ($P = 0.029$; Figures 6D-6F). Laser had no effect in control mice expressing eGFP alone ($P > 0.5$; Figures 7D-7F), and the effects of laser stimulation were significantly different between ChR2 and eGFP mice ($P < 0.001$, bootstrap) and between iC++ and eGFP mice ($P = 0.038$). Furthermore, in GAL-Cre mice injected with AAV2-EF1α-DIO-ChR2-eYFP in their DMH, laser stimulation of the axons in the RPA increased REM sleep ($P < 0.001$, bootstrap) and suppressed NREM sleep ($P = 0.011$; Figures 5D-5F). Together, these results indicate that the RPA-projecting DMH galaninergic neurons are REM promoting.

2.8 Figures

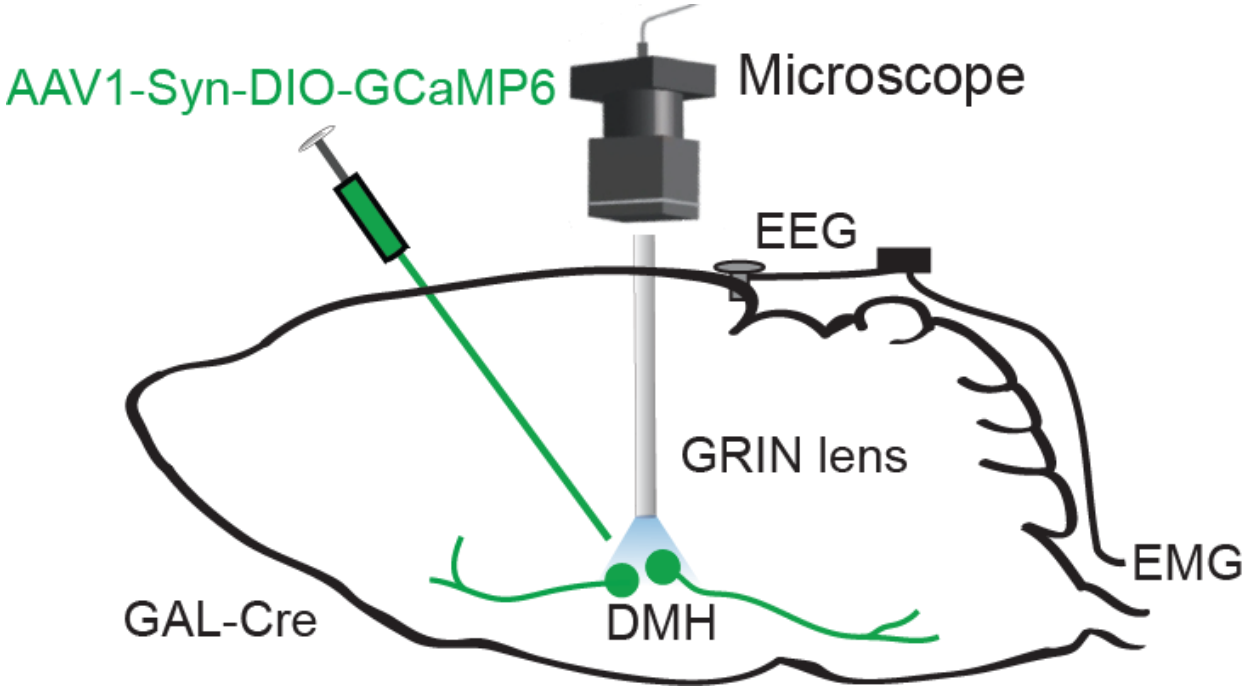

Figure 1A. Schematic of microendoscopic calcium imaging in the DMH

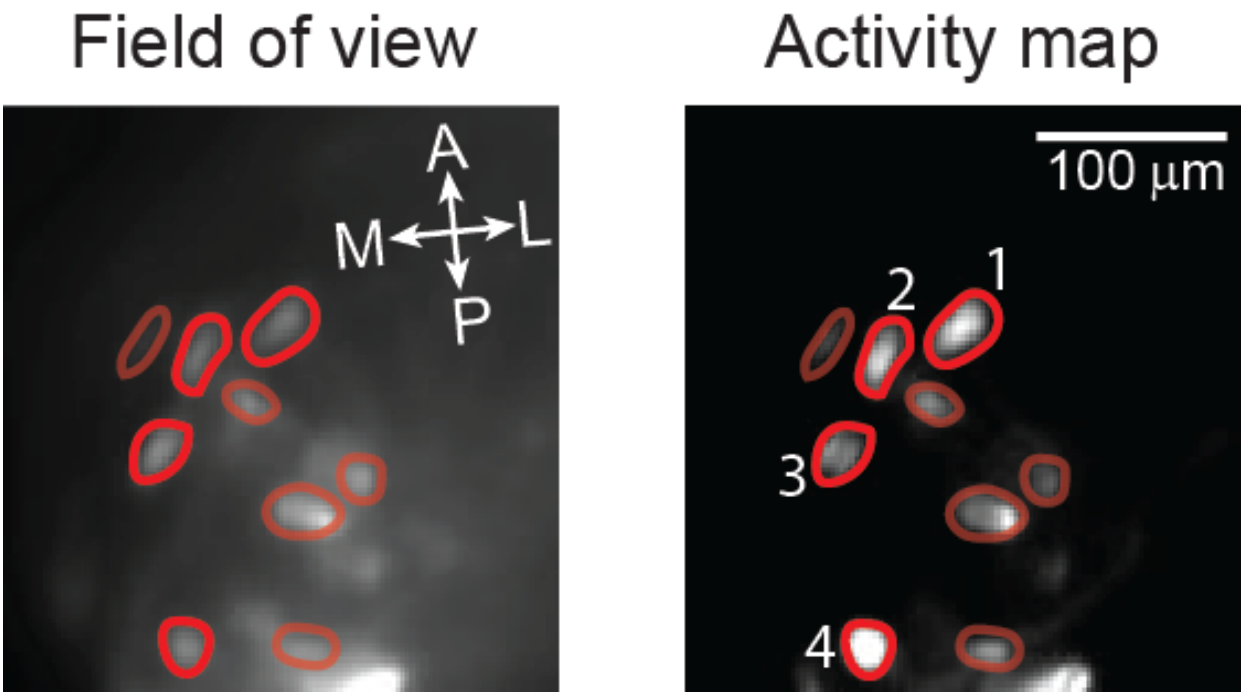

Figure 1B. Example image from DMH microendoscopic calcium imaging

Field of view (left) and activity map (right) of an example imaging session in a GAL-Cre mouse. M, medial; L, lateral; A, anterior; P, posterior. Regions of interest (ROIs) are outlined in red. Numbers indicate ROIs whose calcium traces are plotted in **Figure 1C**.

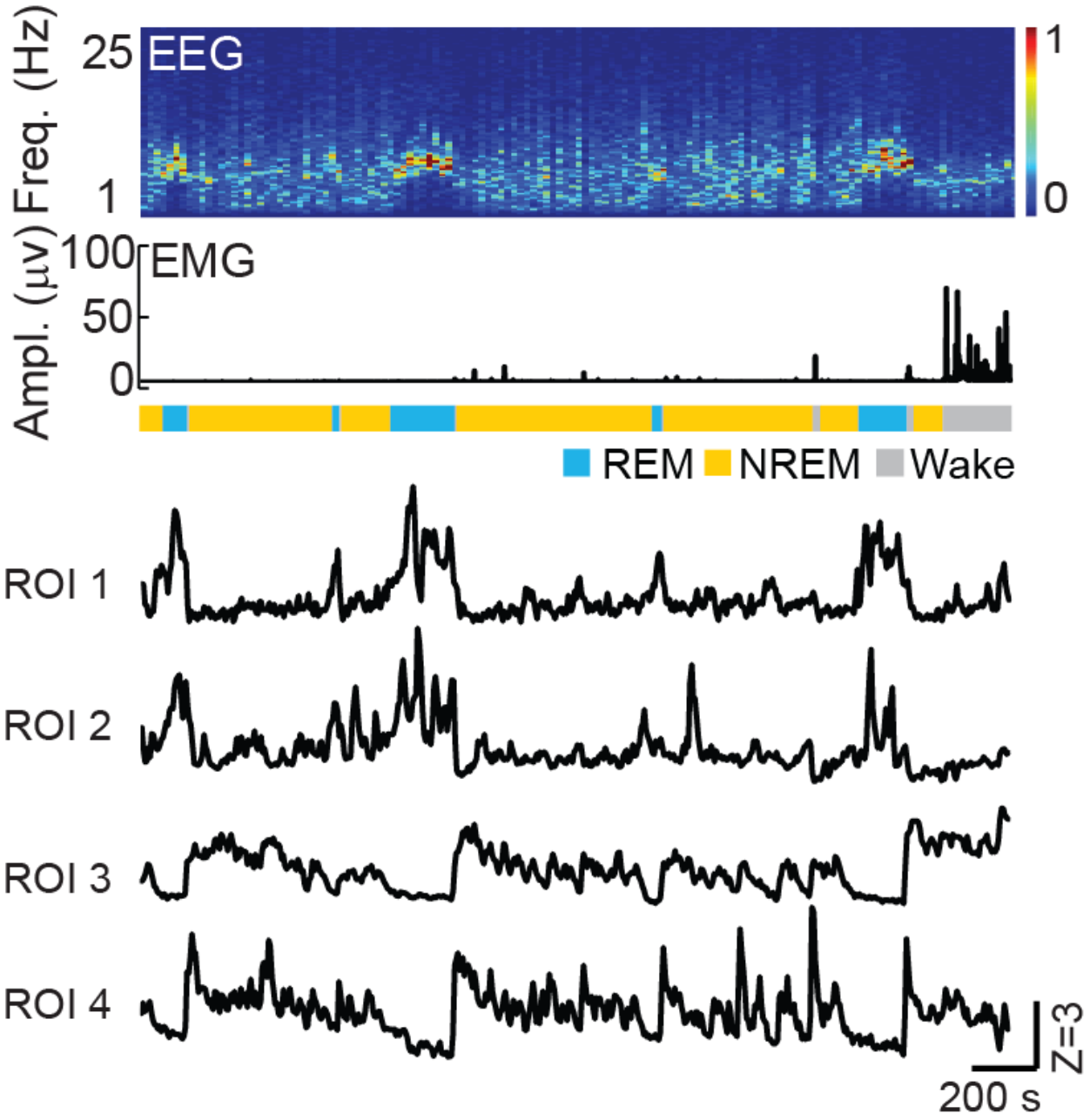

Figure 1C. Example traces from DMH microendoscopic calcium imaging

EEG power spectrogram, EMG trace, brain states (color coded), and calcium traces (Z scored) recorded in the imaging session.

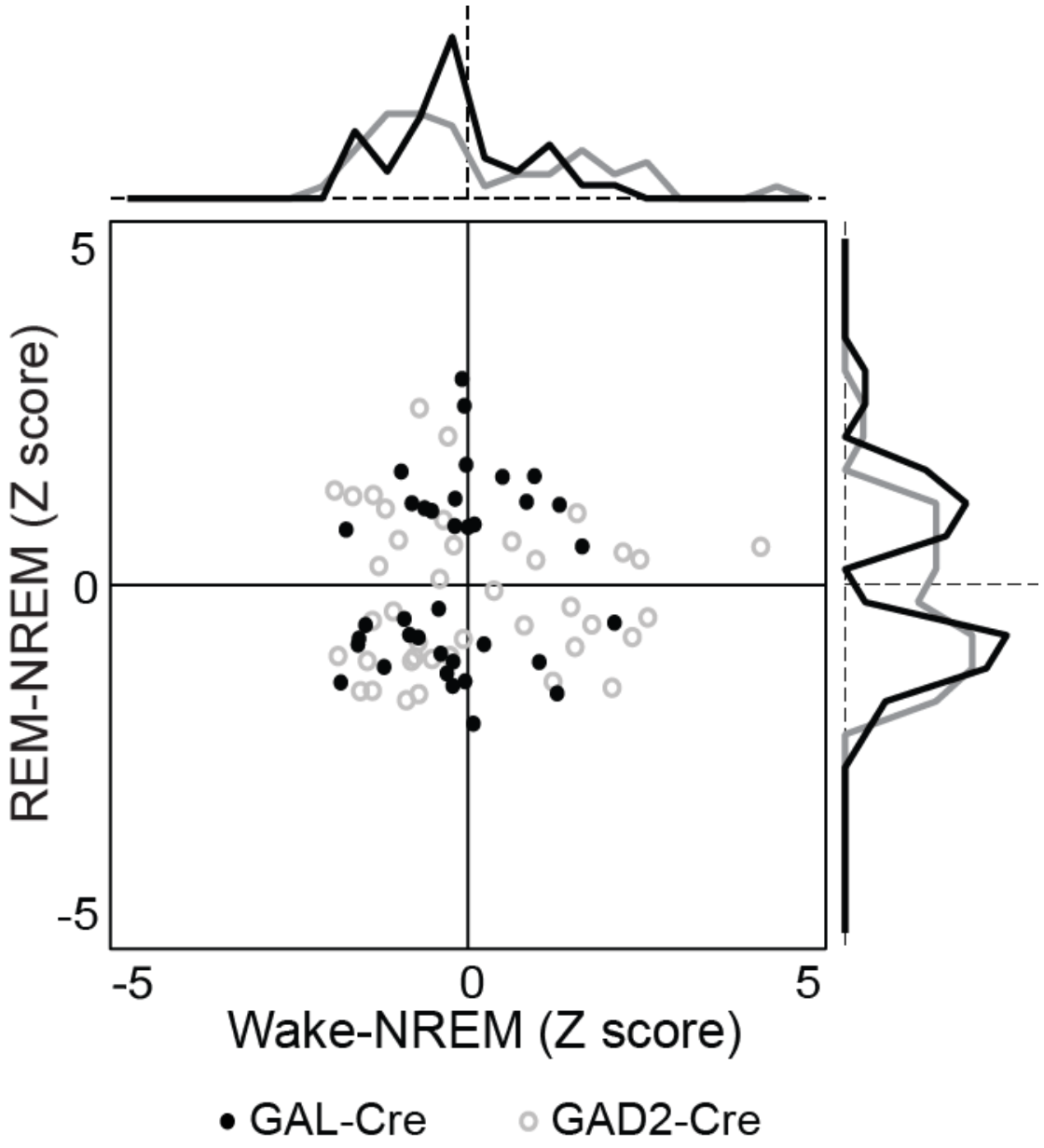

Figure 1D. Quantification of imaging data from DMH galaninergic and GABAergic neurons

REM-NREM activity difference versus wake-NREM activity difference. Each symbol represents one neuron. Black, galaninergic neurons from GAL-Cre mice (n = 36 neurons from 4 mice). Gray, GABAergic neurons from GAD2-Cre mice (n = 40 neurons from 3 mice). Traces on the top and right, distributions of wake-NREM (top) and REM-NREM (right) activity difference for galaninergic (black) and GABAergic (gray) neurons.

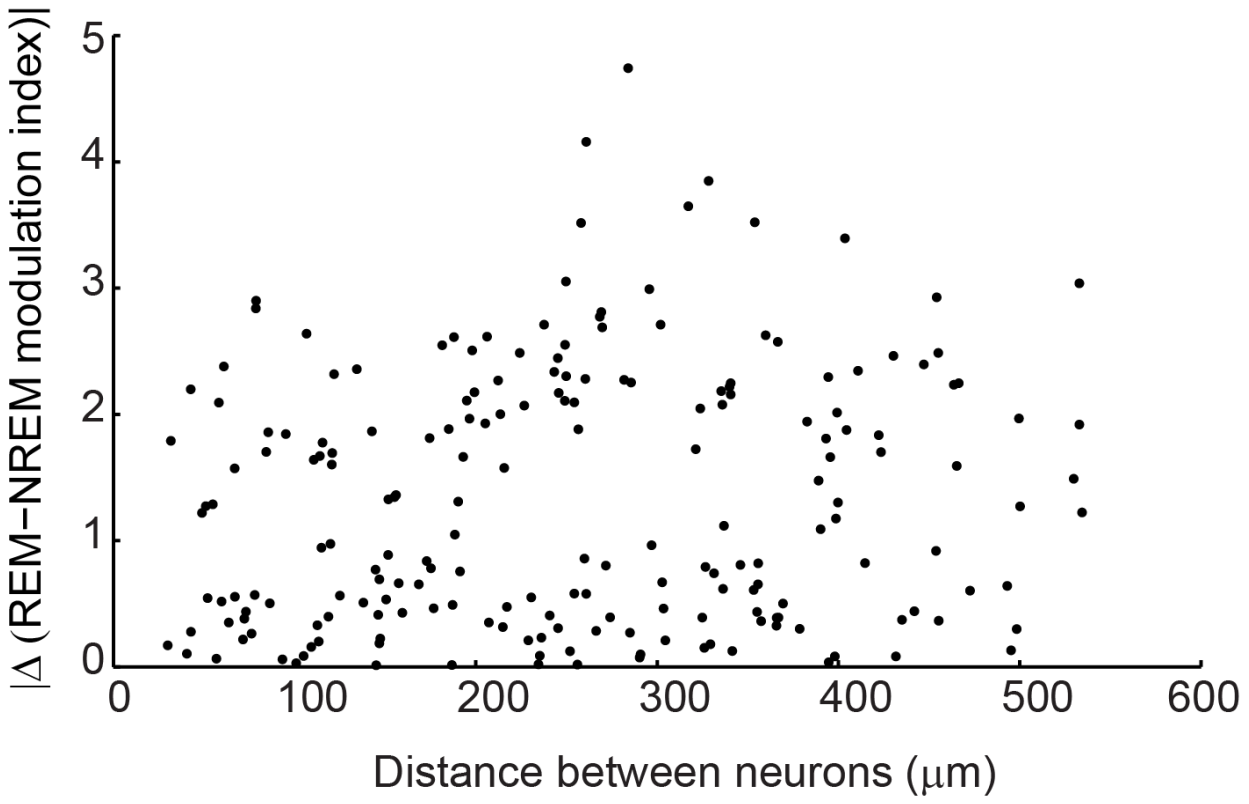

Figure 1E. Difference in REM-NREM modulation index is unrelated to distance between neurons

Each symbol represents one pair of neurons imaged in the same session (n = 201 pairs, from 4 mice). $R^2 = 0.02$.

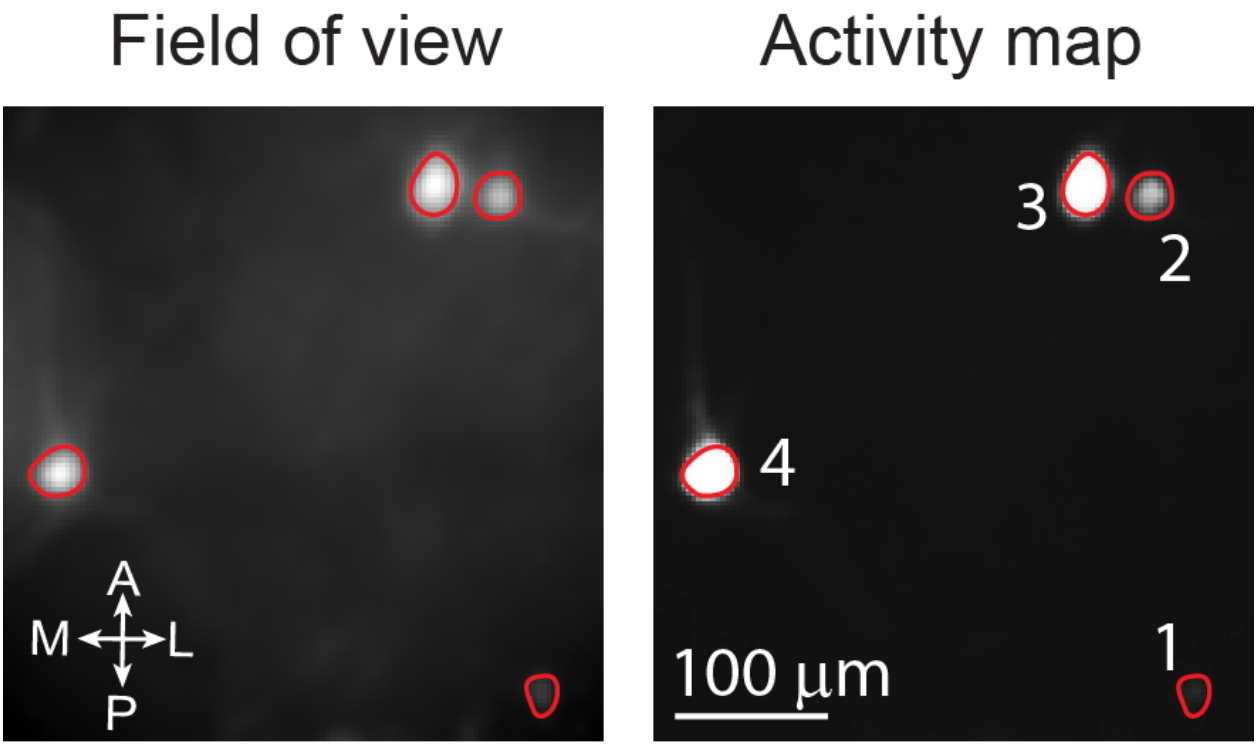

Figure 1F. Example imaging in a GAD2-Cre mouse

Field of view (left) and activity map (right). ROIs are outlined in red. Numbers indicate ROIs whose calcium traces are plotted in **Figure 1G**.

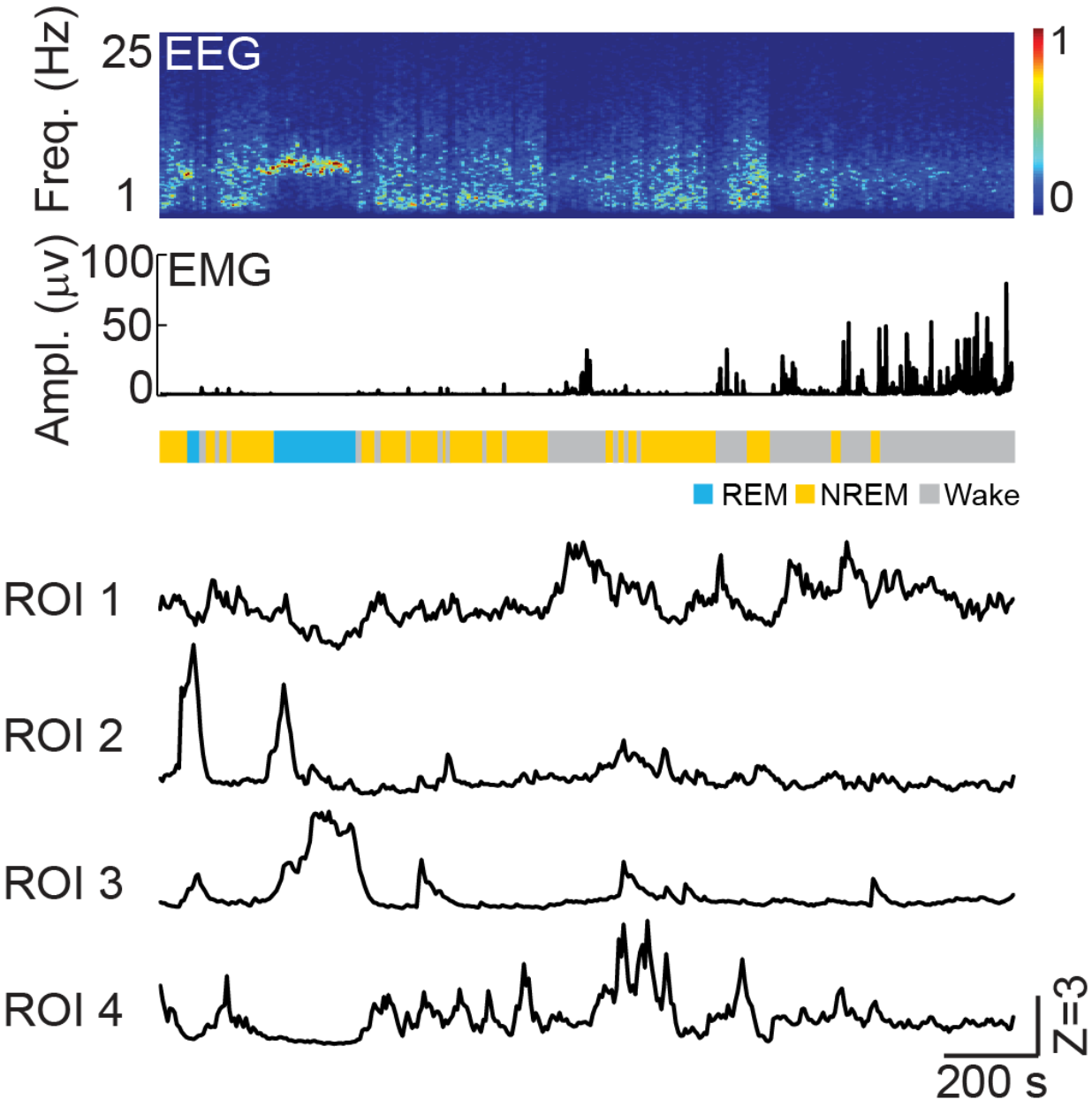

Figure 1G. Example imaging traces in a GAD2-Cre mouse

EEG power spectrogram, EMG trace, brain states (color coded), and calcium traces (Z scored).

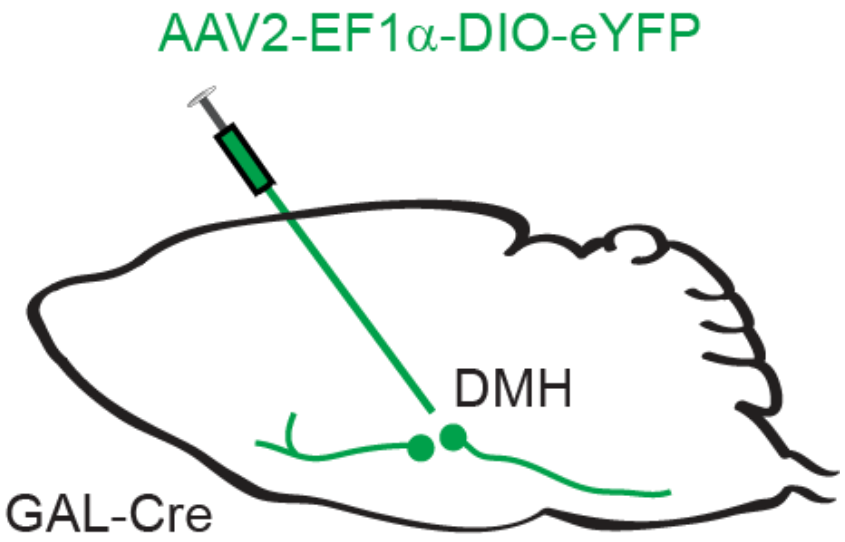

Figure 2A. Schematic of viral injection for anterograde tracing of DMH galaninergic projections

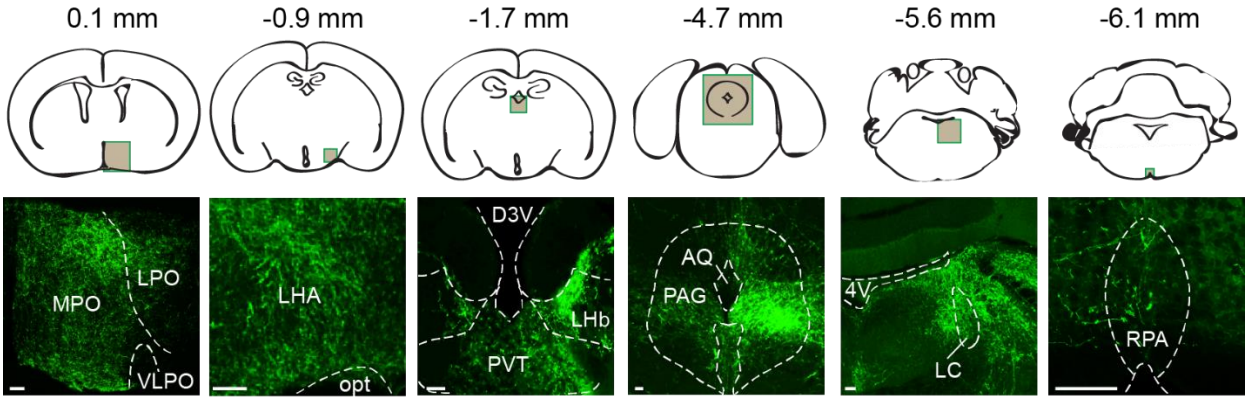

Figure 2B. Fluorescence images of six brain regions with projections from DMH galaninergic neurons (shaded boxes in coronal diagrams above)

POA, preoptic area. LHA, lateral hypothalamus. opt, optic track. LHb, lateral habenula. PVT, paraventricular nucleus of the thalamus. D3V, dorsal 3rd ventricle. PAG, periaqueductal gray. AQ, cerebral aqueduct. LC, locus coeruleus. 4V, 4th ventricle. RPA, raphe pallidus. Scale bar, 100 μm.

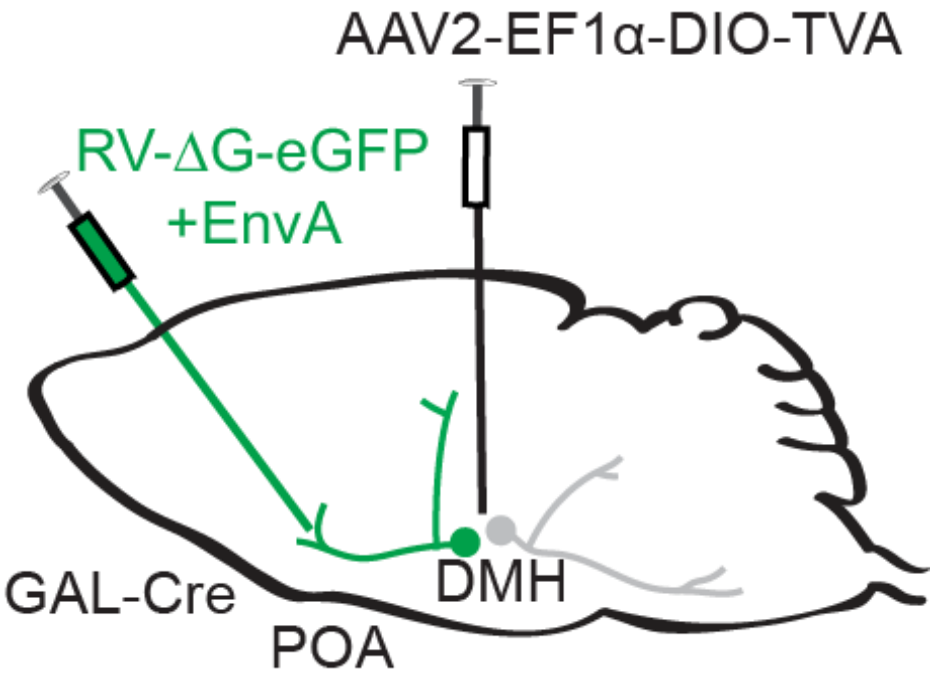

Figure 2C. Schematic of viral strategy for labeling axon collaterals of POA-projecting DMH galaninergic neurons

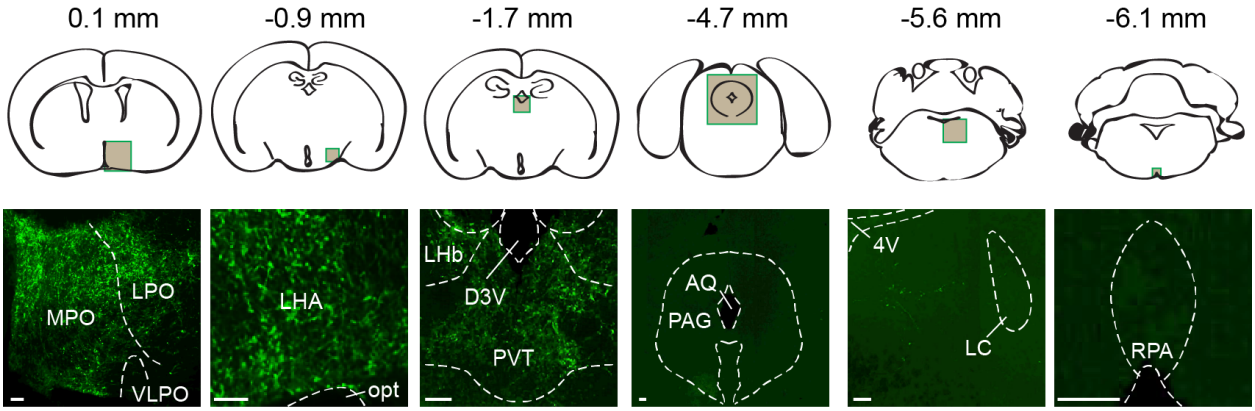

Figure 2D. Fluorescence images of six brain regions with projections from DMH POA-projecting galaninergic neurons (shaded boxes in coronal diagrams above)

POA, preoptic area. LHA, lateral hypothalamus. opt, optic track. LHb, lateral habenula. PVT, paraventricular nucleus of the thalamus. D3V, dorsal 3rd ventricle. PAG, periaqueductal gray. AQ, cerebral aqueduct. LC, locus coeruleus. 4V, 4th ventricle. RPA, raphe pallidus. Scale bar, 100 μm. *n* = 3 mice.

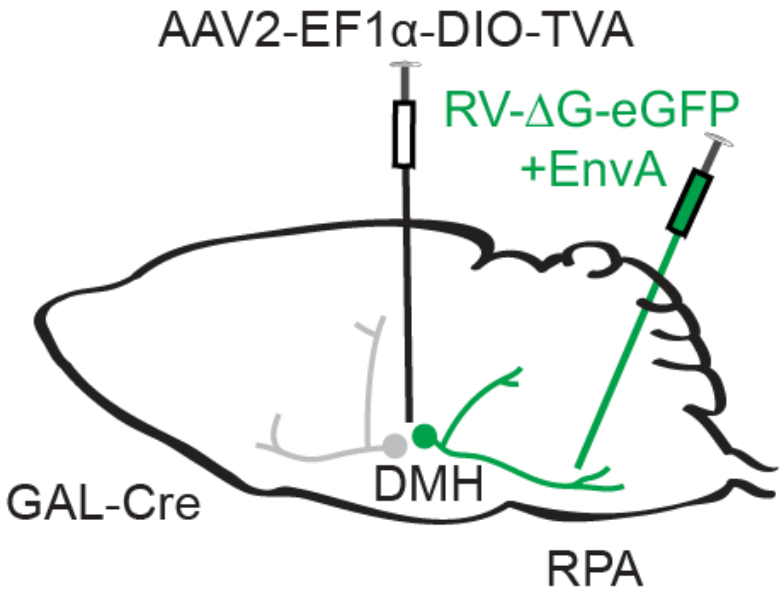

Figure 2E. Schematic of viral strategy for labeling axon collaterals of RPA-projecting DMH galaninergic neurons

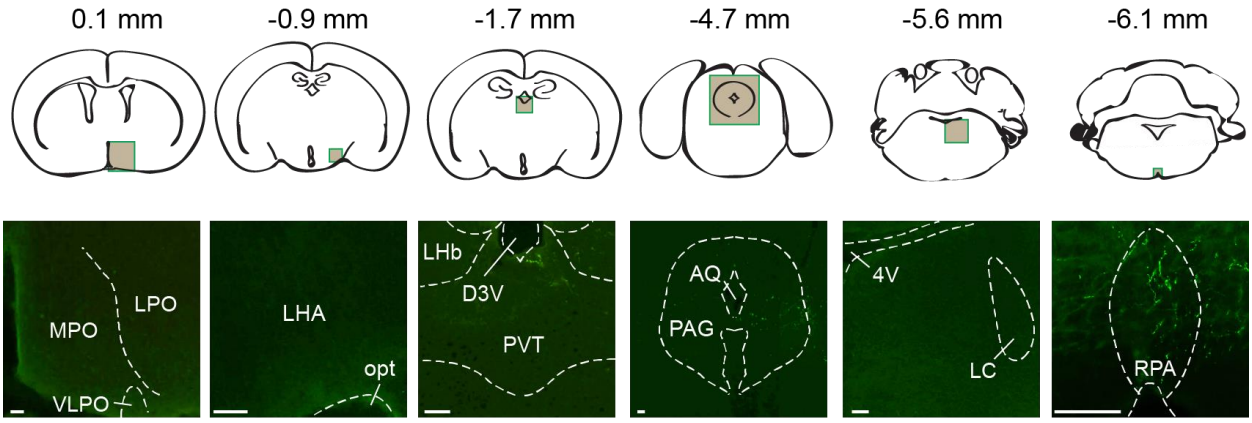

Figure 2F. Fluorescence images of six brain regions with projections from DMH RPA-projecting galaninergic neurons (shaded boxes in coronal diagrams above)

POA, preoptic area. LHA, lateral hypothalamus. opt, optic track. LHb, lateral habenula. PVT, paraventricular nucleus of the thalamus. D3V, dorsal 3rd ventricle. PAG, periaqueductal gray. AQ, cerebral aqueduct. LC, locus coeruleus. 4V, 4th ventricle. RPA, raphe pallidus. Scale bar, 100 μm. *n* = 3 mice.

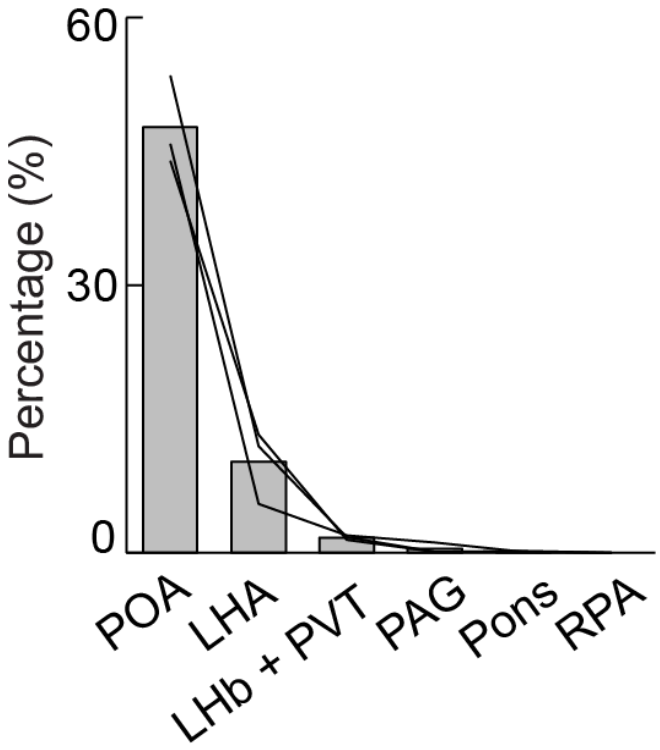

Figure 2G. Percentage of labeled axons in each area for POA-projecting DMH galaninergic neurons

Each line represents data from one mouse (*n* = 3 mice). Bar, average across mice.

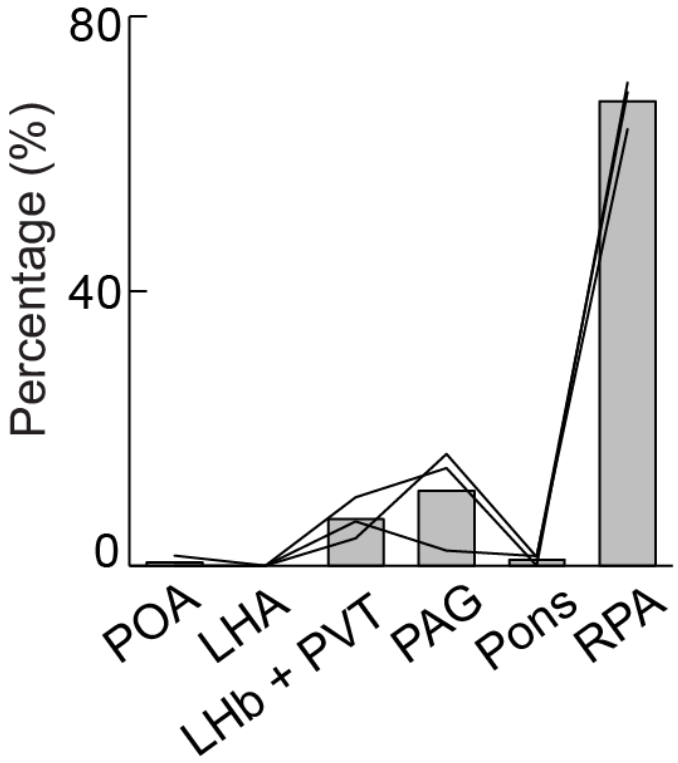

Figure 2H. Percentage of labeled axons in each area for RPA-projecting DMH galaninergic neurons

Each line represents data from one mouse (*n* = 3 mice). Bar, average across mice.

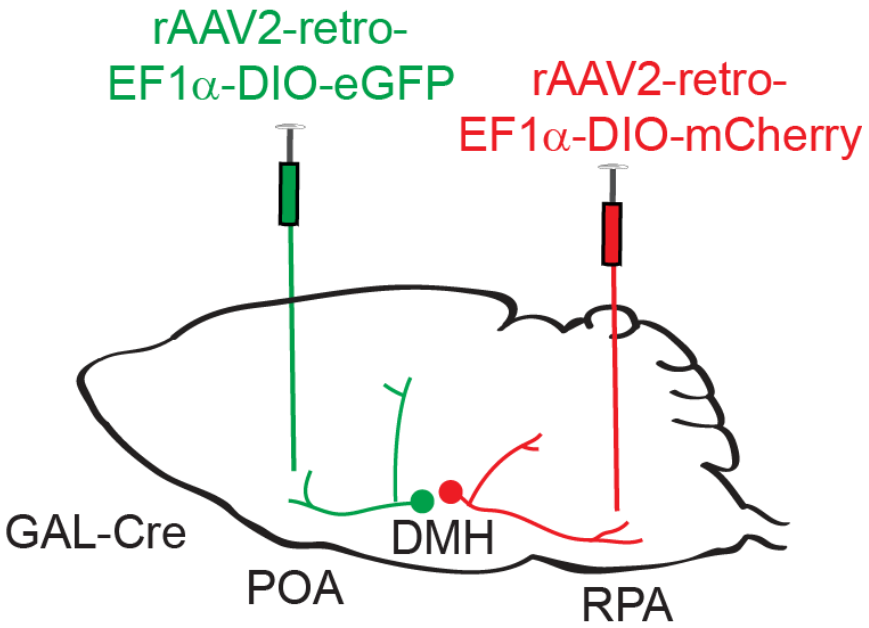

Figure 2I. Schematic of viral injection for simultaneous retrograde tracing from POA and RPA

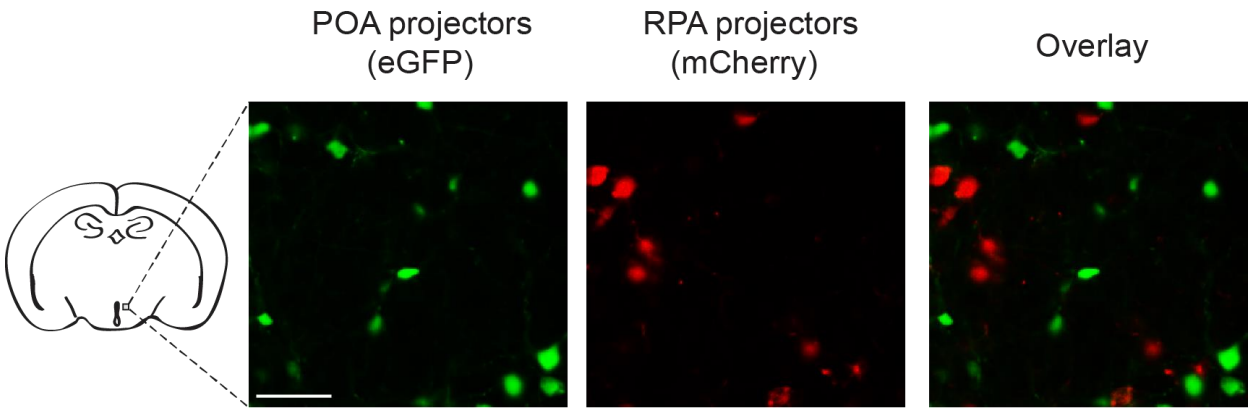

Figure 2J. Example images from the simultaneous retrograde tracing experiments

Fluorescence images of DMH showing neurons expressing eGFP and mCherry. Scale bar, 50 μm.

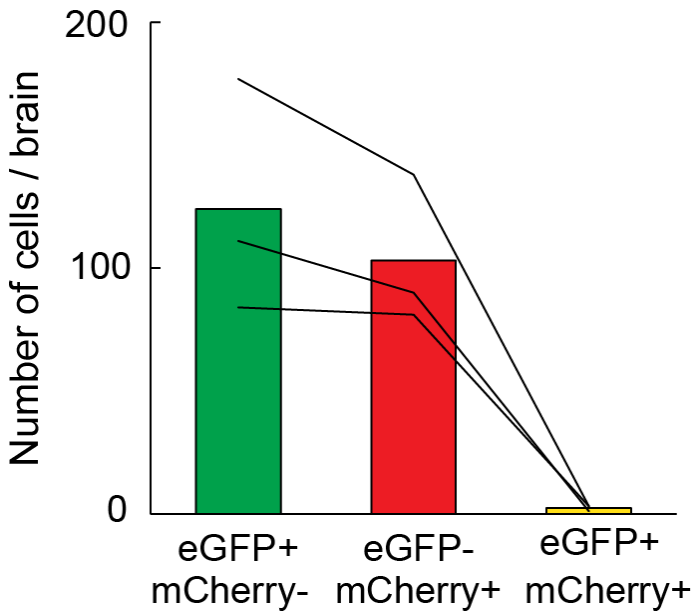

Figure 2K. Quantification of the simultaneous retrograde tracing data

Number of neurons expressing each marker alone or both. Each line represents data from one mouse (*n* = 3 mice).

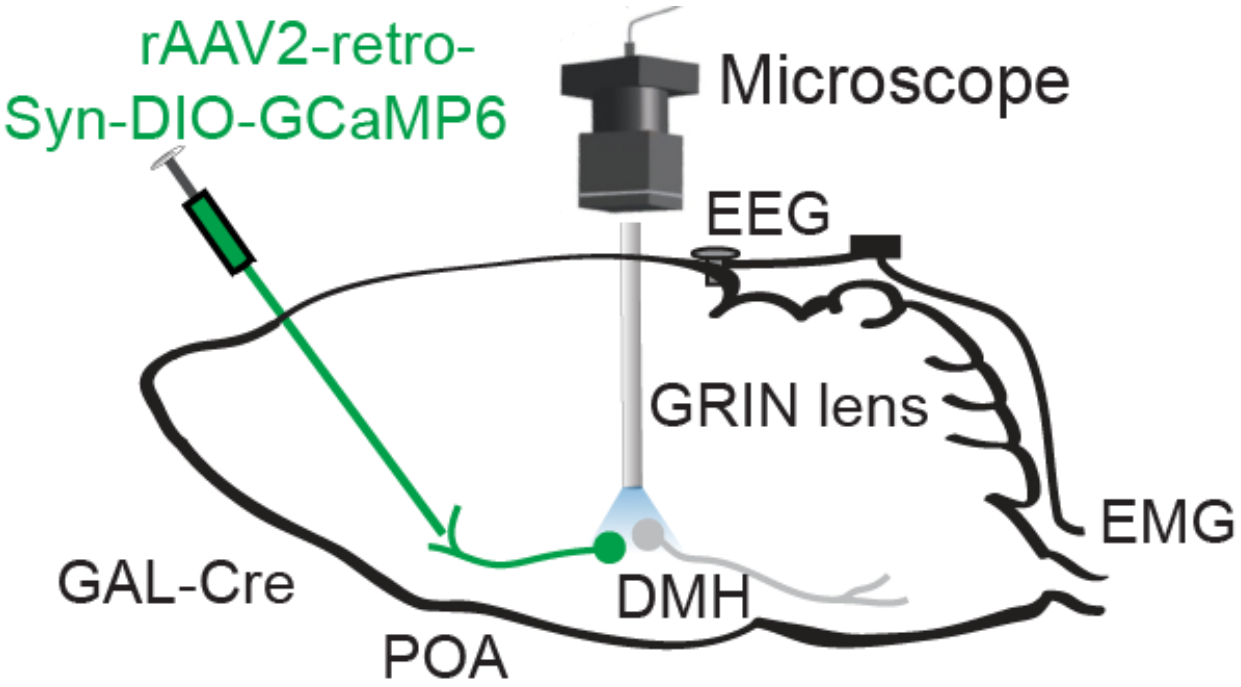

Figure 3A. Schematic of calcium imaging of POA-projecting DMH galaninergic neurons

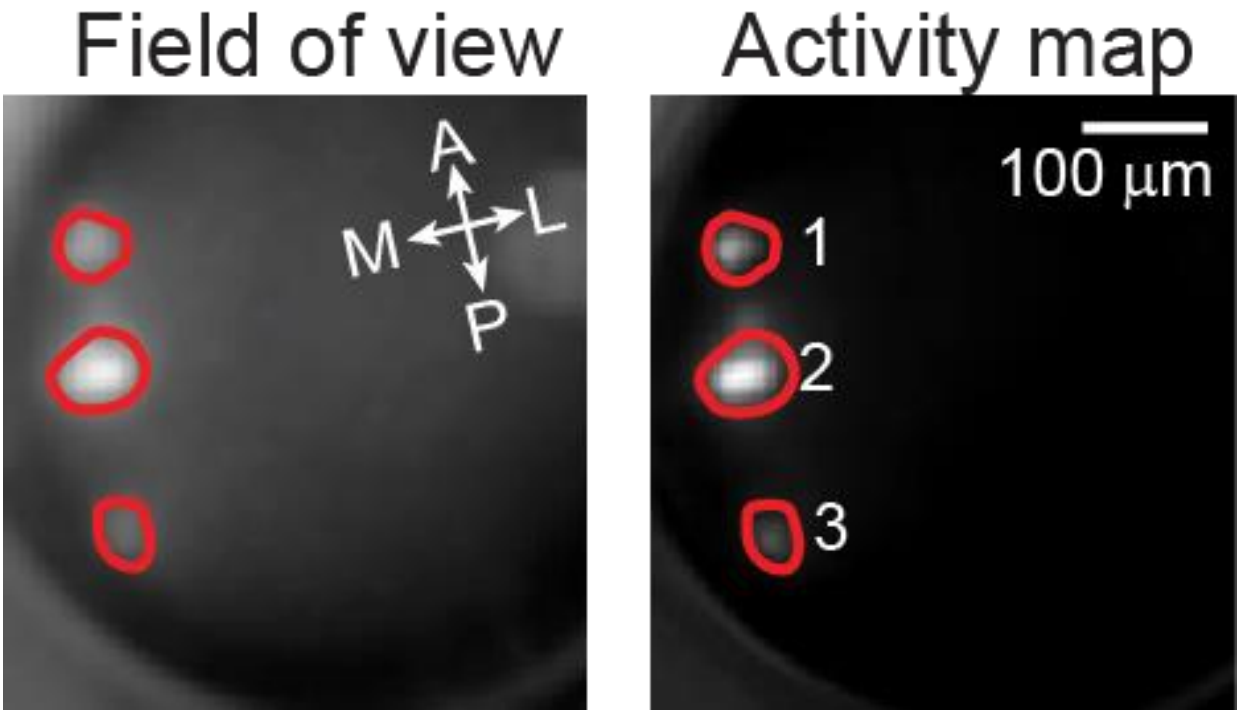

Figure 3B. Example image from microendoscopic calcium imaging of POA-projecting DMH galaninergic neurons

Field of view (left) and activity map (right) of an example imaging session. ROIs are outlined in red. Numbers indicate ROIs whose calcium traces are plotted in **Figure 3C**.

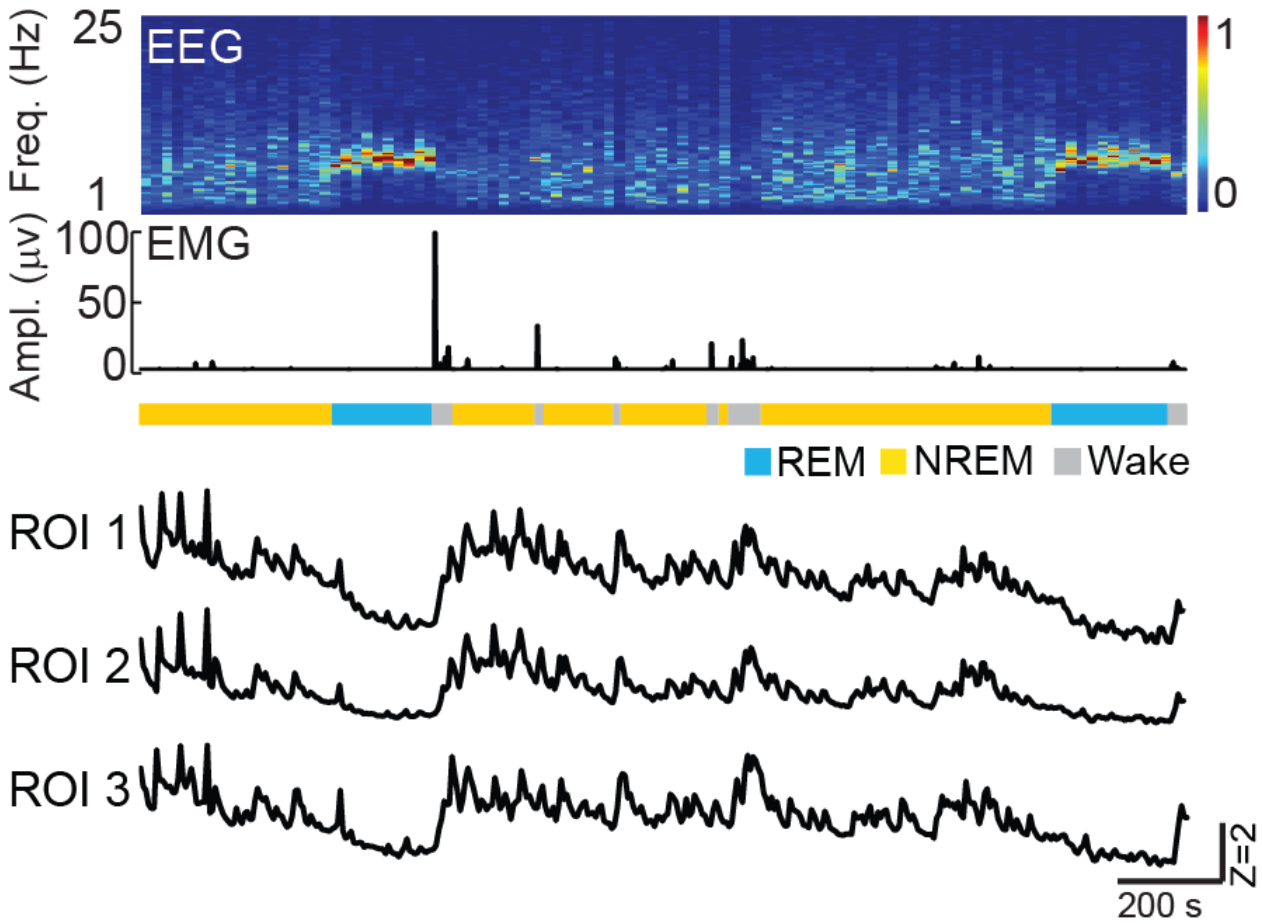

Figure 3C. Example traces from microendoscopic calcium imaging of POA-projecting DMH galaninergic neurons

EEG power spectrogram, EMG trace, brain states (color coded), and calcium traces (Z scored) recorded in the imaging session.

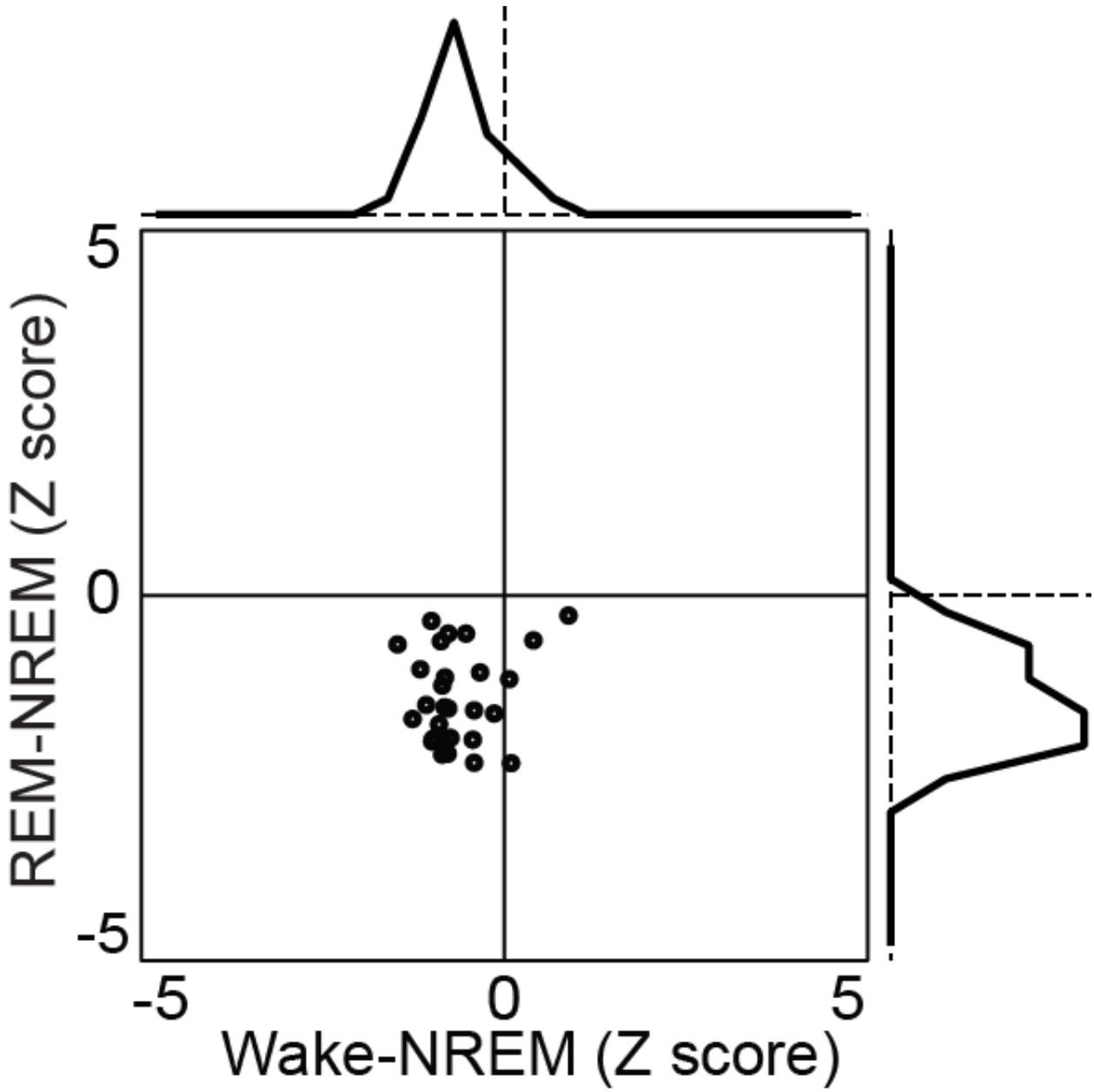

Figure 3D. Quantification of imaging data from POA-projecting DMH neurons

REM-NREM activity difference versus wake-NREM activity difference. Traces on the top and right: distributions of wake-NREM and REM-NREM activity differences for POA-projecting DMH galaninergic neurons (n = 28 cells from 3 mice).

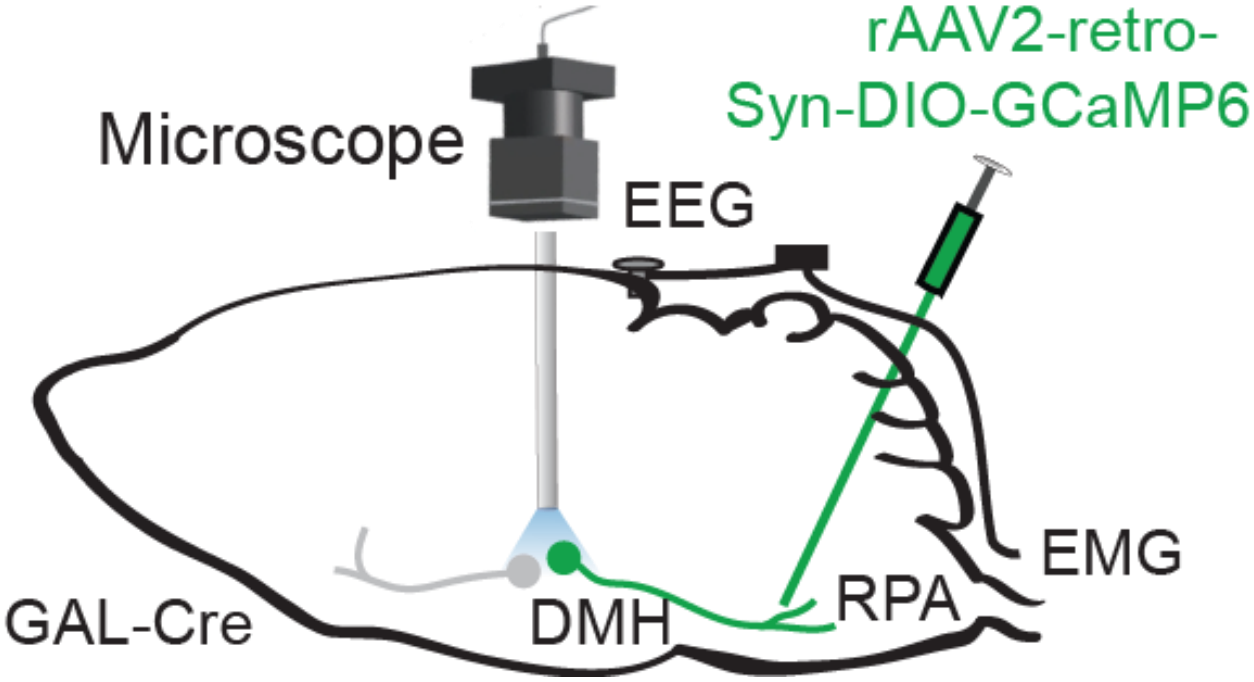

Figure 3E. Schematic of calcium imaging of RPA-projecting DMH galaninergic neurons

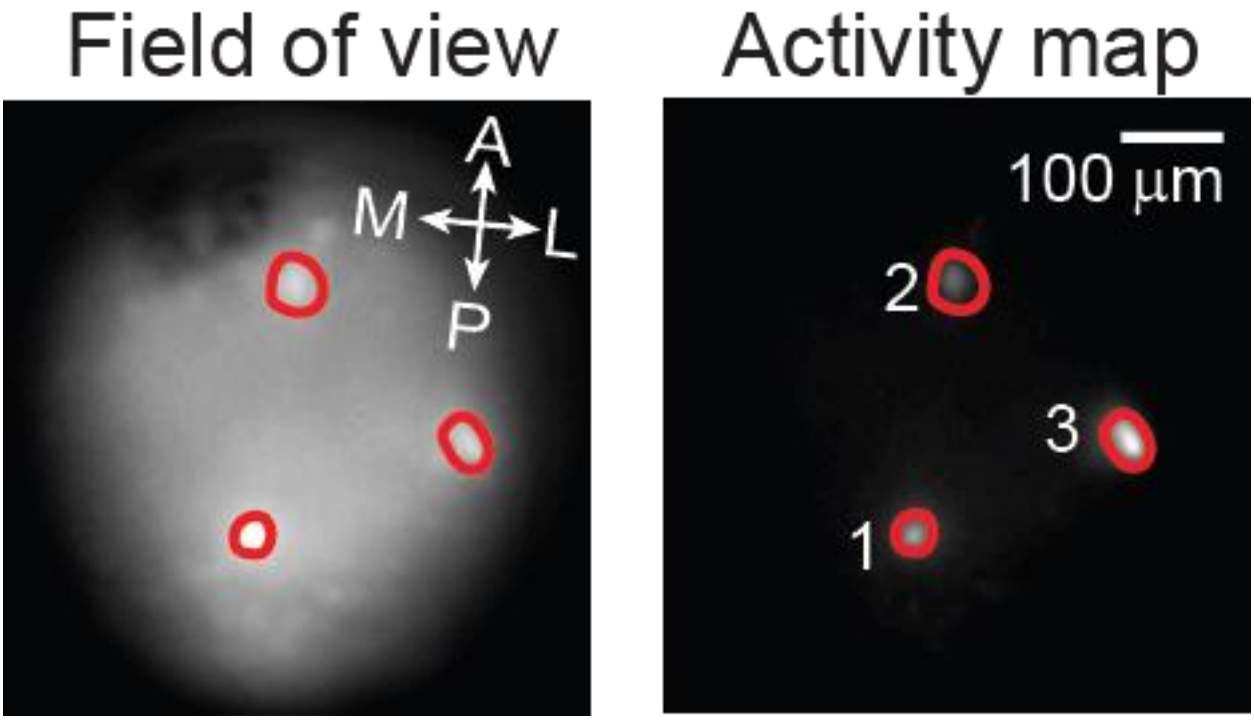

Figure 3F. Example image from microendoscopic calcium imaging of RPA-projecting DMH galaninergic neurons

Field of view (left) and activity map (right) of an example imaging session. ROIs are outlined in red. Numbers indicate ROIs whose calcium traces are plotted in **Figure 3G**.

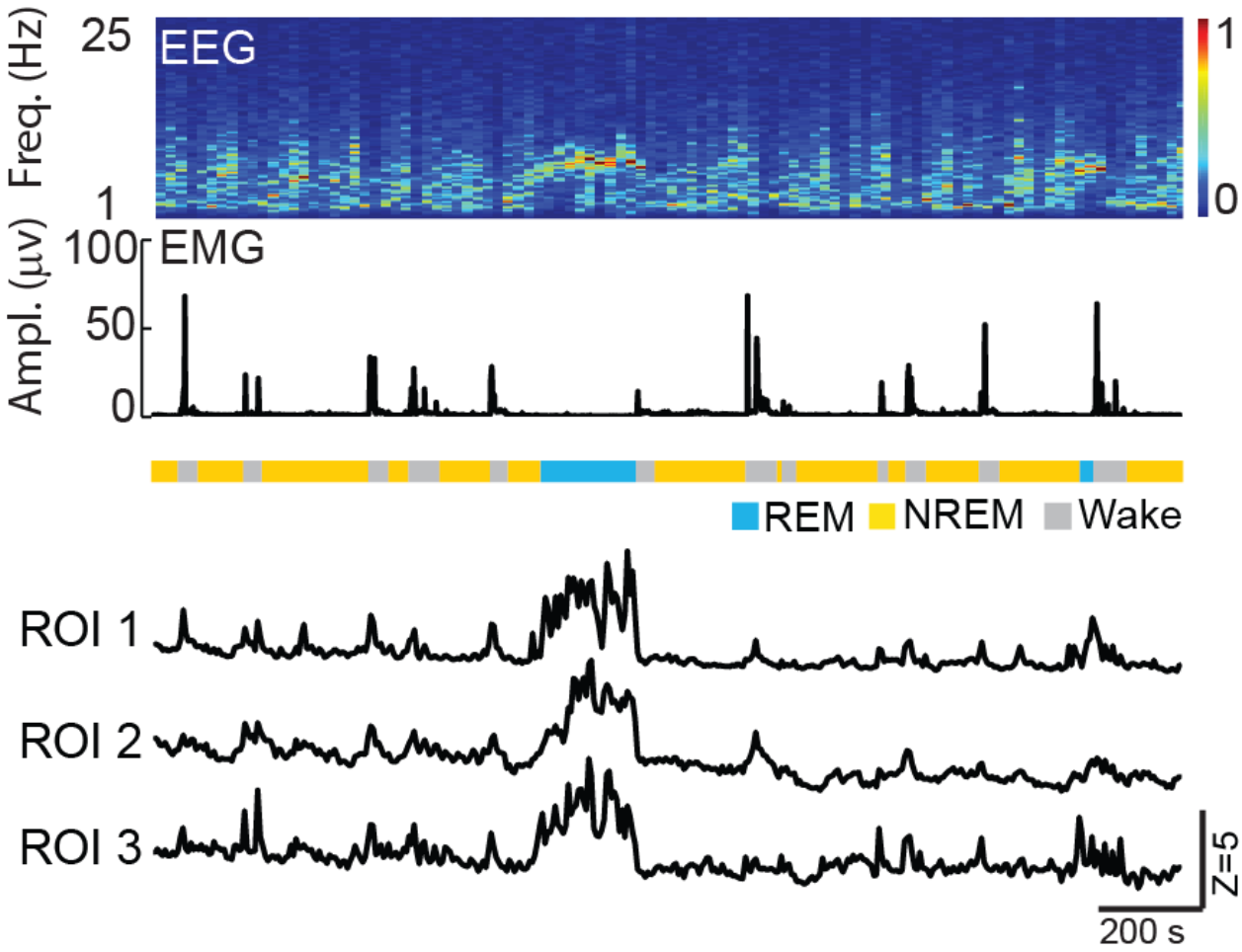

Figure 3G. Example traces from microendoscopic calcium imaging of RPA-projecting DMH galaninergic neurons

EEG power spectrogram, EMG trace, brain states (color coded), and calcium traces (Z scored) recorded in the imaging session.

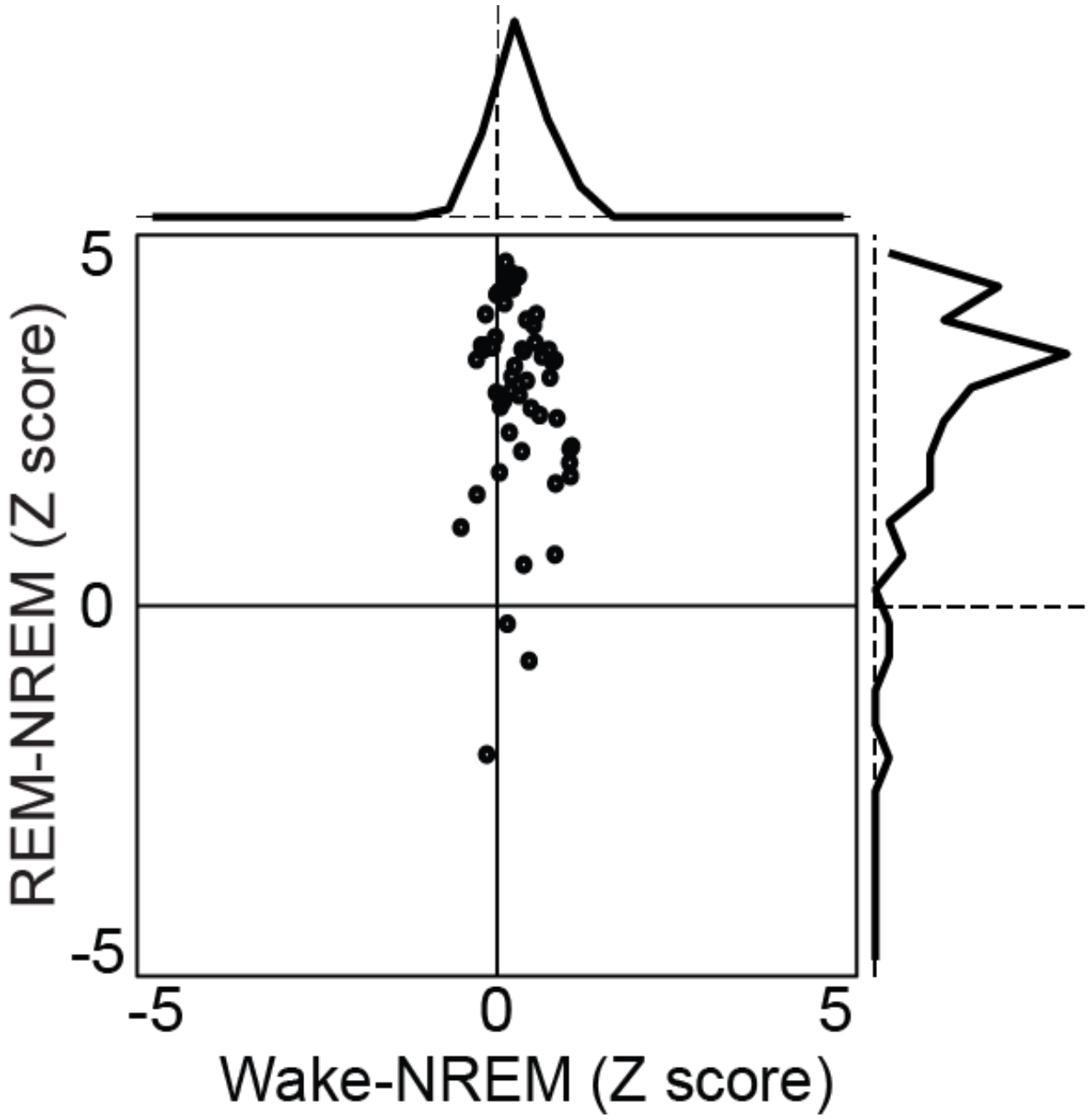

Figure 3H. Quantification of imaging data from RPA-projecting DMH neurons

REM-NREM activity difference versus wake-NREM activity difference. Traces on the top and right: distributions of wake-NREM and REM-NREM activity differences for RPA-projecting DMH galaninergic neurons (n = 28 cells from 3 mice).

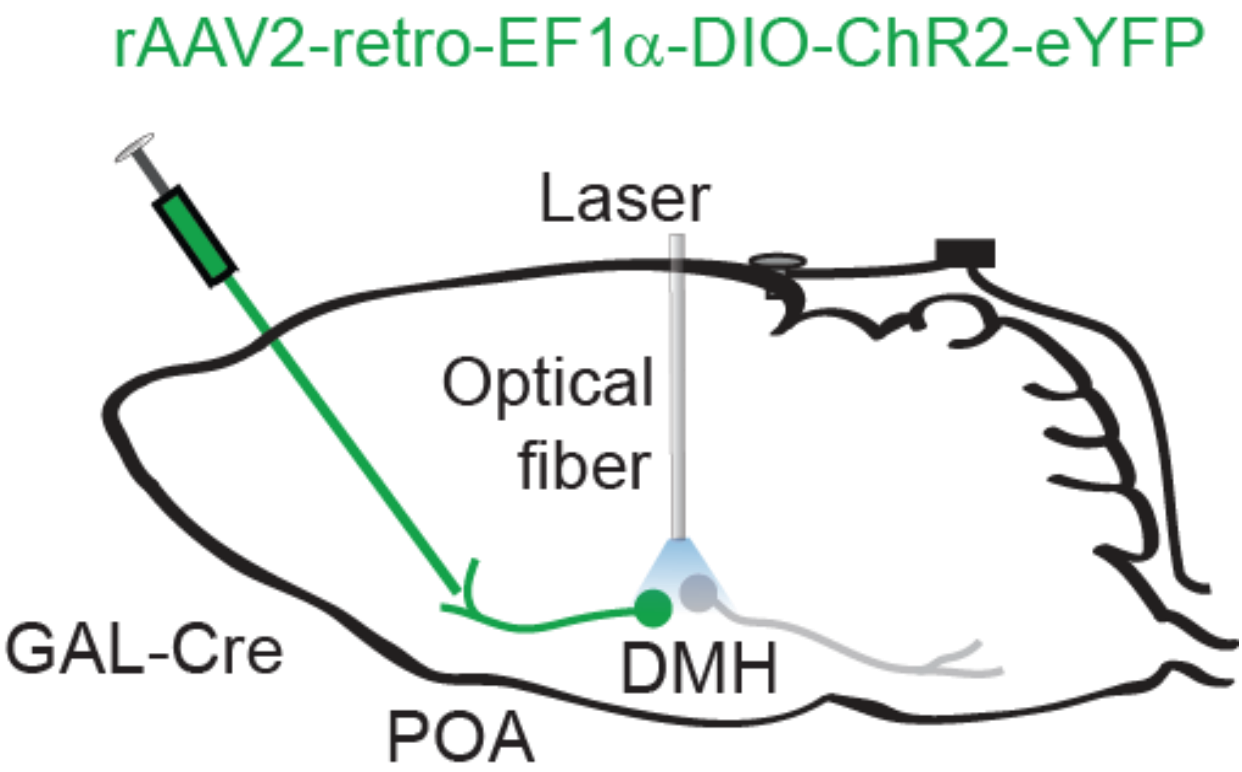

Figure 4A. Schematic of optogenetic activation experiments of POA-projecting DMH galaninergic neurons

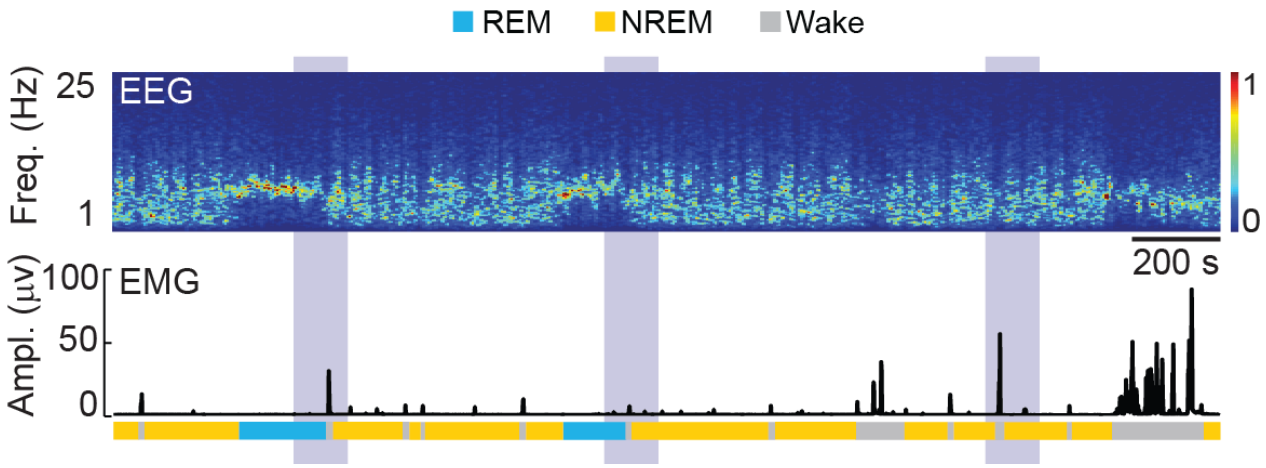

Figure 4B. Example traces from optogenetic activation experiments of POA-projecting DMH galaninergic neurons

An example experiment showing EEG power spectrogram, EMG trace and brain states (color coded). Purple shading, laser stimulation period.

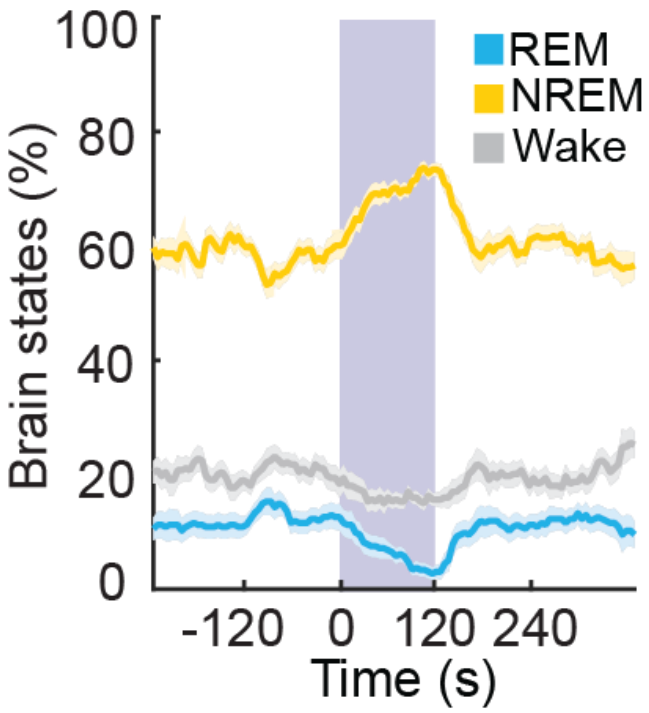

Figure 4C. Quantification of optogenetic activation experiments of POA-projecting DMH galaninergic neurons

Percentage of time in NREM, REM, or wake state before, during, and after laser stimulation (purple shading), averaged from 6 mice. Shading of each trace, ±SEM.

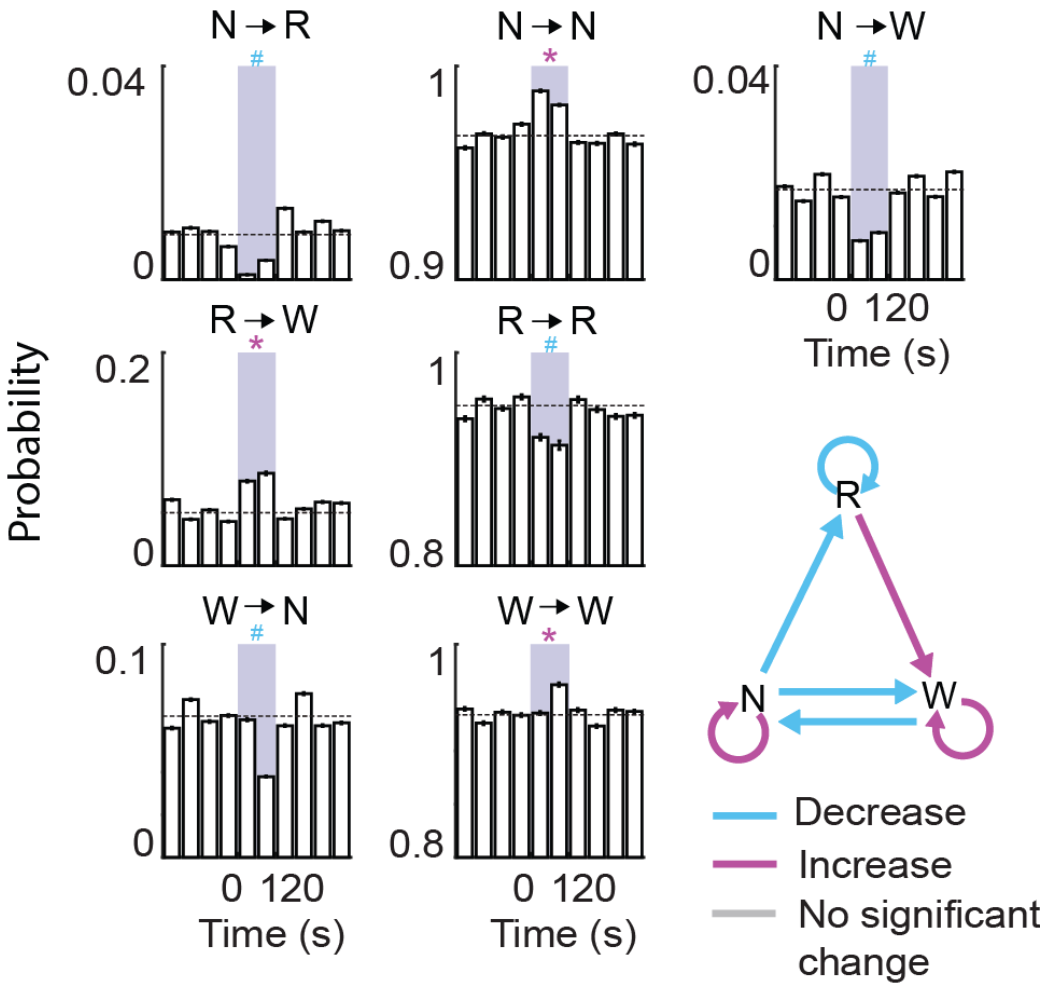

Figure 4D. Transition analysis of optogenetic activation experiments of POA-projecting DMH galaninergic neurons

Transition probability within each 10 s period with optogenetic activation of POA-projecting DMH galaninergic neurons (n = 6 mice). Shown in each bar is the transition probability averaged across six consecutive 10 s bins within each 60 s. Error bar, 95% confidence interval (bootstrap). The baseline transition probability (gray dashed line) was averaged across all time bins within 240 s before laser onset. Direct wake→ REM and REM→ NREM transitions were not observed and the corresponding plots were omitted. Bottom right diagram indicates transition probabilities that are significantly increased, decreased, or unaffected by laser stimulation.

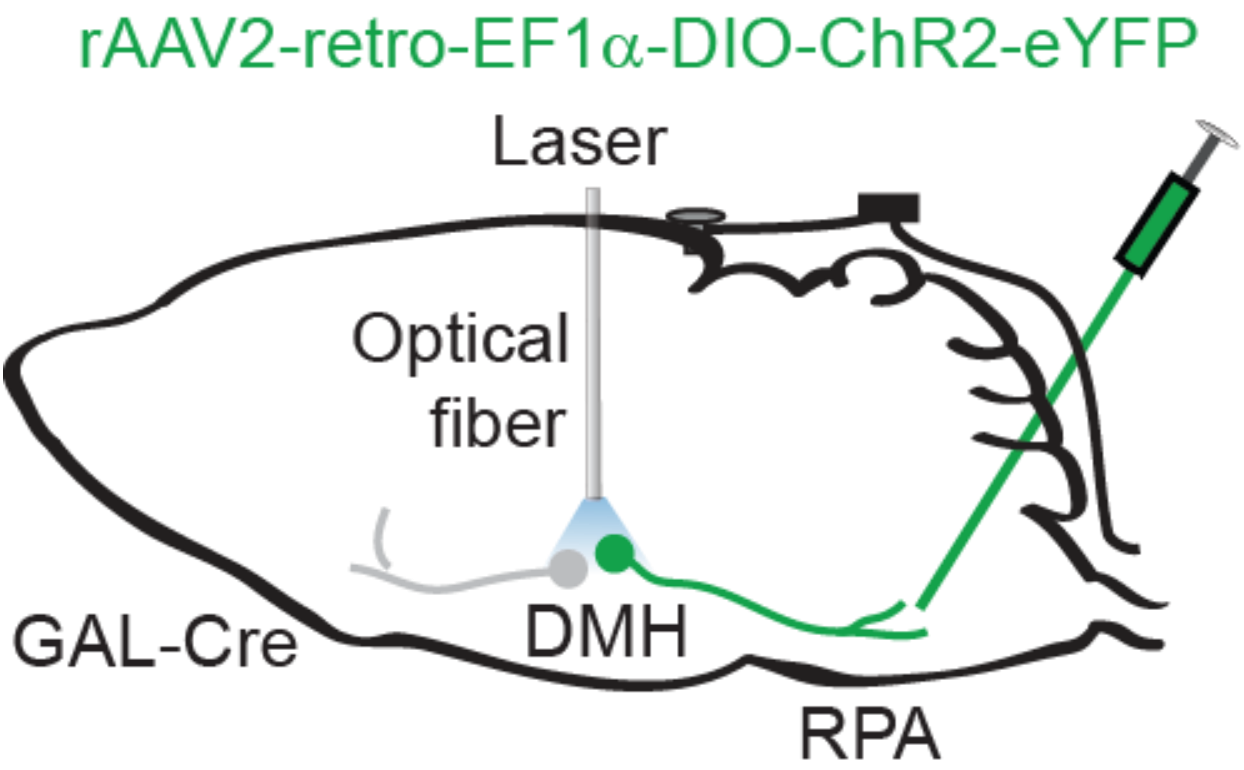

Figure 4E. Schematic of optogenetic activation experiments of RPA-projecting DMH galaninergic neurons

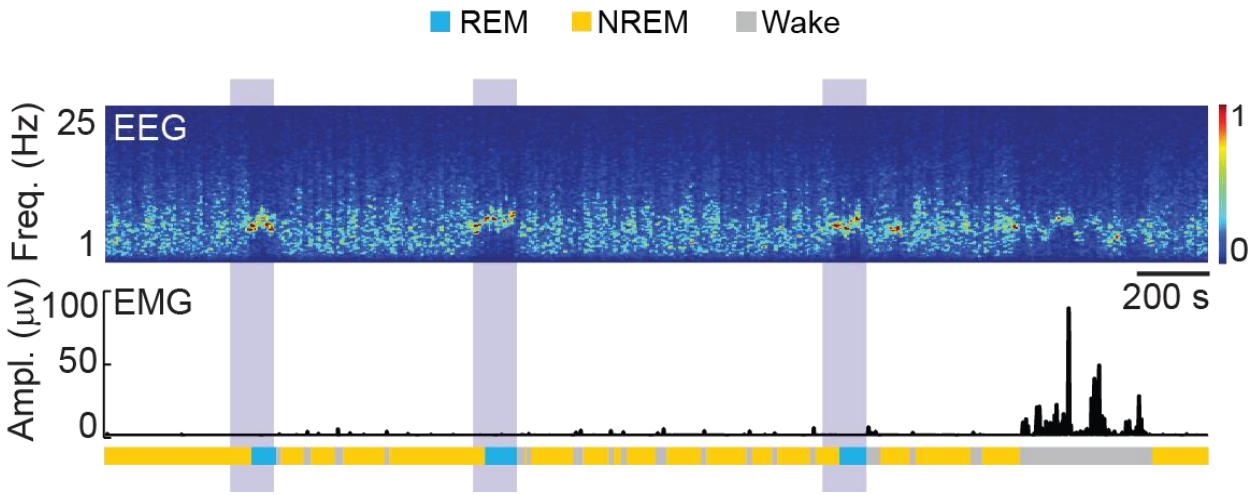

Figure 4F. Example traces from optogenetic activation experiments of RPA-projecting DMH galaninergic neurons

An example experiment showing EEG power spectrogram, EMG trace and brain states (color coded). Purple shading, laser stimulation period.

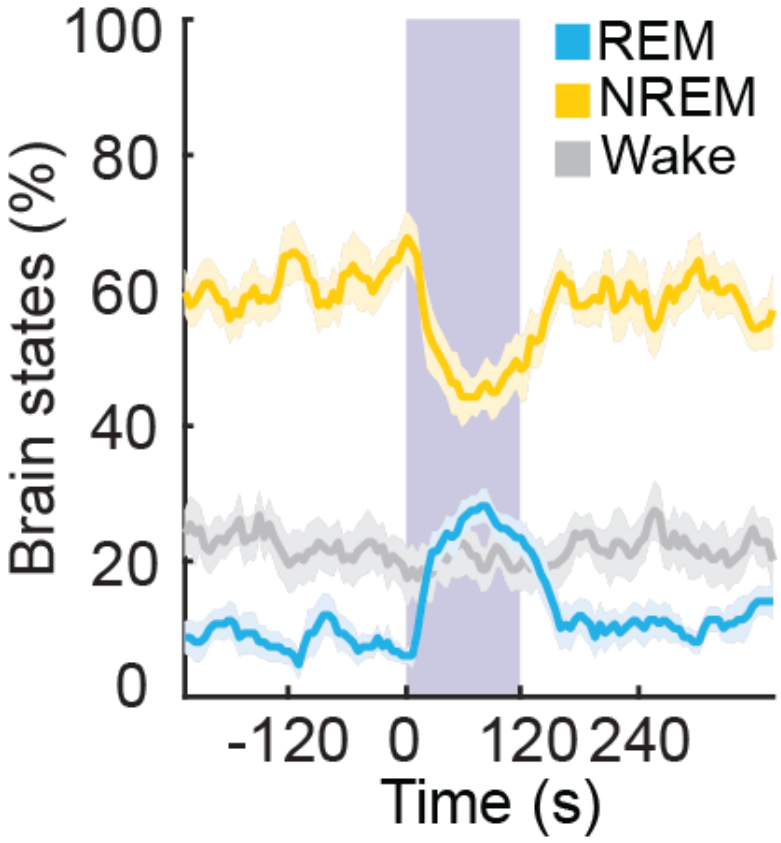

Figure 4G. Quantification of optogenetic activation experiments of RPA-projecting DMH galaninergic neurons

Percentage of time in NREM, REM, or wake state before, during, and after laser stimulation (purple shading), averaged from 4 mice. Shading of each trace, ±SEM.

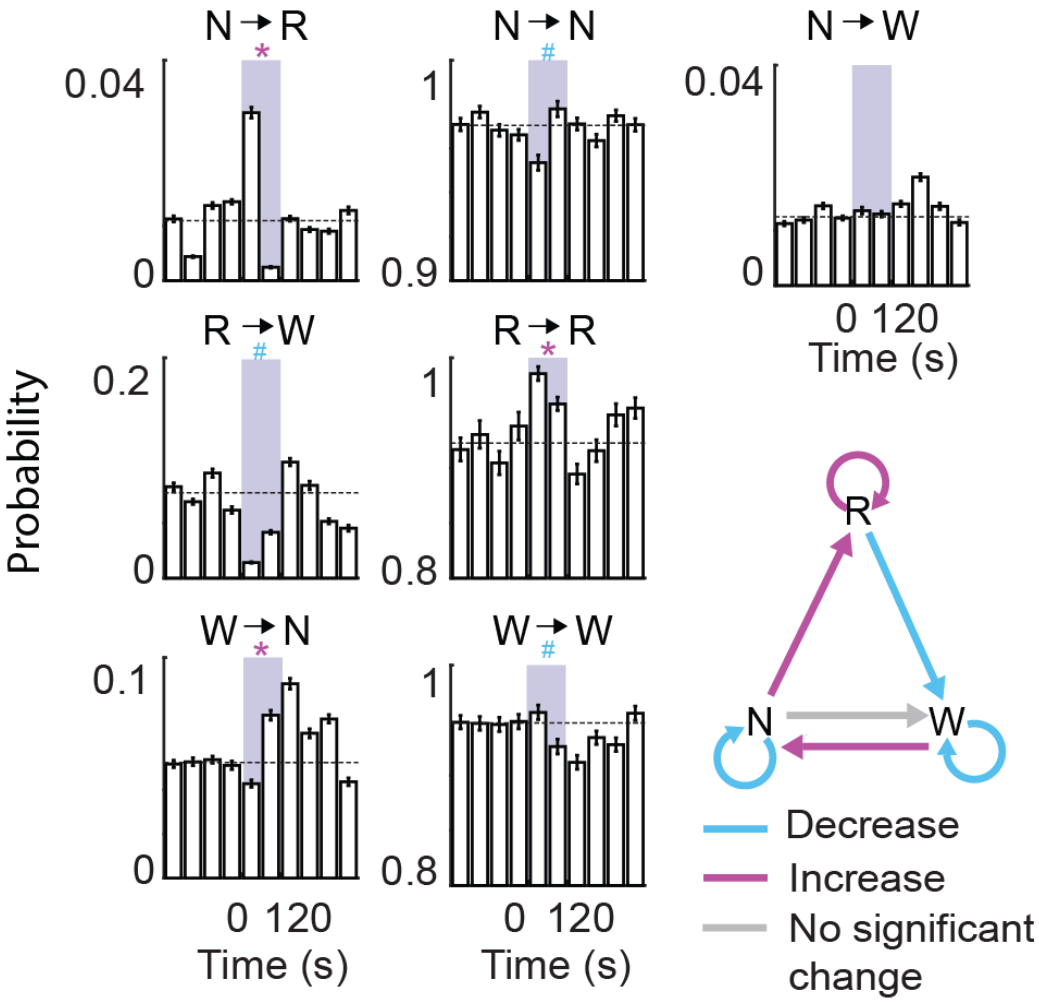

Figure 4H. Transition analysis of optogenetic activation experiments of RPA-projecting DMH galaninergic neurons

Transition probability within each 10 s period with optogenetic activation of RPA-projecting DMH galaninergic neurons (n = 4 mice). Shown in each bar is the transition probability averaged across six consecutive 10 s bins within each 60 s. Error bar, 95% confidence interval (bootstrap). The baseline transition probability (gray dashed line) was averaged across all time bins within 240 s before laser onset. Direct wake→ REM and REM→ NREM transitions were not observed and the corresponding plots were omitted. Bottom right diagram indicates transition probabilities that are significantly increased, decreased, or unaffected by laser stimulation.

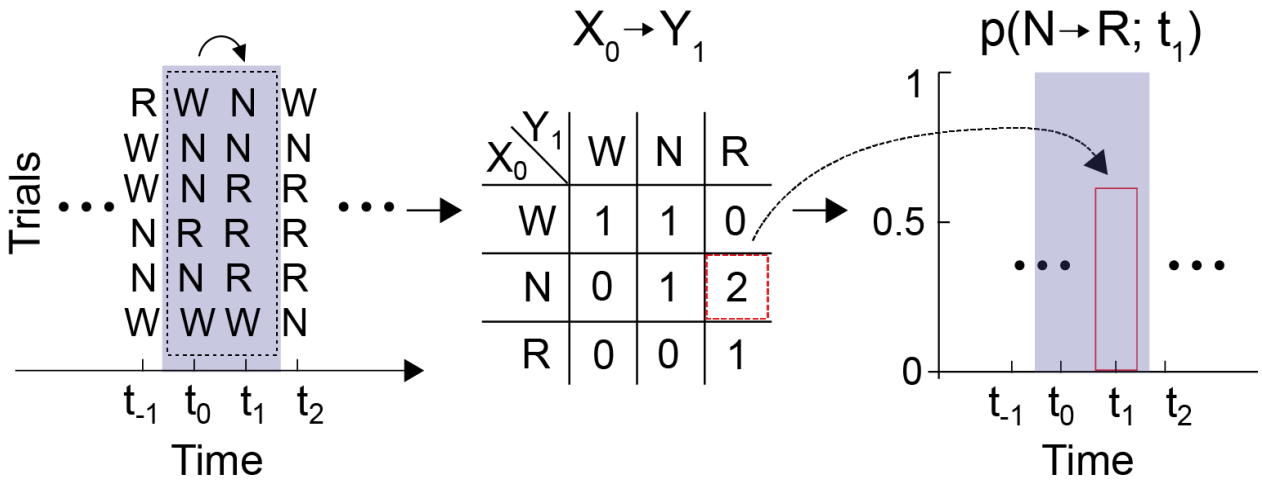

Figure 4I. Schematic illustrating the calculation of transition probability.

For the transition probability at a given time bin (*i*), I first identified all the trials (*n*) in which the animal was in state *X* (*X* could be wake, NREM, or REM) in the preceding time bin ($i - 1$). Among these *n* trials, I identified the subset of trials (*m*) in which the animal transitioned into state *Y* in the current time bin (*i*). The $X \rightarrow Y$ transition probability for time bin *i* was computed as m/n.

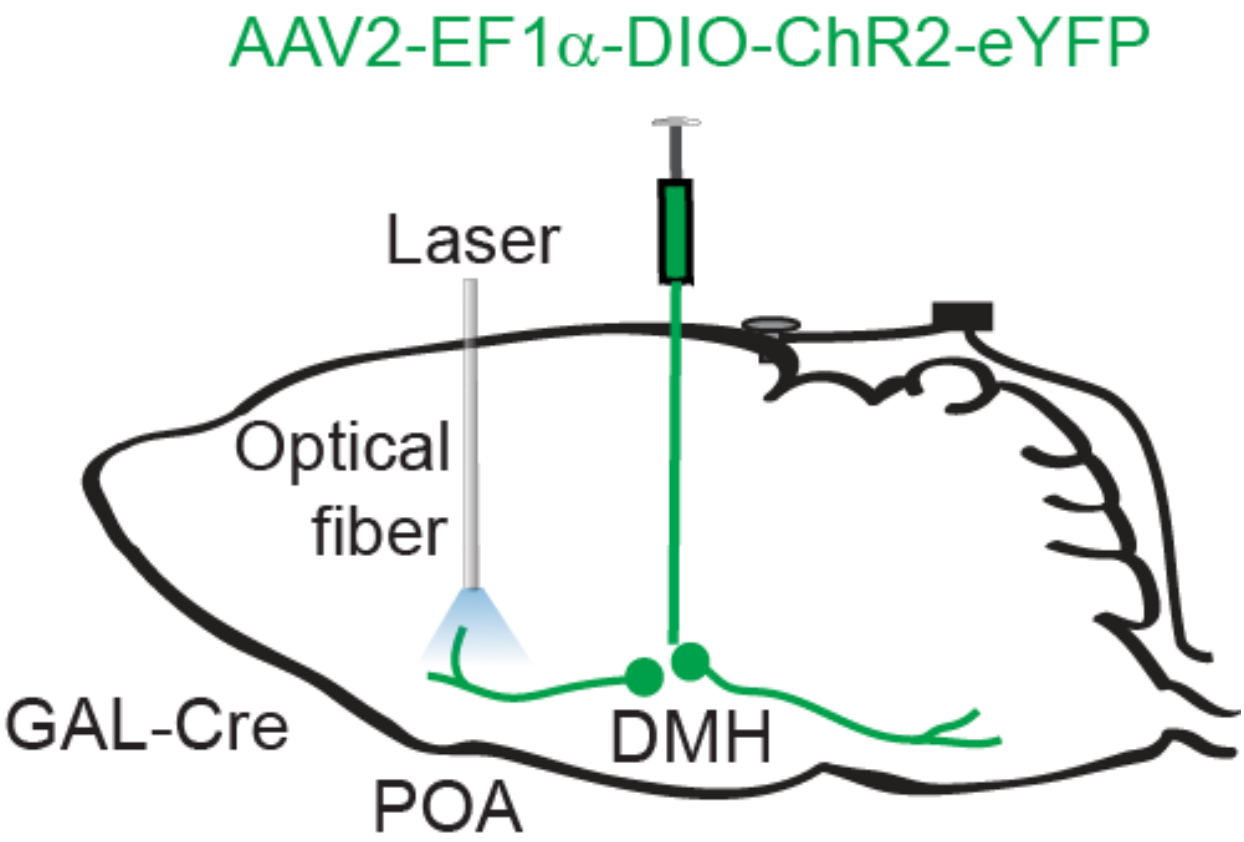

Figure 5A. Schematic of optogenetic activation experiments of DMH galaninergic axons in the POA

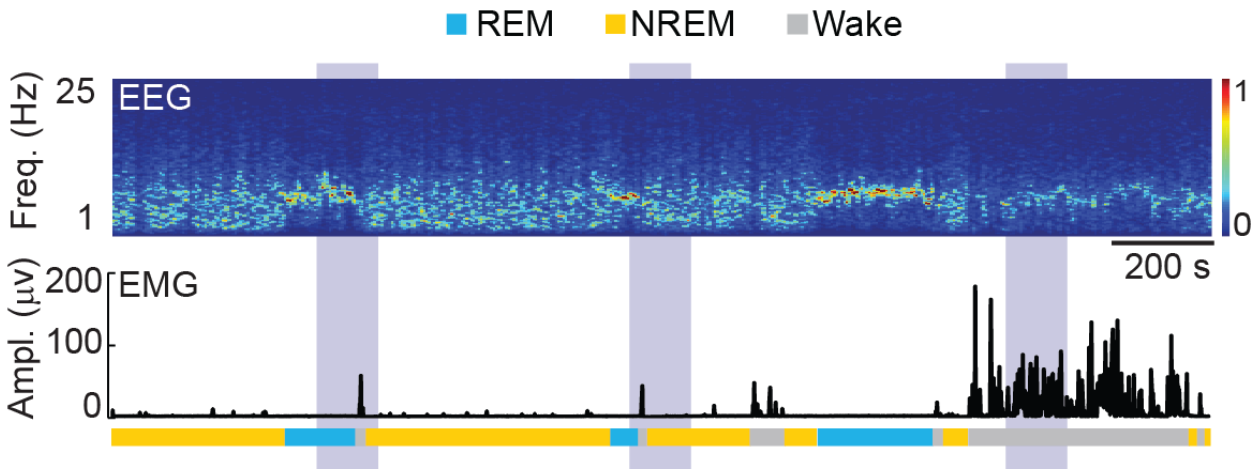

Figure 5B. Example traces from optogenetic activation experiments of DMH galaninergic axons at POA

An example experiment showing EEG power spectrogram, EMG trace and brain states (color coded). Purple shading, laser stimulation period.

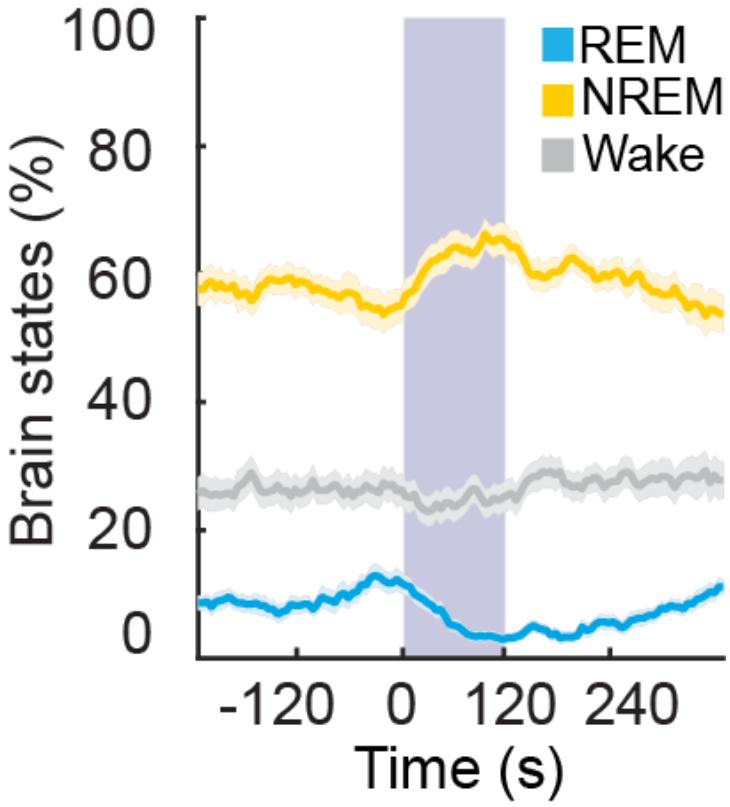

Figure 5C. Quantification of optogenetic activation experiments of DMH galaninergic axons at POA

Percentage of time in NREM, REM, or wake state before, during, and after laser stimulation (purple shading), averaged from 6 mice. Shading of each trace, ±SEM.

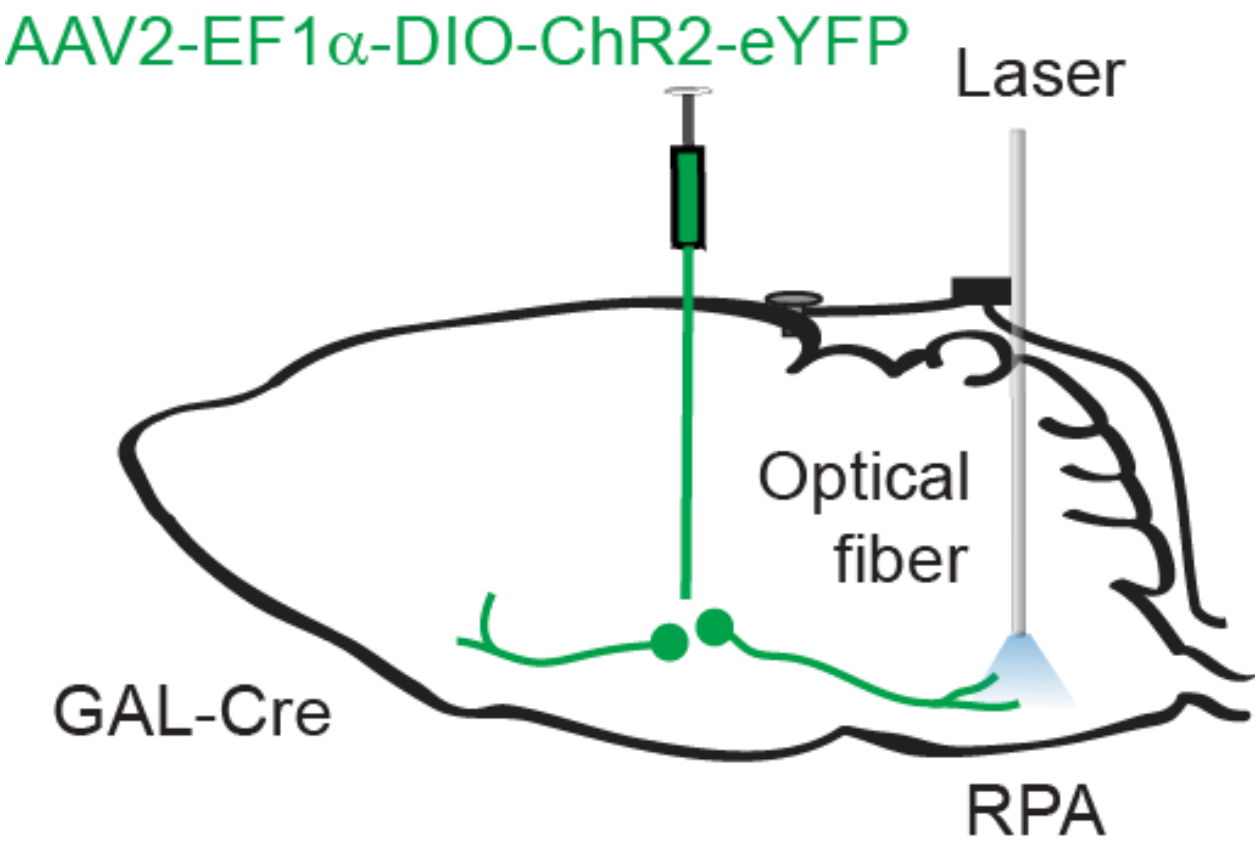

Figure 5D. Schematic of optogenetic activation experiments of DMH galaninergic axons in the RPA

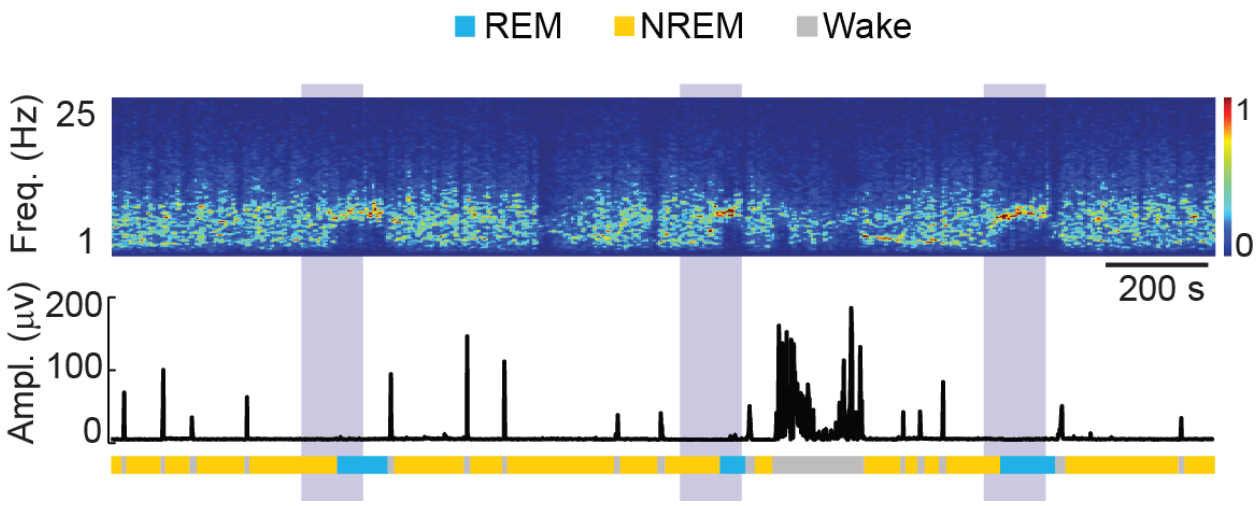

Figure 5E. Example traces from optogenetic activation experiments of DMH galaninergic axons at RPA

An example experiment showing EEG power spectrogram, EMG trace and brain states (color coded). Purple shading, laser stimulation period.

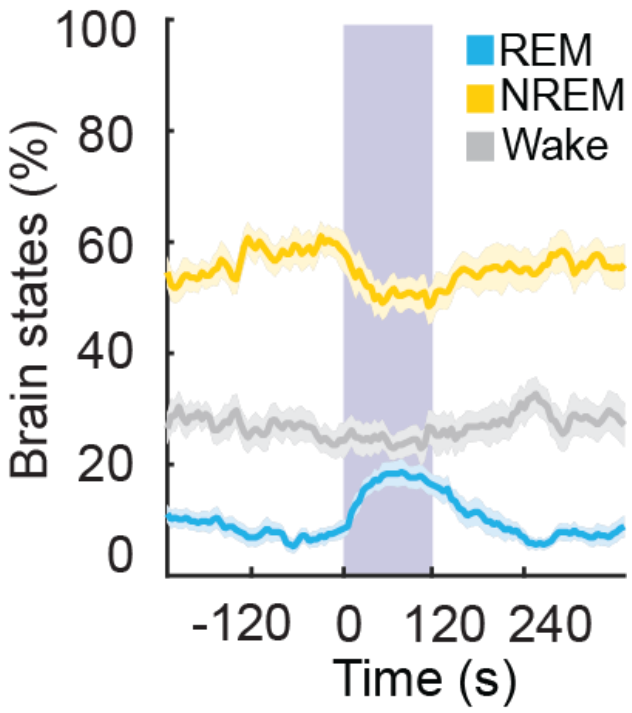

Figure 5F. Quantification of optogenetic activation experiments of DMH galaninergic axons at RPA

Percentage of time in NREM, REM, or wake state before, during, and after laser stimulation (purple shading), averaged from 4 mice. Shading of each trace, ±SEM.

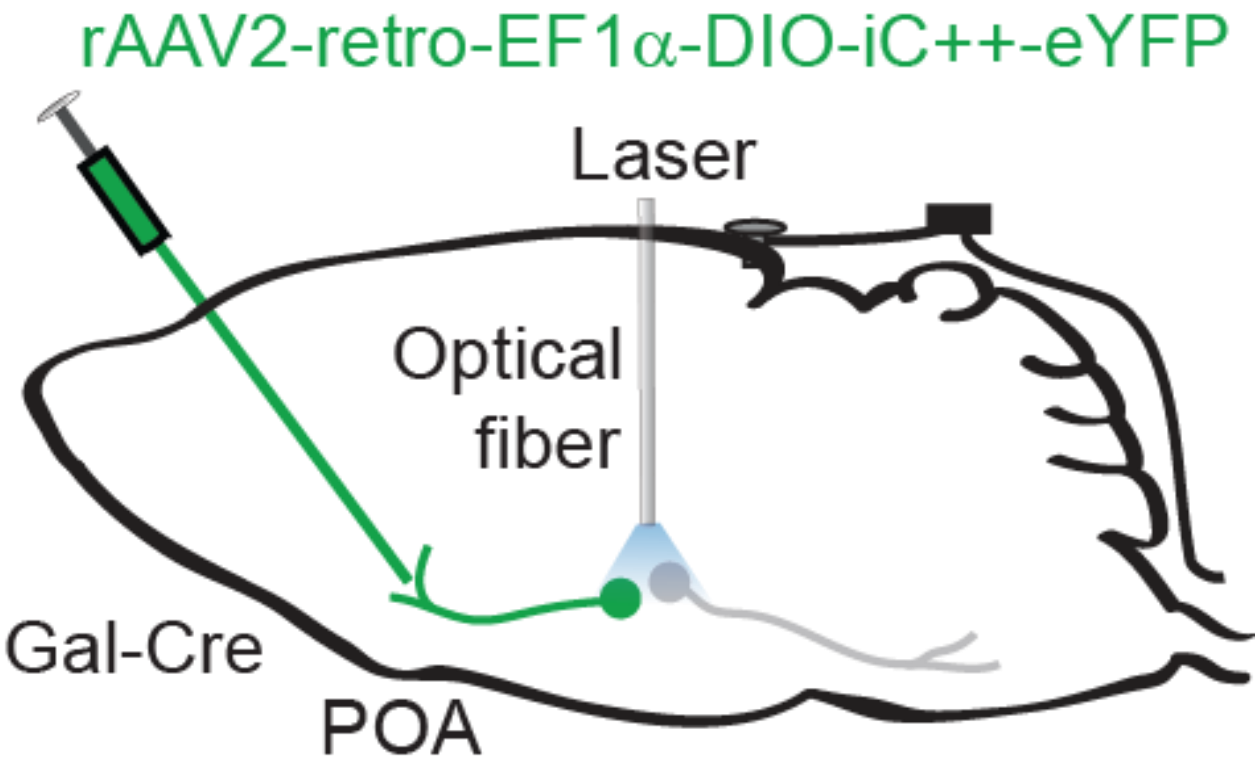

Figure 6A. Schematic of optogenetic inhibition experiments of POA-projecting DMH galaninergic neurons

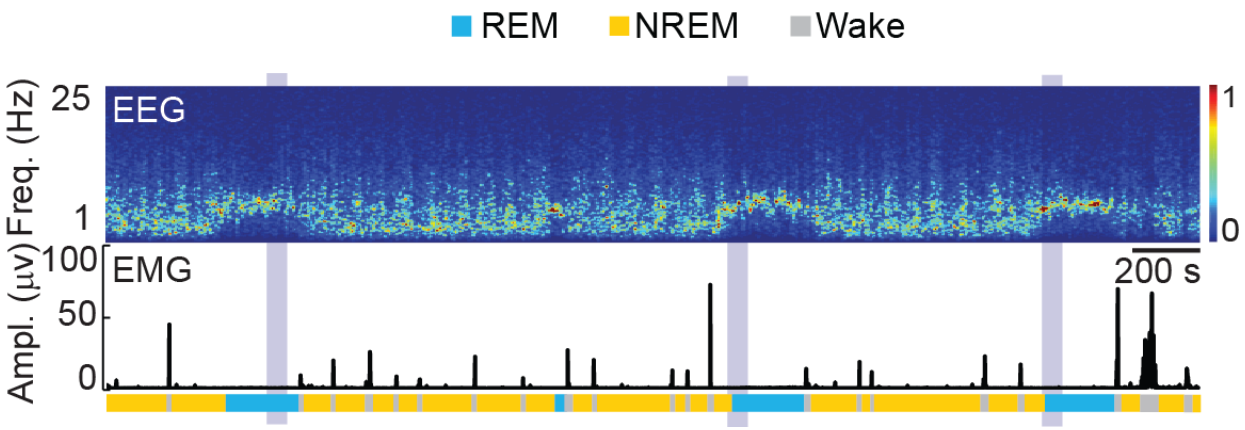

Figure 6B. Example traces from optogenetic inhibition experiments of POA-projecting DMH galaninergic neurons

An example experiment showing EEG power spectrogram, EMG trace and brain states (color coded). Purple shading, laser stimulation period.

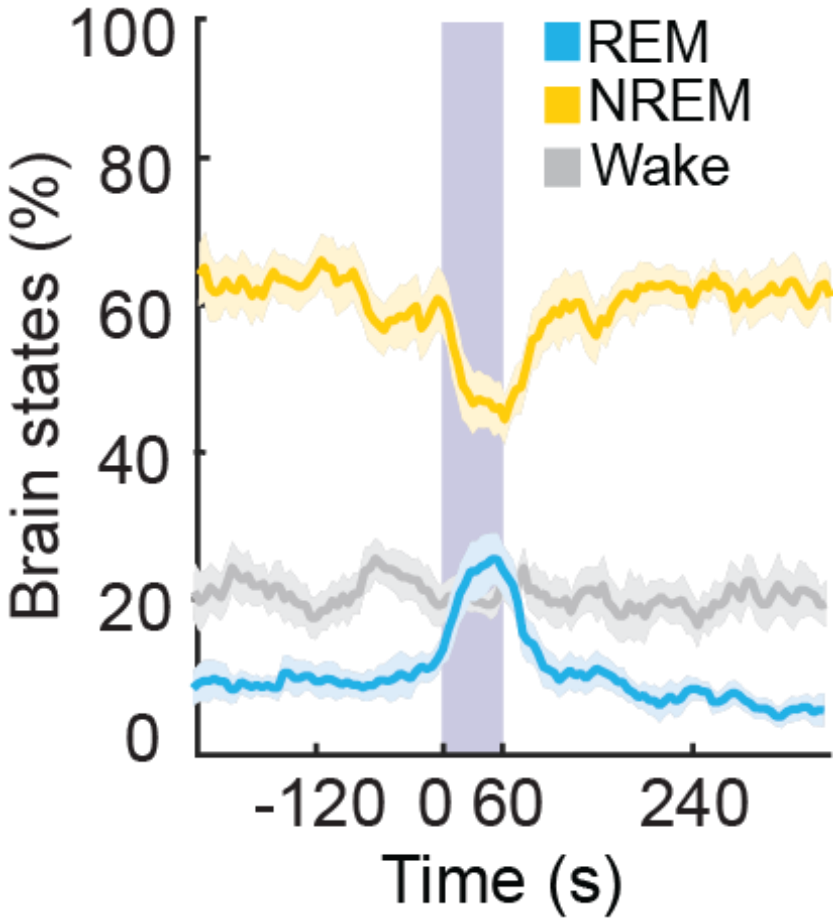

Figure 6C. Quantification of optogenetic inhibition experiments of POA-projecting DMH galaninergic neurons

Percentage of time in NREM, REM, or wake state before, during, and after laser stimulation (purple shading), averaged from 4 mice. Shading of each trace, ±SEM.

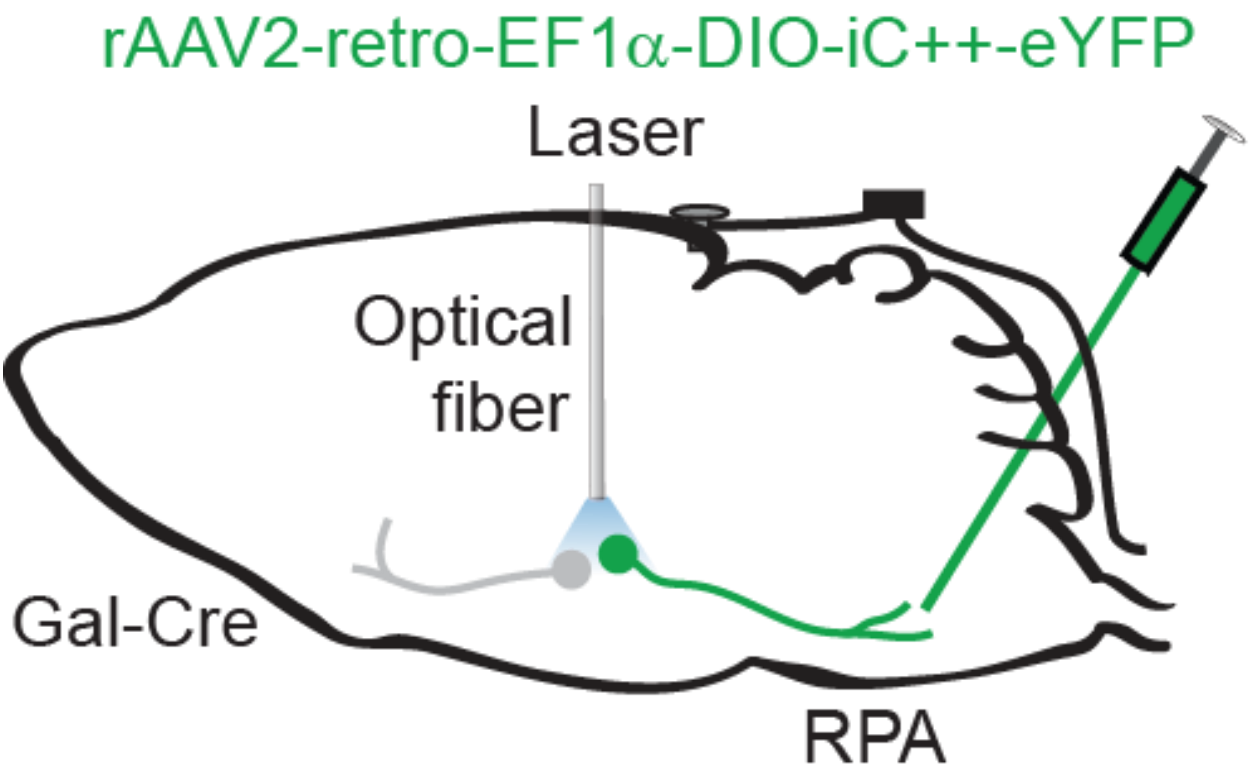

Figure 6D. Schematic of optogenetic inhibition experiments of RPA-projecting DMH galaninergic neurons

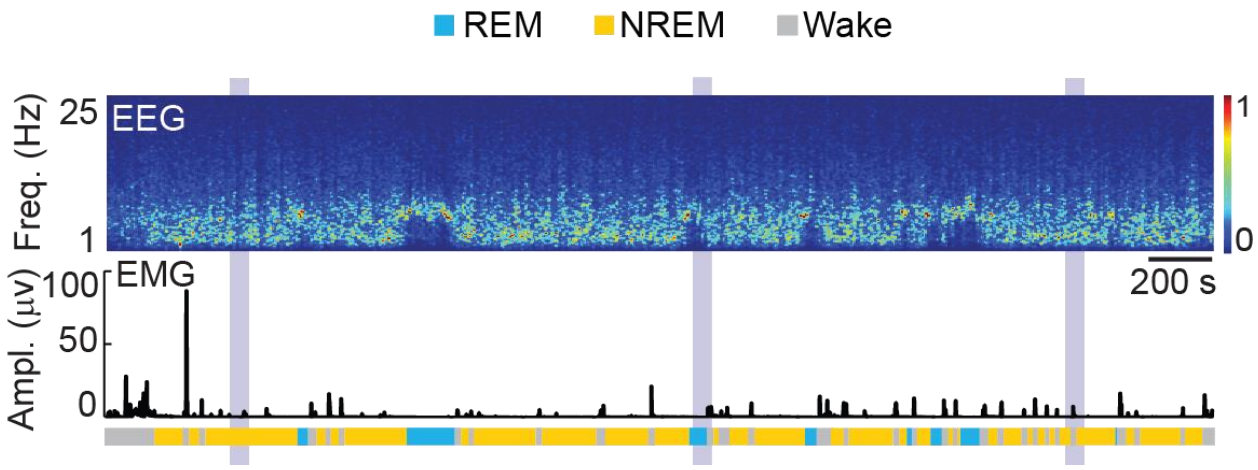

Figure 6E. Example traces from optogenetic inhibition experiments of RPA-projecting DMH galaninergic neurons

An example experiment showing EEG power spectrogram, EMG trace and brain states (color coded). Purple shading, laser stimulation period.

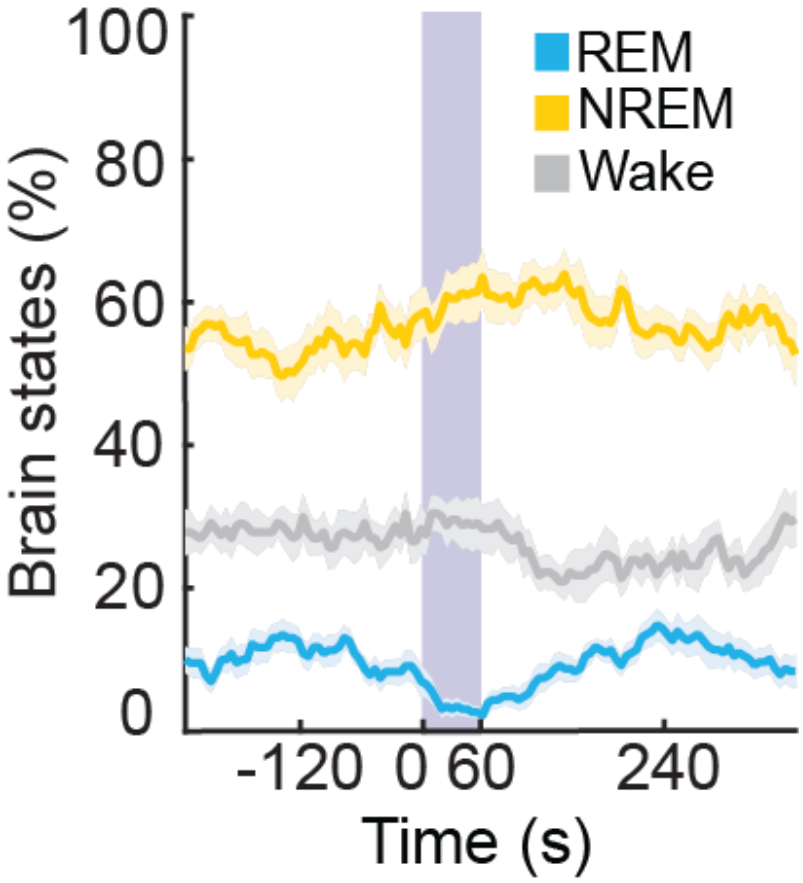

Figure 6F. Quantification of optogenetic inhibition experiments of RPA-projecting DMH galaninergic neurons

Percentage of time in NREM, REM, or wake state before, during, and after laser stimulation (purple shading), averaged from 4 mice. Shading of each trace, ±SEM.

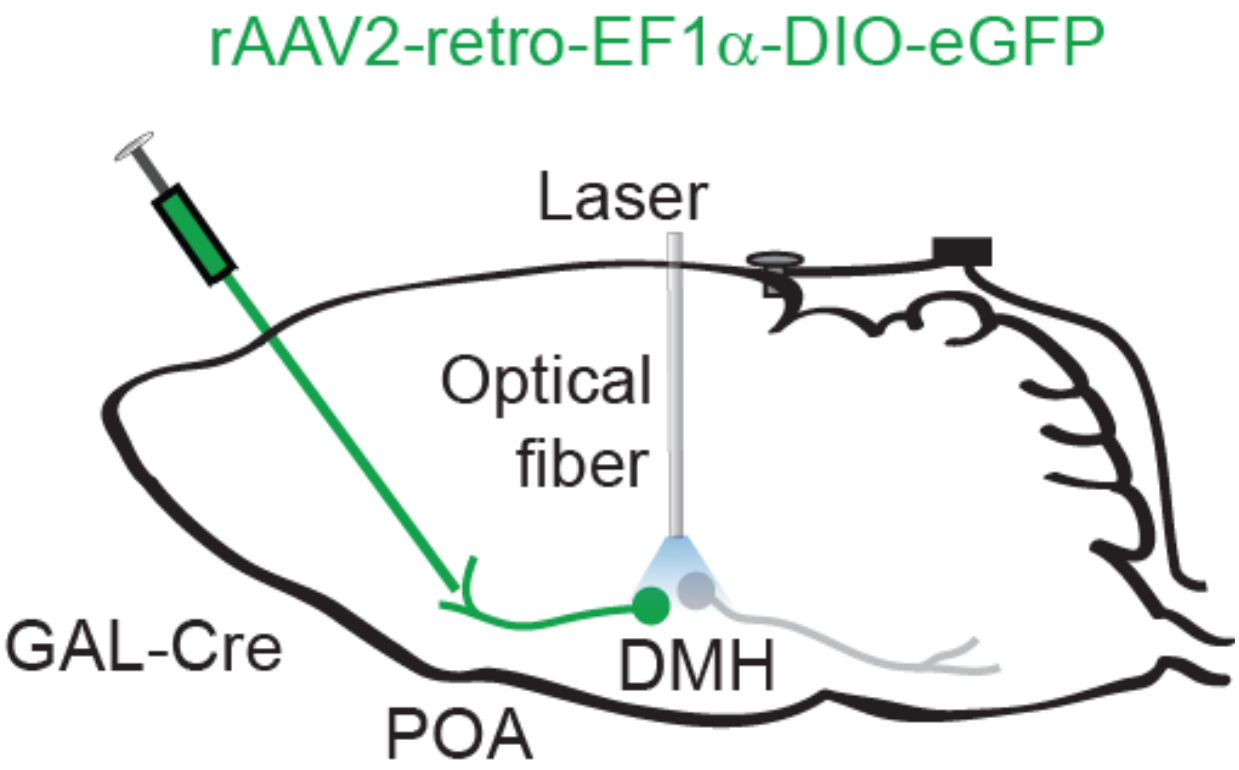

Figure 7A. Schematic of eGFP control experiments for POA-projecting DMH galaninergic neurons.

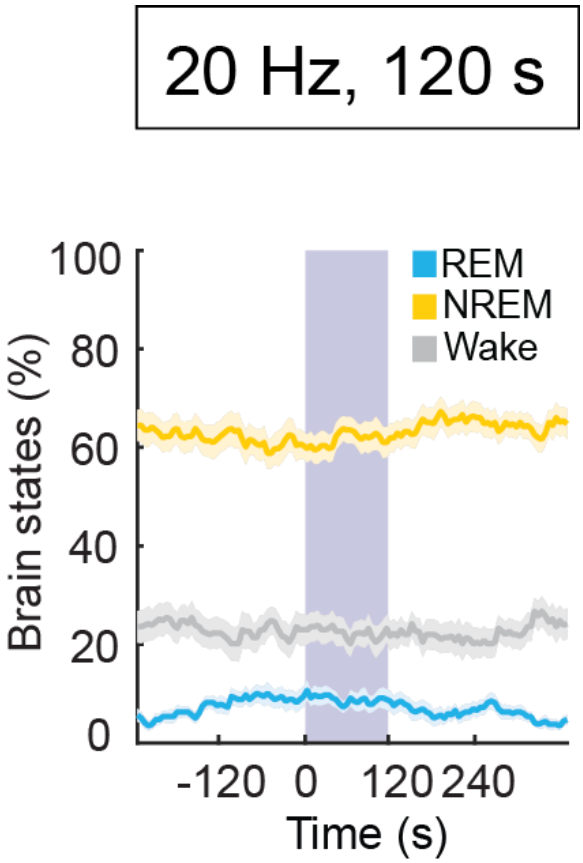

Figure 7B. Quantification of eGFP control experiments for POA-projecting DMH galaninergic neurons

Percentage of time in NREM, REM, or wake state before, during, and after laser stimulation (purple shading, 20 Hz, 120 s), averaged from 4 mice. Shading of each trace, ±SEM.

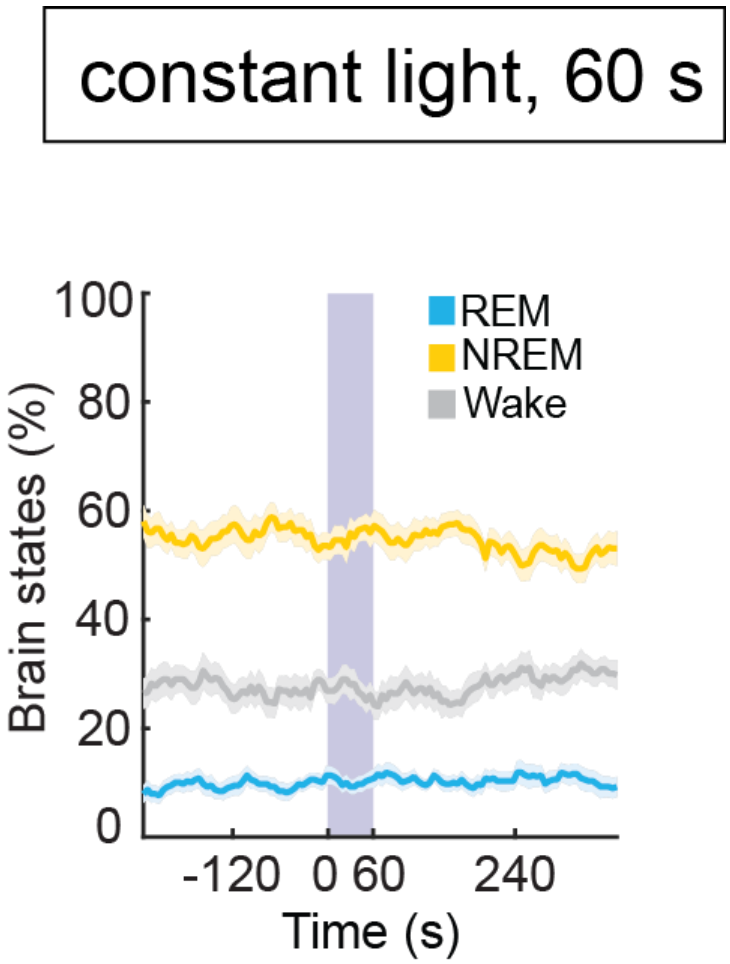

Figure 7C. Quantification of eGFP control experiments for POA-projecting DMH galaninergic neurons

Percentage of time in NREM, REM, or wake state before, during, and after laser stimulation (purple shading, constant light, 60s.), averaged from 4 mice. Shading of each trace, ±SEM.

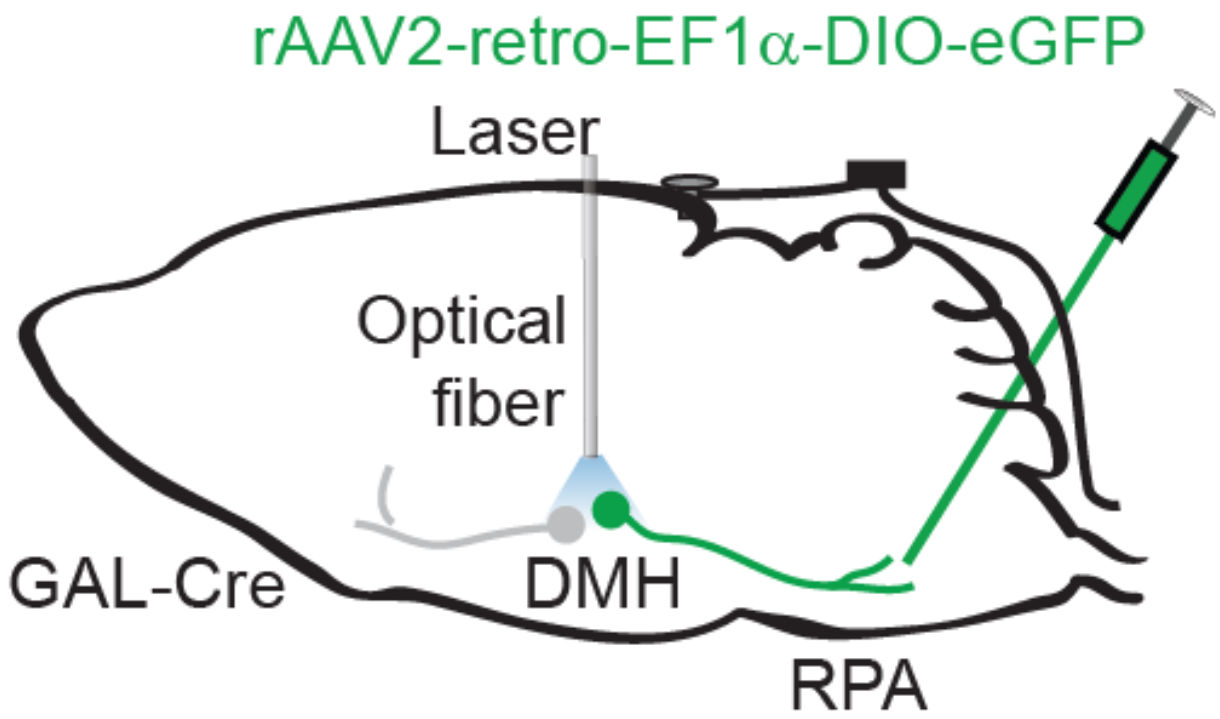

Figure 7D. Schematic of eGFP control experiments for RPA-projecting DMH galaninergic neurons

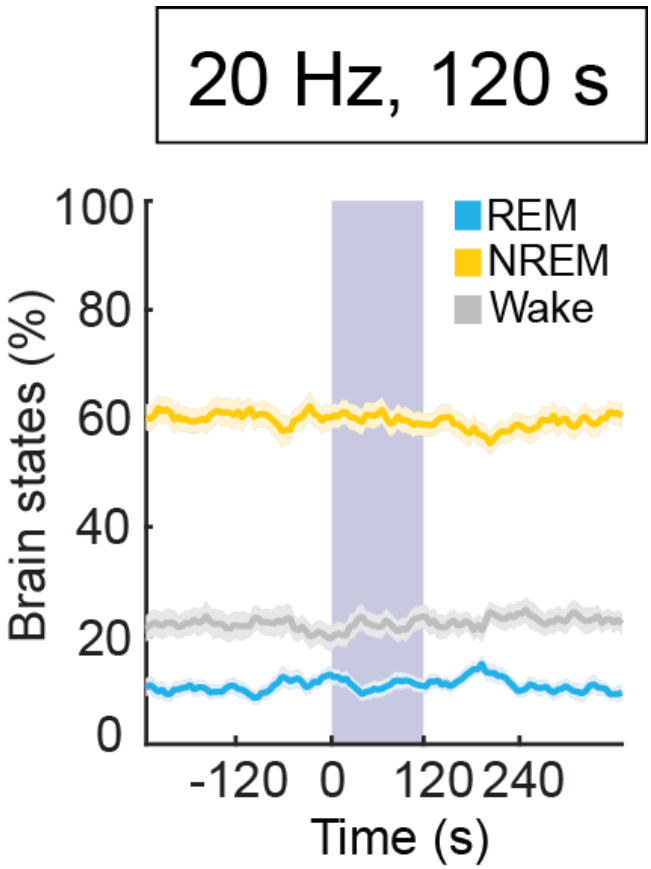

Figure 7E. Quantification of eGFP control experiments for RPA-projecting DMH galaninergic neurons

Percentage of time in NREM, REM, or wake state before, during, and after laser stimulation (purple shading, 20 Hz, 120 s), averaged from 4 mice. Shading of each trace, ±SEM.

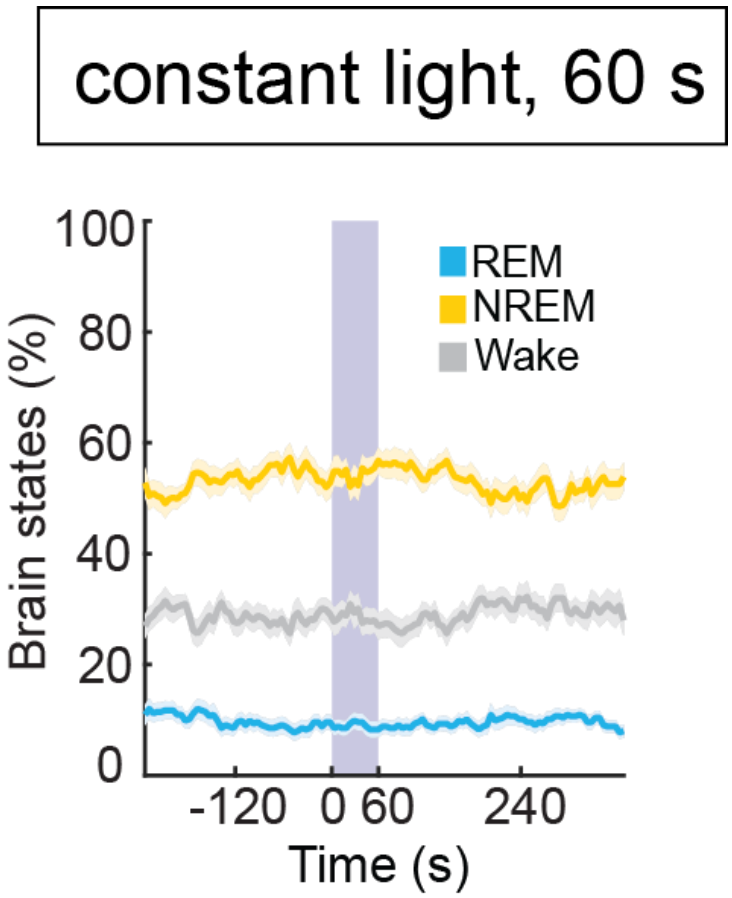

Figure 7F. Quantification of eGFP control experiments for RPA-projecting DMH galaninergic neurons

Percentage of time in NREM, REM, or wake state before, during, and after laser stimulation (purple shading, constant light, 60s.), averaged from 4 mice. Shading of each trace, ±SEM.

Chapter 3. Conclusion and Implications

3.1 Summary of the Research

Vivid dreams occur during rapid-eye-movement (REM) sleep. My research identifies and segregates a heterogeneous population of hypothalamic neurons which can switch ON or OFF the REM sleep, the dream state of the brain.

REM sleep is characterized by skeletal muscle paralysis and desynchronized electroencephalogram (EEG) and is thought to be important for certain types of memory. Understanding the mechanisms regulating REM sleep is important for improving the treatments of REM sleep disorders such as narcolepsy and REM sleep behavior disorder. Based on previous lesion studies, the dorsomedial hypothalamus (DMH) is thought to be involved in sleep regulation. However, the underlying neural mechanism remains unclear.

In my doctoral research, I apply several novel techniques to dissect the DMH circuits regulating REM sleep. I expressed genetic-encoded calcium indicators (GCaMP) in the DMH of transgenic mice and performed *in vivo* microendoscopic calcium imaging to understand the correlation between DMH neuron activity and brain states. I found that there are two distinct subtypes of inhibitory neurons within the DMH: one group has the highest activity during REM sleep, and the other group has the lowest activity during REM sleep. Since these two groups of neurons have different firing patterns, I hypothesize that they may innervate to different brain regions. Using a retrograde viral tracing tool, I expressed GCaMP into selective DMH neurons based on their projections. To determine the causal functions of these neurons, I retrogradely expressed a light-gated ion channel (channelehodopsin, ChR2) to activate each group of DMH neurons by light. I found that preoptic-area-projecting neurons have the lowest activity during REM sleep, and activating them switched REM sleep to non-REM sleep, while the brainstem-projecting neurons show the opposite effect. Optical activation of DMH axons in the preoptic-area or in the brainstem switch off and on REM sleep, respectively, suggesting that these regions may be the downstream targets mediating the brain state changes.

This study reveals a new neural mechanism for REM sleep regulation in the DMH. The strategy I apply to segregate a heterogeneous population of neurons can also be applied to other circuit studies.

3.2 Discussion and Future Directions

Using cell-type- and projection-target-specific imaging and optogenetic manipulations, I have revealed a novel hypothalamic mechanism regulating the REM-NREM switch. While the DMH GABAergic neurons exhibit highly diverse brain-state-dependent calcium activity (Figure 1D, gray dots), the neuropeptide galanin labels two distinct subpopulations that are either REM-on or REM-off (Figs. 1D, black dots). Retrograde labeling based on their axon projections then allowed us to isolate each of the two subsets and demonstrate their opposing effects on REM vs. NREM sleep.

The REM-promoting effect of RPA-projecting neurons could be partly mediated by their GABA and/or galanin synaptic inhibition of the serotoninergic neurons in the RPA, which are known to be REM-off and may modulate other REM-sleep promoting neurons, such as GABAergic neurons in the ventral medulla (Heym et al., 1982; Trulson and Trulson, 1982; Weber et al., 2015). The POA-projecting neurons, on the other hand, could suppress REM sleep through multiple projections (Figures 2C, 2D and 2G). In addition to the REM-promoting neurons in the POA (Chung et al., 2017; Lu et al., 2006), the REM-active, REM-promoting MCH neurons (Blanco-Centurion et al., 2016; Ferreira et al., 2017; Hassani et al., 2009; Jego et al., 2013) are located well within the axonal field of the POA-projecting neurons. Whether and how the DMH galaninergic neurons interact with these sleep-related neurons remain to the elucidated. Interestingly, the DMH, POA, and RPA are all key brain structures involved in thermoregulation (Morrison and Nakamura, 2011), an important homeostatic process closely related to sleep generation. In future studies it would be of great interest to investigate the relationship between the neurons controlling sleep and those regulating body temperature.

The nature of the inputs that give rise to the REM-on versus REM-off activity of the DMH galaninergic neurons remains unknown. A promising approach is to map the monosynaptic inputs to POA- or RPA-projecting galaninergic neurons using the "cell-type-specific tracing the relationship between input and output" (cTRIO) method (Beier et al., 2015; Schwarz et al., 2015). Such whole-brain mapping will provide an anatomical blueprint to guide functional identification of the REM- and NREM-sleep-related inputs. Another useful approach is to combine retrograde labeling and gene expression profiling to identify molecular markers specific for the POA- and RPA-projecting populations (Chung et al., 2017). Uncovering the genetic identity of each population will greatly facilitate selective targeting of these neurons for further circuit analysis.

My results demonstrate a striking circuit motif in which two groups of neurons, residing in the same nucleus and using the same neurotransmitters (both GABA and galanin), promote two mutually exclusive brain states. The spatial intermingling between these two groups raises the intriguing possibility of local reciprocal inhibition, and their physical proximity could greatly improve the efficiency of the neuronal circuit in regulating the switch between REM and NREM sleep.

References

Adamantidis, A., Salvert, D., Goutagny, R., Lakaye, B., Gervasoni, D., Grisar, T., Luppi, P.-H., and Fort, P. (2008). Sleep architecture of the melanin-concentrating hormone receptor 1-knockout mice. European Journal of Neuroscience *27*, 1793-1800.

Adamantidis, A.R., Zhang, F., Aravanis, A.M., Deisseroth, K., and de Lecea, L. (2007). Neural substrates of awakening probed with optogenetic control of hypocretin neurons. Nature *450*, 420.

Anaclet, C., Ferrari, L., Arrigoni, E., Bass, C.E., Saper, C.B., Lu, J., and Fuller, P.M. (2014). The GABAergic parafacial zone is a medullary slow wave sleep-promoting center. Nat Neurosci *17*, 1217-1224.

Aserinsky, E. (1996). Memories of famous neuropsychologists. Journal of the History of the Neurosciences *5*, 213-227.

Aserinsky, E., and Kleitman, N. (1953). Regularly occurring periods of eye motility, and concomitant phenomena, during sleep. Science *118*, 273-274.

Aston-Jones, G., and Bloom, F. (1981). Activity of norepinephrine-containing locus coeruleus neurons in behaving rats anticipates fluctuations in the sleep-waking cycle. The Journal of Neuroscience *1*, 876-886.

Aston-Jones, G., Chen, S., Zhu, Y., and Oshinsky, M.L. (2001). A neural circuit for circadian regulation of arousal. Nat Neurosci *4*, 732-738.

Beier, K.T., Steinberg, E.E., DeLoach, K.E., Xie, S., Miyamichi, K., Schwarz, L., Gao, X.J., Kremer, E.J., Malenka, R.C., and Luo, L. (2015). Circuit Architecture of VTA Dopamine Neurons Revealed by Systematic Input-Output Mapping. Cell *162*, 622-634.

Berndt, A., Lee, S.Y., Wietek, J., Ramakrishnan, C., Steinberg, E.E., Rashid, A.J., Kim, H., Park, S., Santoro, A., Frankland, P.W., *et al.* (2016). Structural foundations of optogenetics: Determinants of channelrhodopsin ion selectivity. Proc Natl Acad Sci U S A *113*, 822-829.

Blanco-Centurion, C., Gerashchenko, D., and Shiromani, P.J. (2007). Effects of Saporin-Induced Lesions of Three Arousal Populations on Daily Levels of Sleep and Wake. The Journal of Neuroscience *27*, 14041-14048.

Blanco-Centurion, C., Liu, M., Konadhode, R.P., Zhang, X., Pelluru, D., van den Pol, A.N., and Shiromani, P.J. (2016). Optogenetic activation of melanin-concentrating hormone neurons increases non-rapid eye movement and rapid eye movement sleep during the night in rats. Eur J Neurosci *44*, 2846-2857.

Boissard, R., Fort, P., Gervasoni, D., Barbagli, B., and Luppi, P.H. (2003). Localization of the GABAergic and non-GABAergic neurons projecting to the sublaterodorsal nucleus and potentially gating paradoxical sleep onset. Eur J Neurosci *18*, 1627-1639.

Boissard, R., Gervasoni, D., Schmidt, M.H., Barbagli, B., Fort, P., and Luppi, P.-H. (2002). The rat ponto-medullary network responsible for paradoxical sleep onset and maintenance: a combined microinjection and functional neuroanatomical study. European Journal of Neuroscience *16*, 1959-1973.

Boyden, E.S., Zhang, F., Bamberg, E., Nagel, G., and Deisseroth, K. (2005). Millisecond-timescale, genetically targeted optical control of neural activity. Nature Neuroscience *8*, 1263.

Brown, R.E., Basheer, R., McKenna, J.T., Strecker, R.E., and McCarley, R.W. (2012). Control of sleep and wakefulness. Physiol Rev *92*, 1087-1187.

Burgess, C., Lai, D., Siegel, J., and Peever, J. (2008). An Endogenous Glutamatergic Drive onto Somatic Motoneurons Contributes to the Stereotypical Pattern of Muscle Tone across the Sleep–Wake Cycle. The Journal of Neuroscience *28*, 4649-4660.
Callaway, E.M., and Luo, L. (2015). Monosynaptic Circuit Tracing with Glycoprotein-Deleted Rabies Viruses. The Journal of Neuroscience *35*, 8979-8985.
Chamberlin, N.L., Arrigoni, E., Chou, T.C., Scammell, T.E., Greene, R.W., and Saper, C.B. (2003). Effects of adenosine on gabaergic synaptic inputs to identified ventrolateral preoptic neurons. Neuroscience *119*, 913-918.
Chen, T.-W., Wardill, T.J., Sun, Y., Pulver, S.R., Renninger, S.L., Baohan, A., Schreiter, E.R., Kerr, R.A., Orger, M.B., Jayaraman, V., *et al.* (2013). Ultra-sensitive fluorescent proteins for imaging neuronal activity. Nature *499*, 295-300.
Chou, T.C., Bjorkum, A.A., Gaus, S.E., Lu, J., Scammell, T.E., and Saper, C.B. (2002). Afferents to the Ventrolateral Preoptic Nucleus. The Journal of Neuroscience *22*, 977-990.
Chou, T.C., Scammell, T.E., Gooley, J.J., Gaus, S.E., Saper, C.B., and Lu, J. (2003). Critical role of dorsomedial hypothalamic nucleus in a wide range of behavioral circadian rhythms. J Neurosci *23*, 10691-10702.
Chung, S., Weber, F., Zhong, P., Tan, C.L., Nguyen, T.N., Beier, K.T., Hörmann, N., Chang, W.-C., Zhang, Z., Do, J.P., *et al.* (2017). Identification of preoptic sleep neurons using retrograde labelling and gene profiling. Nature *545*, 477-481.
Clement, O., Sapin, E., Berod, A., Fort, P., and Luppi, P.H. (2011). Evidence that neurons of the sublaterodorsal tegmental nucleus triggering paradoxical (REM) sleep are glutamatergic. Sleep *34*, 419-423.
Cox, J., Pinto, L., and Dan, Y. (2016). Calcium imaging of sleep–wake related neuronal activity in the dorsal pons. Nature Communications *7*, 10763.
Crochet, S., Onoe, H., and Sakai, K. (2006). A potent non-monoaminergic paradoxical sleep inhibitory system: a reverse microdialysis and single-unit recording study. European Journal of Neuroscience *24*, 1404-1412.
Dement, W. (1958). The occurrence of low voltage, fast, electroencephalogram patterns during behavioral sleep in the cat. Electroencephalography and clinical neurophysiology *10*, 291-296.
Dement, W. (1960). The Effect of Dream Deprivation. Science *131*, 1705-1707.
Do, J.P., Xu, M., Lee, S.H., Chang, W.C., Zhang, S., Chung, S., Yung, T.J., Fan, J.L., Miyamichi, K., Luo, L., *et al.* (2016). Cell type-specific long-range connections of basal forebrain circuit. Elife *5*.
Elias, C.F., Lee, C.E., Kelly, J.F., Ahima, R.S., Kuhar, M., Saper, C.B., and Elmquist, J.K. (2001). Characterization of CART neurons in the rat and human hypothalamus. The Journal of Comparative Neurology *432*, 1-19.
Estabrooke, I.V., McCarthy, M.T., Ko, E., Chou, T.C., Chemelli, R.M., Yanagisawa, M., Saper, C.B., and Scammell, T.E. (2001). Fos Expression in Orexin Neurons Varies with Behavioral State. The Journal of Neuroscience *21*, 1656-1662.
Ferreira, J.G.P., Bittencourt, J.C., and Adamantidis, A. (2017). Melanin-concentrating hormone and sleep. Curr Opin Neurobiol *44*, 152-158.
Findlay, A.L., and Hayward, J.N. (1969). Spontaneous activity of single neurones in the hypothalamus of rabbits during sleep and waking. J Physiol *201*, 237-258.
Gallopin, T., Fort, P., Eggermann, E., Cauli, B., Luppi, P.-H., Rossier, J., Audinat, E., Mühlethaler, M., and Serafin, M. (2000). Identification of sleep-promoting neurons in vitro. Nature *404*, 992.

Gaus, S.E., Strecker, R.E., Tate, B.A., Parker, R.A., and Saper, C.B. (2002). Ventrolateral preoptic nucleus contains sleep-active, galaninergic neurons in multiple mammalian species. Neuroscience *115*, 285-294.
Gerashchenko, D., Blanco-Centurion, C., Greco, M.A., and Shiromani, P.J. (2003). Effects of lateral hypothalamic lesion with the neurotoxin hypocretin-2–saporin on sleep in Long–Evans rats. Neuroscience *116*, 223-235.
Gerfen, C.R., Paletzki, R., and Heintz, N. (2013). GENSAT BAC cre-recombinase driver lines to study the functional organization of cerebral cortical and basal ganglia circuits. Neuron *80*, 1368-1383.
Ghosh, K.K., Burns, L.D., Cocker, E.D., Nimmerjahn, A., Ziv, Y., Gamal, A.E., and Schnitzer, M.J. (2011). Miniaturized integration of a fluorescence microscope. Nat Methods *8*, 871-878.
Hallanger, A.E., Levey, A.I., Lee, H.J., Rye, D.B., and Wainer, B.H. (1987). The origins of cholinergic and other subcortical afferents to the thalamus in the rat. The Journal of Comparative Neurology *262*, 105-124.
Hassani, O.K., Lee, M.G., and Jones, B.E. (2009). Melanin-concentrating hormone neurons discharge in a reciprocal manner to orexin neurons across the sleep-wake cycle. Proc Natl Acad Sci U S A *106*, 2418-2422.
Hayashi, Y., Kashiwagi, M., Yasuda, K., Ando, R., Kanuka, M., Sakai, K., and Itohara, S. (2015). Cells of a common developmental origin regulate REM/non-REM sleep and wakefulness in mice. Science *350*, 957-961.
Hendricks, J.C., Morrison, A.R., and Mann, G.L. (1982). Different behaviors during paradoxical sleep without atonia depend on pontine lesion site. Brain Research *239*, 81-105.
Heym, J., Steinfels, G.F., and Jacobs, B.L. (1982). Activity of serotonin-containing neurons in the nucleus raphe pallidus of freely moving cats. Brain Research *251*, 259-276.
Hobson, J.A., McCarley, R.W., and Wyzinski, P.W. (1975). Sleep cycle oscillation: reciprocal discharge by two brainstem neuronal groups. Science *189*, 55-58.
Jego, S., Glasgow, S.D., Herrera, C.G., Ekstrand, M., Reed, S.J., Boyce, R., Friedman, J., Burdakov, D., and Adamantidis, A.R. (2013). Optogenetic identification of a rapid eye movement sleep modulatory circuit in the hypothalamus. Nat Neurosci *16*, 1637-1643.
John, J., Wu, M.-F., Boehmer, L.N., and Siegel, J.M. (2004). Cataplexy-Active Neurons in the Hypothalamus: Implications for the Role of Histamine in Sleep and Waking Behavior. Neuron *42*, 619-634.
Jones, B.E. (2003). Arousal systems. Frontiers in Bioscience *8*, s438-s451.
Jouvet, M. (1962). [Research on the neural structures and responsible mechanisms in different phases of physiological sleep]. Arch Ital Biol *100*, 125-206.
Ko, E.M., Estabrooke, I.V., McCarthy, M., and Scammell, T.E. (2003). Wake-related activity of tuberomammillary neurons in rats. Brain research *992*, 220-226.
Köhler, C., Ericson, H., Watanabe, T., Polak, J., Palay, S.L., Palay, V., and Chan-Palay, V. (1986). Galanin immunoreactivity in hypothalamic histamine neurons: Further evidence for multiple chemical messengers in the tuberomammillary nucleus. The Journal of Comparative Neurology *250*, 58-64.
Konadhode, R.R., Pelluru, D., Blanco-Centurion, C., Zayachkivsky, A., Liu, M., Uhde, T., Glen, W.B., Jr., van den Pol, A.N., Mulholland, P.J., and Shiromani, P.J. (2013). Optogenetic stimulation of MCH neurons increases sleep. J Neurosci *33*, 10257-10263.
Krout, K.E., Belzer, R.E., and Loewy, A.D. (2002). Brainstem projections to midline and intralaminar thalamic nuclei of the rat. The Journal of Comparative Neurology *448*, 53-101.

Lee, M.G., Hassani, O.K., and Jones, B.E. (2005). Discharge of Identified Orexin/Hypocretin Neurons across the Sleep-Waking Cycle. The Journal of Neuroscience *25*, 6716-6720.
Lu, J., Bjorkum, A.A., Xu, M., Gaus, S.E., Shiromani, P.J., and Saper, C.B. (2002). Selective Activation of the Extended Ventrolateral Preoptic Nucleus during Rapid Eye Movement Sleep. The Journal of Neuroscience *22*, 4568-4576.
Lu, J., Greco, M.A., Shiromani, P., and Saper, C.B. (2000). Effect of Lesions of the Ventrolateral Preoptic Nucleus on NREM and REM Sleep. The Journal of Neuroscience *20*, 3830-3842.
Lu, J., Sherman, D., Devor, M., and Saper, C.B. (2006). A putative flip–flop switch for control of REM sleep. Nature *441*, 589-594.
Luppi, P.-H., ClÉMent, O., and Fort, P. (2013). Brainstem structures involved in rapid eye movement sleep behavior disorder. Sleep and Biological Rhythms *11*, 9-14.
Luppi, P.-H., Gervasoni, D., Verret, L., Goutagny, R., Peyron, C., Salvert, D., Leger, L., and Fort, P. (2006). Paradoxical (REM) sleep genesis: The switch from an aminergic–cholinergic to a GABAergic–glutamatergic hypothesis. Journal of Physiology-Paris *100*, 271-283.
Maheshri, N., Koerber, J.T., Kaspar, B.K., and Schaffer, D.V. (2006). Directed evolution of adeno-associated virus yields enhanced gene delivery vectors. Nat Biotech *24*, 198-204.
McCarley, R., and Hobson, J. (1975). Neuronal excitability modulation over the sleep cycle: a structural and mathematical model. Science *189*, 58-60.
McCormick, D.A. (1989). Cholinergic and noradrenergic modulation of thalamocortical processing. Trends in Neurosciences *12*, 215-221.
McGinty, D.J., and Sterman, M.B. (1968). Sleep Suppression after Basal Forebrain Lesions in the Cat. Science *160*, 1253-1255.
Mileykovskiy, B.Y., Kiyashchenko, L.I., and Siegel, J.M. (2005). Behavioral Correlates of Activity in Identified Hypocretin/Orexin Neurons. Neuron *46*, 787-798.
Miyamichi, K., Amat, F., Moussavi, F., Wang, C., Wickersham, I., Wall, N.R., Taniguchi, H., Tasic, B., Huang, Z.J., He, Z., *et al.* (2011). Cortical representations of olfactory input by trans-synaptic tracing. Nature *472*, 191-196.
Morrison, A.R. (2011). The discovery of REM sleep: the death knell of the passive theory of sleep. In Rapid Eye Movement Sleep: Regulation and Function, A.R. Morrison, B.N. Mallick, R.W. McCarley, and S.R. Pandi-Perumal, eds. (Cambridge: Cambridge University Press), pp. 31-39.
Morrison, S.F., and Nakamura, K. (2011). Central neural pathways for thermoregulation. Front Biosci (Landmark Ed) *16*, 74-104.
Moruzzi, G., Magoun, HW. (1949). Brain stem reticular formation and activation of the EEG. Electroencephalogr Clin Neurophysiol, 455-473.
Mukamel, E.A., Nimmerjahn, A., and Schnitzer, M.J. (2009). Automated Analysis of Cellular Signals from Large-Scale Calcium Imaging Data. Neuron *63*, 747-760.
Nauta, W.J.H. (1946). HYPOTHALAMIC REGULATION OF SLEEP IN RATS. AN EXPERIMENTAL STUDY. Journal of Neurophysiology *9*, 285-316.
Oh, S.W., Harris, J.A., Ng, L., Winslow, B., Cain, N., Mihalas, S., Wang, Q., Lau, C., Kuan, L., Henry, A.M., *et al.* (2014). A mesoscale connectome of the mouse brain. Nature *508*, 207-214.
Osakada, F., and Callaway, E.M. (2013). Design and generation of recombinant rabies virus vectors. Nat Protocols *8*, 1583-1601.
Pace-Schott, E.F., and Hobson, J.A. (2002). The Neurobiology of Sleep: Genetics, cellular physiology and subcortical networks. Nature Reviews Neuroscience *3*, 591.
Pinto, L., and Dan, Y. (2015). Cell-Type-Specific Activity in Prefrontal Cortex during Goal-Directed Behavior. Neuron *87*, 437-450.

Ranson, S.W. (1939). Somnolence caused by hypothalamic lesions in the monkey. Archives of Neurology & Psychiatry *41*, 1-23.
Rasmussen, K., Heym, J., and Jacobs, B.L. (1984). Activity of serotonin-containing neurons in nucleus centralis superior of freely moving cats. Experimental Neurology *83*, 302-317.
Resendez, S.L., Jennings, J.H., Ung, R.L., Namboodiri, V.M.K., Zhou, Z.C., Otis, J.M., Nomura, H., McHenry, J.A., Kosyk, O., and Stuber, G.D. (2016). Visualization of cortical, subcortical and deep brain neural circuit dynamics during naturalistic mammalian behavior with head-mounted microscopes and chronically implanted lenses. Nat Protocols *11*, 566-597.
Romanov, R.A., Zeisel, A., Bakker, J., Girach, F., Hellysaz, A., Tomer, R., Alpar, A., Mulder, J., Clotman, F., Keimpema, E., *et al.* (2017). Molecular interrogation of hypothalamic organization reveals distinct dopamine neuronal subtypes. Nat Neurosci *20*, 176-188.
Sakai, K., and Jouvet, M. (1980). Brain stem PGO-on cells projecting directly to the cat dorsal lateral geniculate nucleus. Brain Research *194*, 500-505.
Saper, C.B. (1985). Organization of cerebral cortical afferent systems in the rat. II. Hypothalamocortical projections. The Journal of Comparative Neurology *237*, 21-46.
Saper, C.B., Chou, T.C., and Scammell, T.E. (2001). The sleep switch: hypothalamic control of sleep and wakefulness. Trends in Neurosciences *24*, 726-731.
Saper, C.B., Fuller, P.M., Pedersen, N.P., Lu, J., and Scammell, T.E. (2010). Sleep state switching. Neuron *68*, 1023-1042.
Sapin, E., Lapray, D., Berod, A., Goutagny, R., Leger, L., Ravassard, P., Clement, O., Hanriot, L., Fort, P., and Luppi, P.H. (2009). Localization of the brainstem GABAergic neurons controlling paradoxical (REM) sleep. PLoS One *4*, e4272.
Sastre, J.P., Buda, C., Kitahama, K., and Jouvet, M. (1996). Importance of the ventrolateral region of the periaqueductal gray and adjacent tegmentum in the control of paradoxical sleep as studied by muscimol microinjections in the cat. Neuroscience *74*, 415-426.
Scammell, T.E., Arrigoni, E., and Lipton, J.O. (2017). Neural Circuitry of Wakefulness and Sleep. Neuron *93*, 747-765.
Schwarz, L.A., Miyamichi, K., Gao, X.J., Beier, K.T., Weissbourd, B., DeLoach, K.E., Ren, J., Ibanes, S., Malenka, R.C., Kremer, E.J., *et al.* (2015). Viral-genetic tracing of the input-output organization of a central noradrenaline circuit. Nature *524*, 88-92.
Sherin, J.E., Elmquist, J.K., Torrealba, F., and Saper, C.B. (1998). Innervation of Histaminergic Tuberomammillary Neurons by GABAergic and Galaninergic Neurons in the Ventrolateral Preoptic Nucleus of the Rat. The Journal of Neuroscience *18*, 4705-4721.
Sherin, J.E., Shiromani, P.J., McCarley, R.W., and Saper, C.B. (1996). Activation of Ventrolateral Preoptic Neurons During Sleep. Science *271*, 216-219.
Shouse, M.N., and Siegel, J.M. (1992). Pontine regulation of REM sleep components in cats: integrity of the pedunculopontine tegmentum (PPT) is important for phasic events but unnecessary for atonia during REM sleep. Brain Research *571*, 50-63.
Starzl, T.E., Taylor, C.W., and Magoun, H.W. (1951). ASCENDING CONDUCTION IN RETICULAR ACTIVATING SYSTEM, WITH SPECIAL REFERENCE TO THE DIENCEPHALON. Journal of neurophysiology *14*, 461-477.
Steiger, A., and Holsboer, F. (1997). Neuropeptides and human sleep. Sleep *20*, 1038-1052.
Steininger, T.L., Alam, M.N., Gong, H., Szymusiak, R., and McGinty, D. (1999). Sleep–waking discharge of neurons in the posterior lateral hypothalamus of the albino rat. Brain Research *840*, 138-147.

Strecker, R.E., Morairty, S., Thakkar, M.M., Porkka-Heiskanen, T., Basheer, R., Dauphin, L.J., Rainnie, D.G., Portas, C.M., Greene, R.W., and McCarley, R.W. (2000). Adenosinergic modulation of basal forebrain and preoptic/anterior hypothalamic neuronal activity in the control of behavioral state. Behavioural Brain Research *115*, 183-204.
Suntsova, N., Szymusiak, R., Alam, M.N., Guzman-Marin, R., and McGinty, D. (2002). Sleep-waking discharge patterns of median preoptic nucleus neurons in rats. The Journal of Physiology *543*, 665-677.
Takahashi, K., Kayama, Y., Lin, J.S., and Sakai, K. (2010). Locus coeruleus neuronal activity during the sleep-waking cycle in mice. Neuroscience *169*, 1115-1126.
Tervo, D.Gowanlock R., Hwang, B.-Y., Viswanathan, S., Gaj, T., Lavzin, M., Ritola, Kimberly D., Lindo, S., Michael, S., Kuleshova, E., Ojala, D., *et al.* (2016). A Designer AAV Variant Permits Efficient Retrograde Access to Projection Neurons. Neuron *92*, 372-382.
Trulson, M.E., Jacobs, B.L., and Morrison, A.R. (1981). Raphe unit activity during REM sleep in normal cats and in pontine lesioned cats displaying REM sleep without atonia. Brain Research *226*, 75-91.
Trulson, M.E., and Trulson, V.M. (1982). Activity of nucleus raphe pallidus neurons across the sleep-waking cycle in freely moving cats. Brain Research *237*, 232-237.
Tsunematsu, T., Ueno, T., Tabuchi, S., Inutsuka, A., Tanaka, K.F., Hasuwa, H., Kilduff, T.S., Terao, A., and Yamanaka, A. (2014). Optogenetic manipulation of activity and temporally controlled cell-specific ablation reveal a role for MCH neurons in sleep/wake regulation. J Neurosci *34*, 6896-6909.
Van Dort, C.J., Zachs, D.P., Kenny, J.D., Zheng, S., Goldblum, R.R., Gelwan, N.A., Ramos, D.M., Nolan, M.A., Wang, K., Weng, F.J., *et al.* (2015). Optogenetic activation of cholinergic neurons in the PPT or LDT induces REM sleep. Proc Natl Acad Sci U S A *112*, 584-589.
Verret, L., Goutagny, R., Fort, P., Cagnon, L., Salvert, D., Léger, L., Boissard, R., Salin, P., Peyron, C., and Luppi, P.-H. (2003). A role of melanin-concentrating hormone producing neurons in the central regulation of paradoxical sleep. BMC Neuroscience *4*, 19.
Vetrivelan, R., Fuller, P.M., Tong, Q., and Lu, J. (2009). Medullary Circuitry Regulating Rapid Eye Movement Sleep and Motor Atonia. The Journal of Neuroscience *29*, 9361-9369.
Vincent, S.R., Hökfelt, T., and Wu, J.Y. (1982). GABA Neuron Systems in Hypothalamus and the Pituitary Gland. Neuroendocrinology *34*, 117-125.
von Economo, C. (1930). Sleep as a problem of localization. J Nerv Ment Dis *71*, 249-259.
Weber, F., Chung, S., Beier, K.T., Xu, M., Luo, L., and Dan, Y. (2015). Control of REM sleep by ventral medulla GABAergic neurons. Nature *526*, 435-438.
Weber, F., and Dan, Y. (2016). Circuit-based interrogation of sleep control. Nature *538*, 51-59.
Webster, H.H., and Jones, B.E. (1988). Neurotoxic lesions of the dorsolateral pontomesencephalic tegmentum-cholinergic cell area in the cat. II. Effects upon sleep-waking states. Brain Research *458*, 285-302.
Wickersham, I.R., Lyon, D.C., Barnard, R.J.O., Mori, T., Finke, S., Conzelmann, K.-K., Young, J.A.T., and Callaway, E.M. (2007). Monosynaptic Restriction of Transsynaptic Tracing from Single, Genetically Targeted Neurons. Neuron *53*, 639-647.
Willie, J.T., Sinton, C.M., Maratos-Flier, E., and Yanagisawa, M. (2008). Abnormal response of melanin-concentrating hormone deficient mice to fasting: Hyperactivity and rapid eye movement sleep suppression. Neuroscience *156*, 819-829.
Wright, J.K.P., Badia, P., and Wauquier, A. (1995). Topographical and Temporal Patterns of Brain Activity During the Transition From Wakefulness to Sleep. Sleep *18*, 880-889.

Xu, M., Chung, S., Zhang, S., Zhong, P., Ma, C., Chang, W.C., Weissbourd, B., Sakai, N., Luo, L., Nishino, S., *et al.* (2015). Basal forebrain circuit for sleep-wake control. Nat Neurosci *18*, 1641-1647.
Zhang, S., Xu, M., Chang, W.-C., Ma, C., Hoang Do, J.P., Jeong, D., Lei, T., Fan, J.L., and Dan, Y. (2016). Organization of long-range inputs and outputs of frontal cortex for top-down control. Nat Neurosci *19*, 1733-1742.